

GEOLOGI FOR SAMFUNNET

GEOLOGY FOR SOCIETY



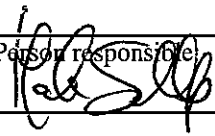
Report no.: 2013.033		ISSN 0800-3416	Grading: open
Title: REE potential of bedrock on Nordkinn Peninsula, Finnmark			
Authors: Julian Schilling		Client:	
County: Finnmark		Commune: Lebesby, Gamvik	
Map-sheet name (M=1:250.000) Nordkapp, Kistrand, Vadsø		Map-sheet no. and -name (M=1:50.000)	
Deposit name and grid-reference: Nordkinn		Number of pages: 83	Price (NOK): 280,-
Fieldwork carried out: 2.-9.7.2012		Date of report: 18.7.2013	Project no.: 348700
Person responsible: 			
<p>Summary:</p> <p>Recently, NGU carried out a low-density soil sampling project on the Nordkinn Peninsula, Finnmark, Northern Norway, that outlined regional-scale anomalies for the REE Peninsula (Reimann et al., 2012). The present report is a follow-up study to the soil sampling project and the present study has involved the mineralogical and compositional characterisation of the metasedimentary bedrock with focus on the economic potential in the rare earth elements (REE) of the area. The REE have been shown to be present in comparable concentration ranges in the soil and hard-rock samples, and the REE results obtained for aliquots of hard-rock samples following AR digestion, 4-Acid leaching and Li-borate fusion/decomposition closely match the results from soil pulps after an Aqua Regia (AR) digestion. Total contents for the REE determined in bedrock using the above methods range between 19 and 429 ppm, indicating an overall limited economic potential for the metasandstones with respect to the REE. The AR leaching method, which is considered to be an incomplete digestion method for most minerals, revealed similarly high REE contents as for the 4-Acid digestion and Li-borate fusion/decomposition methods. In contrast to the AR leaching procedure, the latter two methods are considered to digest samples more completely and hence are expected to produce results closer to total composition. In terms of petrography, essentially all the bedrock samples are characterised by the presence of altered and locally in-situ decomposed LREE-silicates (possibly allanite, a LREE-incorporating, epidote group mineral) and minor REE-phosphates and -carbonates. Secondary, late-stage REE minerals are scarce, implying limited transport of the REE. In conclusion, all of the above preparation methods dissolved the REE more or less completely from the altered (and rare late-stage) minerals, and even the relatively weak AR digestion revealed just as high REE values as the other methods due to the vulnerability of the altered REE phases. Thus, the REE anomalies found in soil samples rather reflect the alteration state of the REE minerals present in the area rather than ore-grade REE concentrations associated with the bedrock. The soil formation process is interpreted to be rather a recent weathering phenomenon than the result of a paleo- (deep[?]) weathering process as positive Ce-anomalies in the soils and opposed negative Ce-anomalies in the bedrock point to an in-situ process, indicating that the soil is the direct weathering product of the underlying bedrock.</p>			
Keywords: REE	Regional-scale REE anomaly in soil	Soil and bedrock petrography	
Whole-rock analyses	Mineralogical and compositional comparative study		

Table of contents

1.1	Introduction	4
1.2	Regional geology	6
2.	Petrography	7
3.	Methods.....	11
4.	Results.....	12
4.1	Major elements	12
4.2	Trace elements	34
5.	Discussion	47
5.1	Weathering.....	47
5.2	REE mineralogy and economic potential	48
7.	Acknowledgements	53
8.	References.....	54
9.	Appendices.....	57

1.1 Introduction

Placer and paleoplacer ore deposits are known to account for a variety of commodities and mineral resources. Minerals locally found to be potentially concentrated to ore-grade in placers are characterised by both high density (i.e., exceeding 2.9 g/cm^3) and resistance to chemical weathering. Potential economic target areas are in-situ weathered bedrock and heavy-mineral-bearing horizons in sediments and sedimentary rocks which may form under fluvial and/or marine conditions. Minerals of potential economic interest found in such settings are typically zircon (e.g., Sircombe & Freeman, 1999; Roy, 1999), cassiterite (Patyk-Kara, 1999), monazite (van Emden et al., 1997), Fe-Ti oxides (Dill, 2007, Bryan et al., 2007, Roy, 1999), diamond (Moore & Moore, 2004) and gold (Giusti, 1986, Minter, 1993).

In the Kalak Nappe Complex, Finnmark, Northern Norway, metamorphosed clastic sediments have been described to contain heavy-mineral layers over a relatively large outcrop area (Roberts & Andersen, 1985; Roberts, 2007, Kirkland et al., 2007). As recently as 2011, the geochemistry group at the Geological Survey of Norway (NGU) carried out a low-density soil sampling programme on the Nordkinn and Varanger Peninsulas and sampled a total of 808 sites, resulting in a density of one sample per 2 km^2 . The soil samples were taken invariably from the mineral soil layer which, on Nordkinn, is assumed to contain the weathering products of the underlying metasandstones and metapelites of the Kalak Nappe. The $<2 \text{ mm}$ fraction of the soil samples was prepared using an Aqua Regia (AR) digestion approach, followed by ICP MS analyses of 65 elements. The results refined the anomalies detected during the course of the earlier, low-density, Nordkalott soil sampling project (Bølviken et al., 1986), the Kola project (Reimann et al., 1996) and re-analysis of the old Nordkalott samples (Reimann et al., 2011), and confirm anomalies for a number of elements, among others the rare earth elements (REE). For the REE, typical values found in the soil samples are as high as a few hundred ppm and rarely even exceed 1000 ppm (Reimann et al., 2012). Given the fact that AR digestion is a relatively mild extraction technique and that the values determined for REE in the soil are promisingly high, the Nordkinn Peninsula thus appeared to yield potential for further exploration, for which more knowledge on the bedrock geology is required. Thus, based on the results presented by Reimann et al. (2011), NGU decided to raise funding from the MINN (Mineral Resources in Northern Norway) and EUrare programs to further explore the REE potential of the Nordkinn area for characterising the outcropping bedrock by means of whole-rock compositional analyses and image-based characterisation of the REE minerals. This approach was necessary as the soil samples reported by Reimann et al. (2012) were analysed as pulp samples and no mineralogical characterisation of the material was carried out. Consequently, the present report summarises the petrographic aspects observed on the macro- and microscales and the whole-rock compositional data obtained for the rock samples. Based on these findings, the present study rates the economic potential of the working area with respect to the REE.

Details on the background of the investigation of the bedrock on Nordkinn Peninsula are as follows. Locally restricted areas were taken into account for bedrock sampling that (i) yielded elevated concentrations of the elements of interest in the soil samples described by Reimann et al. (2012) and/or (ii) have been previously described to display textures such as heavy mineral layers that may point to elevated portions of the potential ore minerals (D. Roberts,

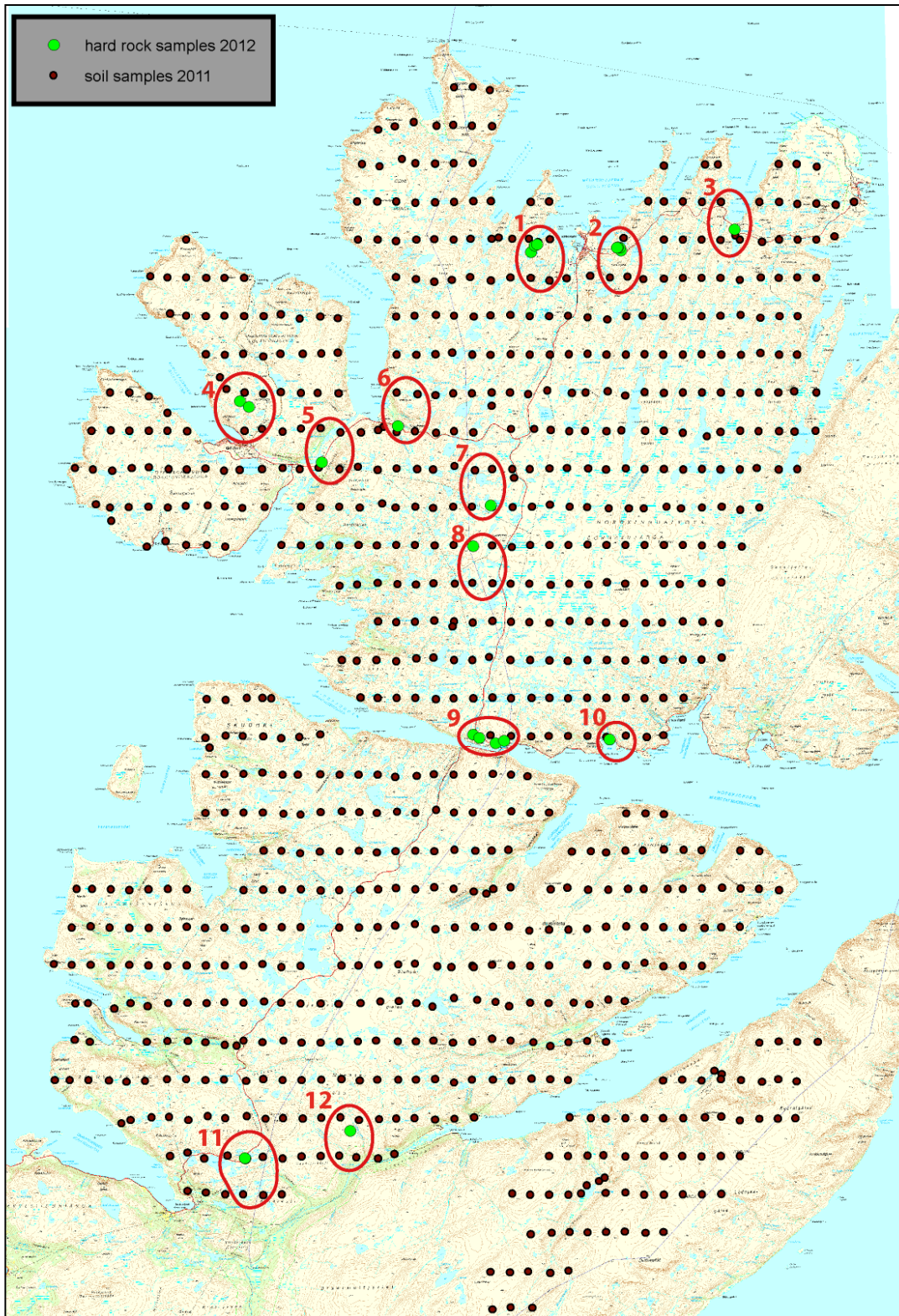


Fig. 1: The Nordkinn Peninsula and adjacent land to the south. Dark-red filled circles are sample sites from Reimann et al. (2012). Green filled circles are bedrock described in the present study. Red open symbols define the localities mentioned in the text, which include both bedrock and adjacent soil samples.

pers. comm. 2012). This led to the definition of 12 locally restricted areas that, where possible, were sampled from outcropping bedrock. From the sample sets obtained, a smaller number of representative samples were chosen (green sites in Fig. 1). In this context, “representative” means that all textural variations observed were included for mineralogical and compositional investigation and compared in terms of major and trace element composition to adjacent soil samples available from Reimann et al. (2012). Hence, all of the 12 defined locations from Fig. 1 marked with red circles include whole rocks and adjacent soil samples.

Aliquots of the bedrock samples were analysed for their major and minor element compositions subsequent to an Aqua Regia digestion, a 4-Acid digestion and a Li-borate fusion/decomposition treatment. Compositional results for the major elements are presented as proportional symbols and compared to the compositions of the soil samples from Reimann et al (2012). Minor and trace elements (including the REE) are shown for each of the defined localities as normalised variation (‘spider’) diagrams for both, hard rock and adjacent soil samples. For normalisation, the average values of the continental crust from Gao & Rudnick (2003) were chosen in order to show the degrees of enrichment compared to common crustal values. Thus, this report addresses the economic potential related to the HFSE- and REE-mineralogy of the metasediments on Nordkinn and establishes a relationship between the elevated REE contents in the soil samples, the analytical methods applied for characterising the soil and hard rock samples, and the petrography of the REE minerals in the bedrock.

1.2 Regional geology

The Nordkinn Peninsula (and adjacent land to the south) is characterised by the occurrence of Neoproterozoic siliciclastic metasedimentary rocks of the Kalak Nappe Complex (Roberts, 1981; 1998; 2006; 2007; Roberts and Siedlecka, 2011; 2012 Siedlecka, 2009; Siedlecka et al., 2006). The origin of the metasedimentary rocks has been subject to discussion and Roberts (2000; 2007) and Roberts and Siedlecka (2012) have concluded that the cross-bedded and folded metapelites of Nordkinn Peninsula derived from basement terranes on the Fennoscandian Shield. In contrast, Kirkland et al. (2007) concluded that the original sediments of the Kalak Nappe Complex were likely to have been deposited in basins along the Laurentian-Amazonian margin and thus may represent material from exotic terranes. A sketch map showing the regional geology of northernmost Norway is shown in Fig. 2 with the working area being highlighted.

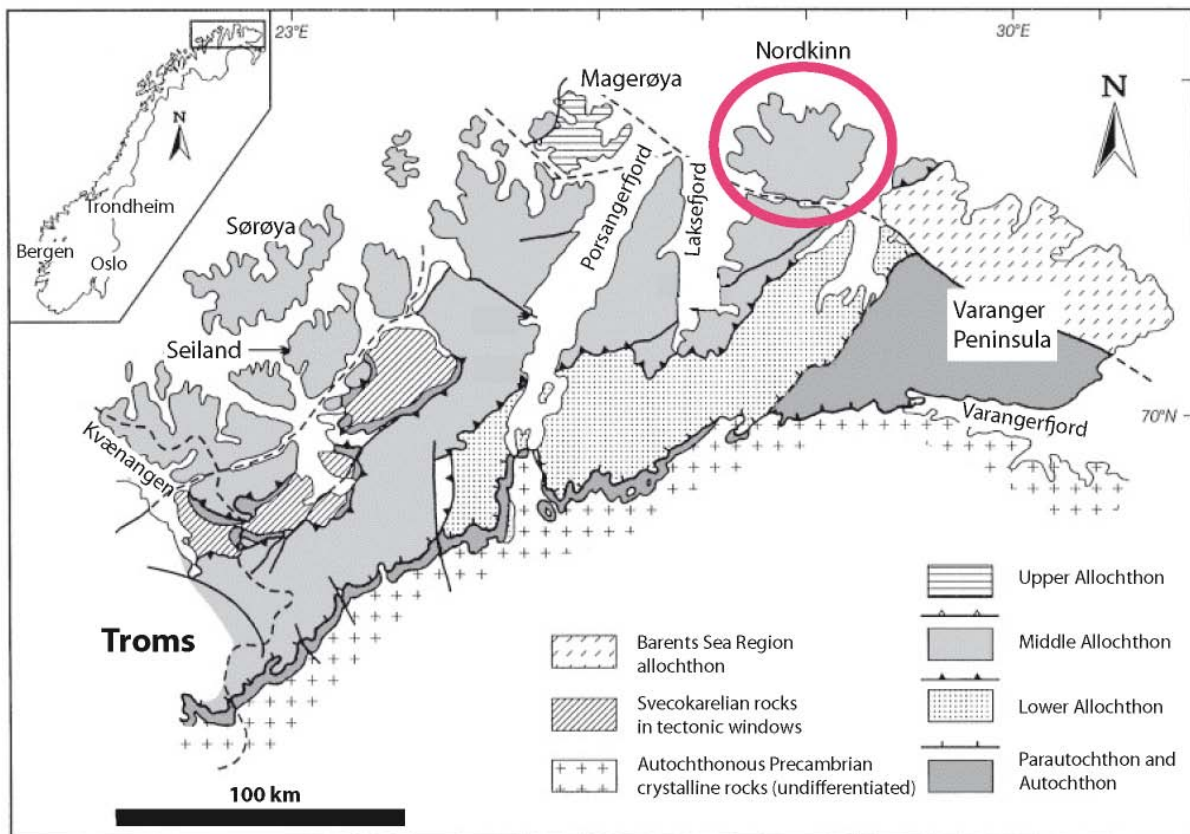


Figure 2: Sketch map showing the major tectonic units of northernmost Norway. The Nordkinn Peninsula is highlighted (red circle). The map is modified after Roberts (1985; 2000).

2. Petrography

Bedrock outcrops providing geochemically fresh and unaltered hard-rock samples are rare in the plains of upland central Nordkinn Peninsula (Fig. 3 a). Geochemically unaltered material was sampled along road-cuts and steeper slopes along the coastline in the pre-defined areas chosen for bedrock sampling (Figs. 3 b-d). In the field, deformed and folded, well bedded metasandstones (lower part of Fig. 3 b; light grey lithology in Fig. 3 c), relatively homogeneous quartzites with and without heavy-mineral layers (Fig. 3 d) and intercalations of metapelite (upper part of Fig. 3 b; dark grey lithology in Fig. 3 c) can be distinguished. The quartzites contain predominantly rounded and cemented quartz grains and biotite and rare muscovite flakes (Fig. 4 a). Locally, heavy-mineral rich horizons contain rounded zircon and magnetite grains (Figs. 4 a, b & g; 5 c); in general, heavy-mineral rich zones are restricted to the metasandstones and quartzites. Grain sizes are relatively homogeneous (Fig. 3 d) and are invariably $<250\ \mu\text{m}$ in the quartzites (Fig. 4 a). Metasandstones are characterised by the occurrence of notable amounts of K-feldspar together with quartz, magnetite, biotite and muscovite. Rounded grains of K-feldspar locally reach up to 1 cm in diameter but grain sizes in the metasandstones are typically $<250\ \mu\text{m}$ (Fig 4 b). The quartz/feldspar ratio varies considerably and transitions between quartzites and metasandstones are common in the studied area. Both quartzites and metasandstones are locally calcite-bearing and calcite appears invariably to be post-sedimentary in origin as it is anhedral in appearance and fills

interstices. Calcite possibly grew into open pore spaces and filled vugs and interstices left from the sedimentation process (Figs 4 a & b). The metapelitic layers vary from sub-mm laminae to m-sized horizons (Figs. 3 b & c; 4 c -f) and are mineralogically dominated by mica, but transitional lithologies with equal amounts of quartz/K-feldspar and mica were found (Figs. 4 c-f). Typical metapelitic layers contain two texturally distinguishable biotite generations, (i) relatively large biotite porphyroblasts and (ii) fine-grained biotite with fine-grained muscovite, variable amounts of rounded quartz, K-feldspar and locally small garnet porphyroblasts (Figs. 4 c-f; cf. Rice and Roberts, 1988). Grain sizes of the metapelites are smaller than in the alternating metapelites and metasandstones and inhomogeneous, ranging from $<50\ \mu\text{m}$ (fine-grained mica) to mm-size (garnet).

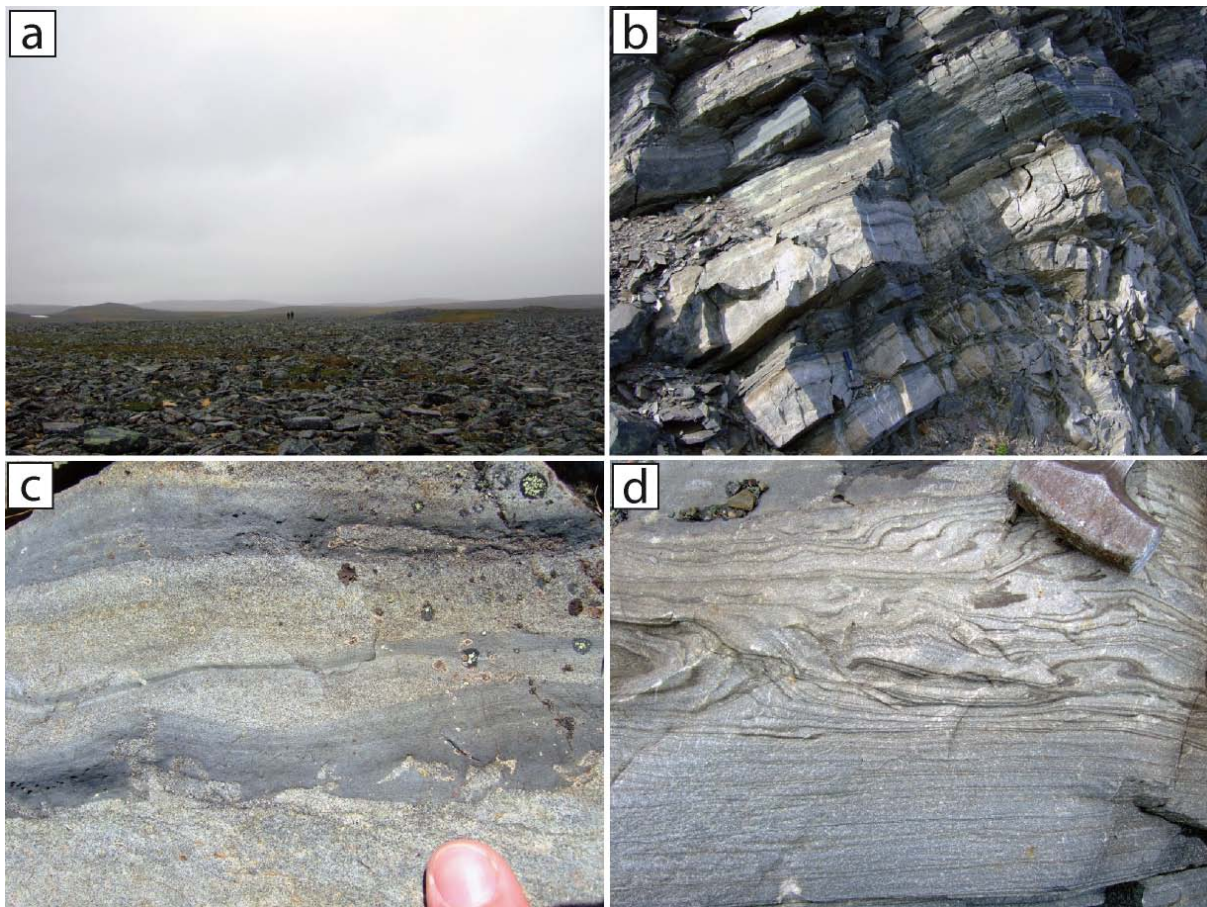


Figure 3: Field aspects of the lithologies from the Nordkinn Peninsula. (a) Blockfield on the central Nordkinn plain; (b) outcrop of metapelites (upper part) and metasandstones (lower part), note hammer for scale; (c) alternating metasandstone (light grey) and metapelite (dark grey) material; (d) penecontemporaneously folded metasandstones with heavy-mineral rich layers.

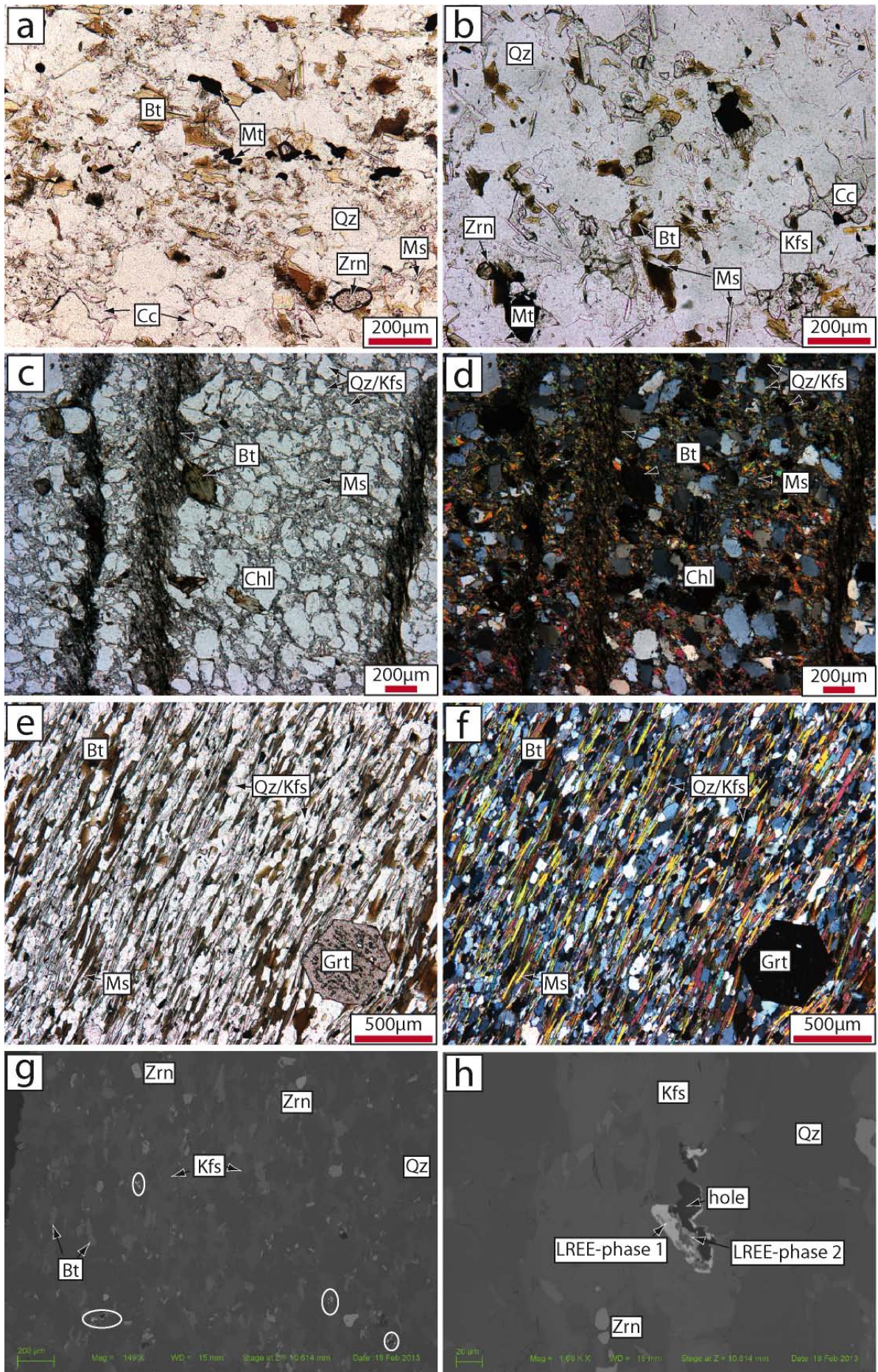


Figure 4: Photomicrographs of bedrock investigated in thin-section: (a and b) heavy-mineral rich metasandstones, PPL; (c and d) metasandstone with μm -thick metapelitic laminae, PPL and XPL; (e and f) metapelite with garnet porphyroblast, PPL (e) and XPL (f); (g) BSEi of heavy-mineral rich metasandstone with REE minerals encircled; (h) BSEi close-up of REE minerals. Mineral abbreviations as suggested by Whitney and Evans (2010).

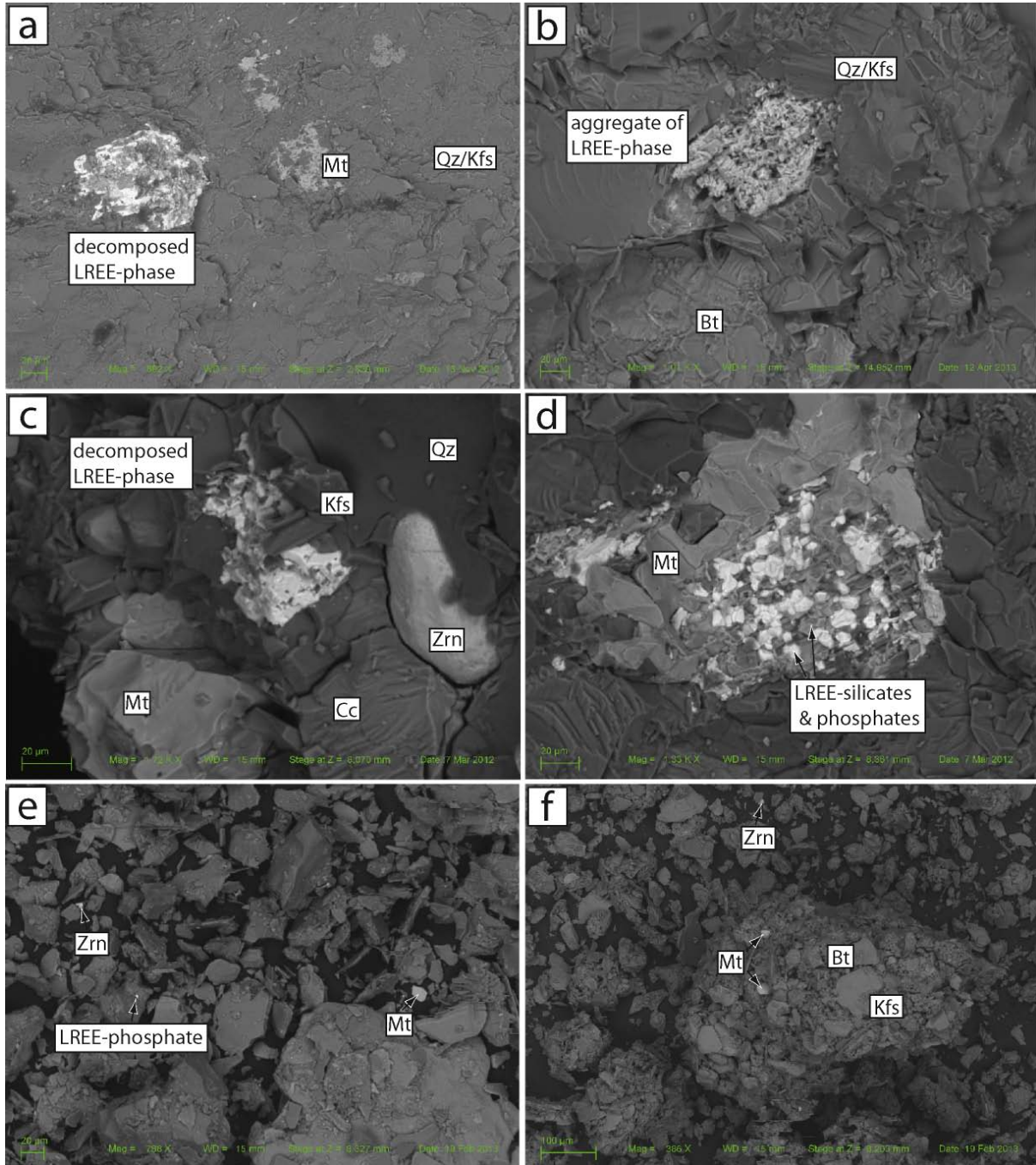


Figure 5: BSEi of sample chips (a – d) and soil sample material (e – f); (a) allanite(?) undergoing strong alteration and (b) replacement by fine-grained mineral aggregates. Note that in both examples the grain shape of the precursor REE-phase (allanite?) is still visible; (c) decomposed LREE-phases are texturally related with euhedral grains of non-REE minerals; (d) overgrowths of intact LREE-phosphates and silicates on magnetite were found in one sample only; (e) the soil samples do not differ mineralogically from the bedrock samples but REE-phases are rare and occur as small constituents or (f) are completely absent. Mineral abbreviations as suggested by Whitney and Evans (2010).

REE phases were identified based on optical properties visible in polarisation microscopy, compositional properties visible in back-scatter electron images (BSEi) and point analyses in EDS mode. In thin-section, REE-minerals commonly occur in multi-mineral aggregates, and in some places holes in the thin-section are associated with the presence of REE minerals (Figs. 4 g-h). Different grey scales in BSEi and point analyses in energy-dispersive spectroscopy (EDS) operation mode point to the presence of different REE phases found associated with REE mineral aggregates, and REE silicates predominate over REE phosphates and REE carbonates. Based on the point spectra obtained, most REE phases are dominated by the light REE (LREE). LREE phases found in the chipped sample material investigated by means of SEM techniques reveal that the REE minerals are strongly altered and partly decomposed (Figs. 5 a-c). It is not only remarkable that REE minerals are altered and decomposed in samples where other minerals such as magnetite occur in alteration textures (Fig. 5 a), but also that REE minerals are altered and decomposed in samples in which essentially all non-REE minerals are texturally unaltered and intact (see e.g. quartz, K-feldspar and biotite in Fig. 5 b and the euhedral K-feldspar crystals in Fig. 5 c adjacent to the LREE phase). In one sample, LREE silicates and phosphates were found as newly grown and intact crystals forming overgrowths on magnetite (Fig. 5 d). In contrast, REE phases in the other samples are corroded and/or decomposed and are interpreted to have undergone in-situ breakdown to extremely fine-grained REE mineral aggregates (note the pseudomorphic replacement of the mineral aggregate after the primary REE mineral in Fig. 5 b). It is assumed that the holes associated with REE phases in the thin-sections described above (Figs. 4 g – h) may be due to partial removal of the fine-grained REE decomposition products during sample preparation.

Aliquots from the <2 mm fractions of the soil samples that were reported by Reimann et al. (2012) to contain the highest REE contents have been investigated by means of BSE imaging and EDS point analyses (Figs. 5 e - f). The soil samples resemble the metasedimentary rocks in terms of major mineralogical composition (i.e., quartz, K-feldspar, biotite and magnetite make up the major volume of the soil samples), but in some soil samples no REE phases at all were identified. This may be a result of sorting effects of the soil material due to movement (i.e. transportation in a container and separating material for the investigation) whereas the proportions separated for the SEM studies did not contain the REE mineral fraction. Alternatively, and possibly more likely, the REE phases were dispersed in the soil samples as extremely fine-grained, possibly sub- μm sized components which were too small to be detected by BSE imaging. The latter interpretation would be in agreement with the observation that extremely fine-grained REE mineral aggregates may have fallen into the sub- μm sized component during weathering and soil formation. The holes associated with REE mineral aggregates documented to occur in thin-section may also have formed as a result of mechanical instability of the secondary REE mineral aggregates during sample preparation.

3. Methods

Bedrock samples from the 2012 fieldwork were taken by the author and whole-rock compositions of 28 selected samples were determined at ACME labs, Vancouver, Canada. Three different preparation techniques from the commercially offered analytical procedures

from ACME labs were chosen to treat three aliquots of each of the 28 samples. Prior to shipping, slices for the preparation of polished thin-sections were cut from the specimen and altered crusts were sawed off. Sample weights ranged between 370 and 790 g and samples were crushed, split and 250 g pulverised at ACME labs, Vancouver, Canada (commercially offered package code R200-250). Aliquots of all samples were analysed by ICP-MS following treatment with 1:1:1 Aqua Regia (AR) digestion (15 g, 1F05-1F09 package), 4 Acid digestion (0.25 g, 1T) and lithium metaborate/tetraborate fusion of 0.2 g sample material, and subsequent ICP ES analyses (major elements, 4A) and AR decomposition of the fusion tablet followed by ICP MS analyses (trace elements, 4B). The 1:1:1 AR digestion is equivalent to the analytical approach applied to the soil samples. Based on the strengths of the acids used for sample powder digestion, it is assumed that the total digestion is closest achieved by the 4AB package, followed by the 1T and 1:1:1 AR digestions.

Soil samples taken in a 2 x 1 km grid during the 2011 fieldwork were dried, sieved and subsequently analysed by ACME labs, Vancouver, Canada. All compositional results from soil samples taken for comparison are from Reimann et al. (2012). Details of the fieldwork, analytical procedure and quality control are given in Reimann et al. (2012).

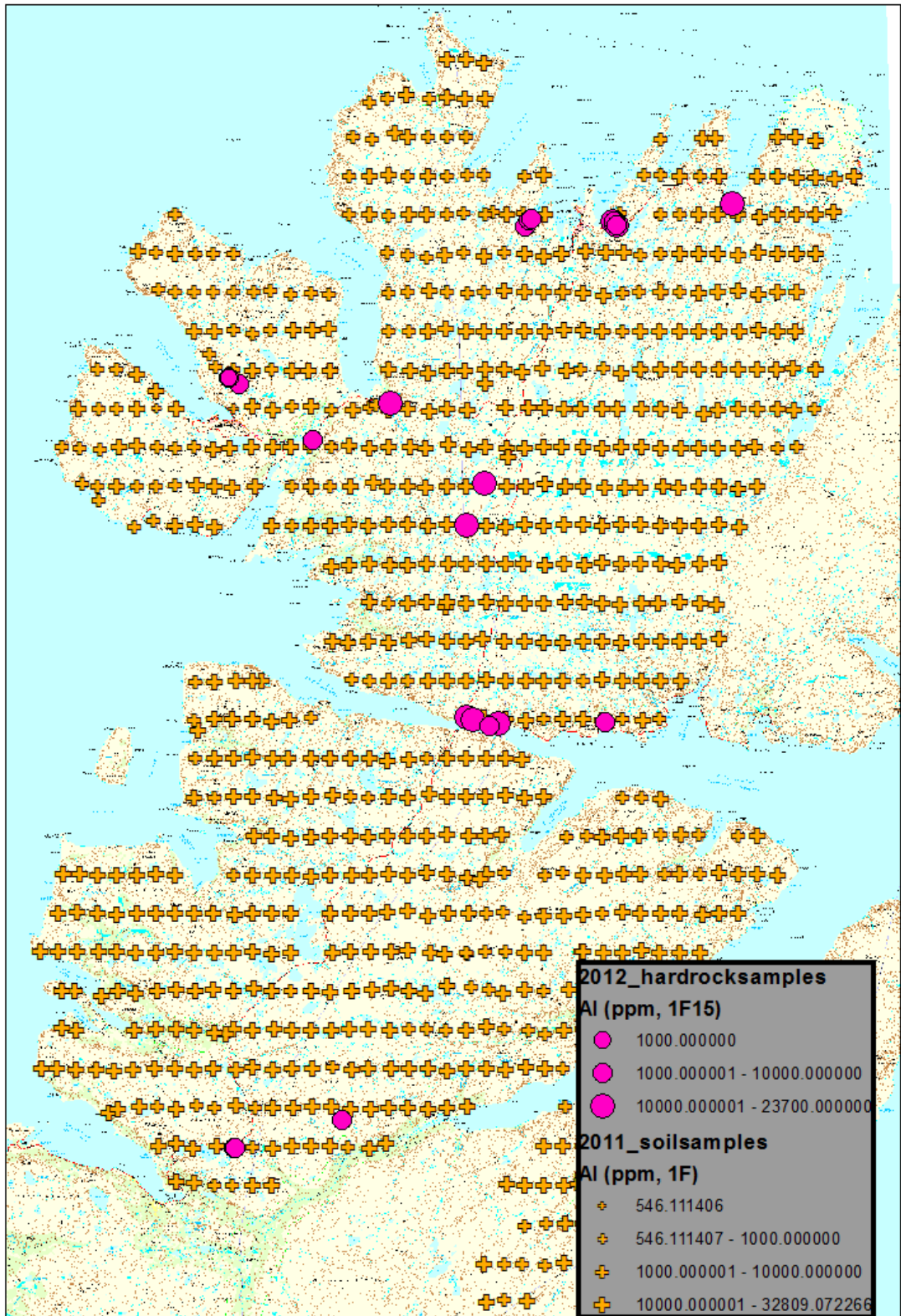
Both polished thinsections and sample pieces of variable size chipped from the rock samples were investigated using qualitative energy-dispersive spectrometry (EDS) on a LEO 1450 VP SEM equipped with an Oxford EDS model 7366 with 10 mm² detector area at NGU, Trondheim, Norway. During operation the acceleration voltage was 15 kV and point analyses in EDS mode were done in variable pressure mode which allowed for analysing the sample material without coating on the samples. Cathodoluminescence (CL) imaging of zircon was done using a Centaurus detector with a sensitivity range between 300 - 600 nm and highest sensitivity around 400 nm. The CL-detector was mounted on the above instrument.

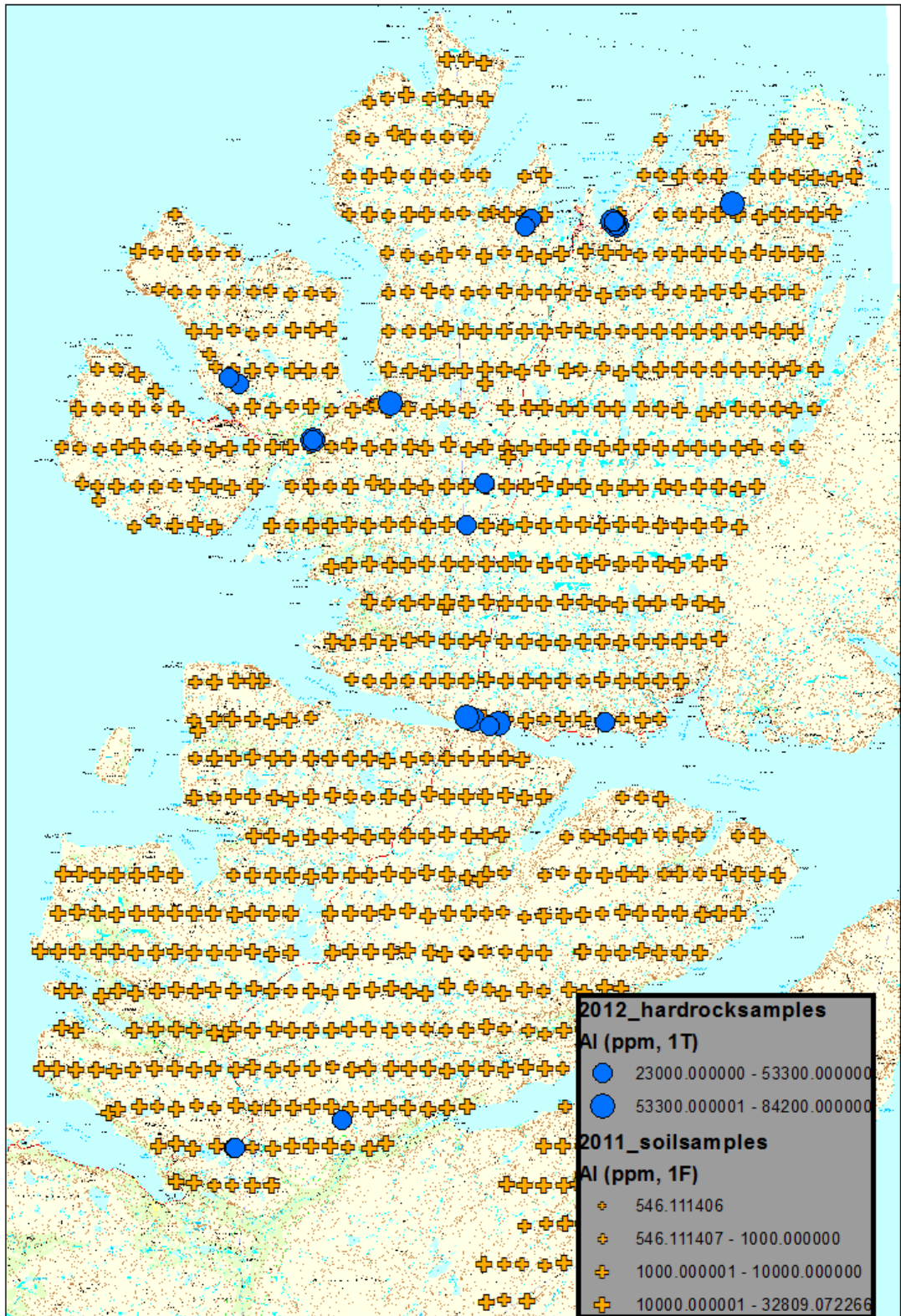
4. Results

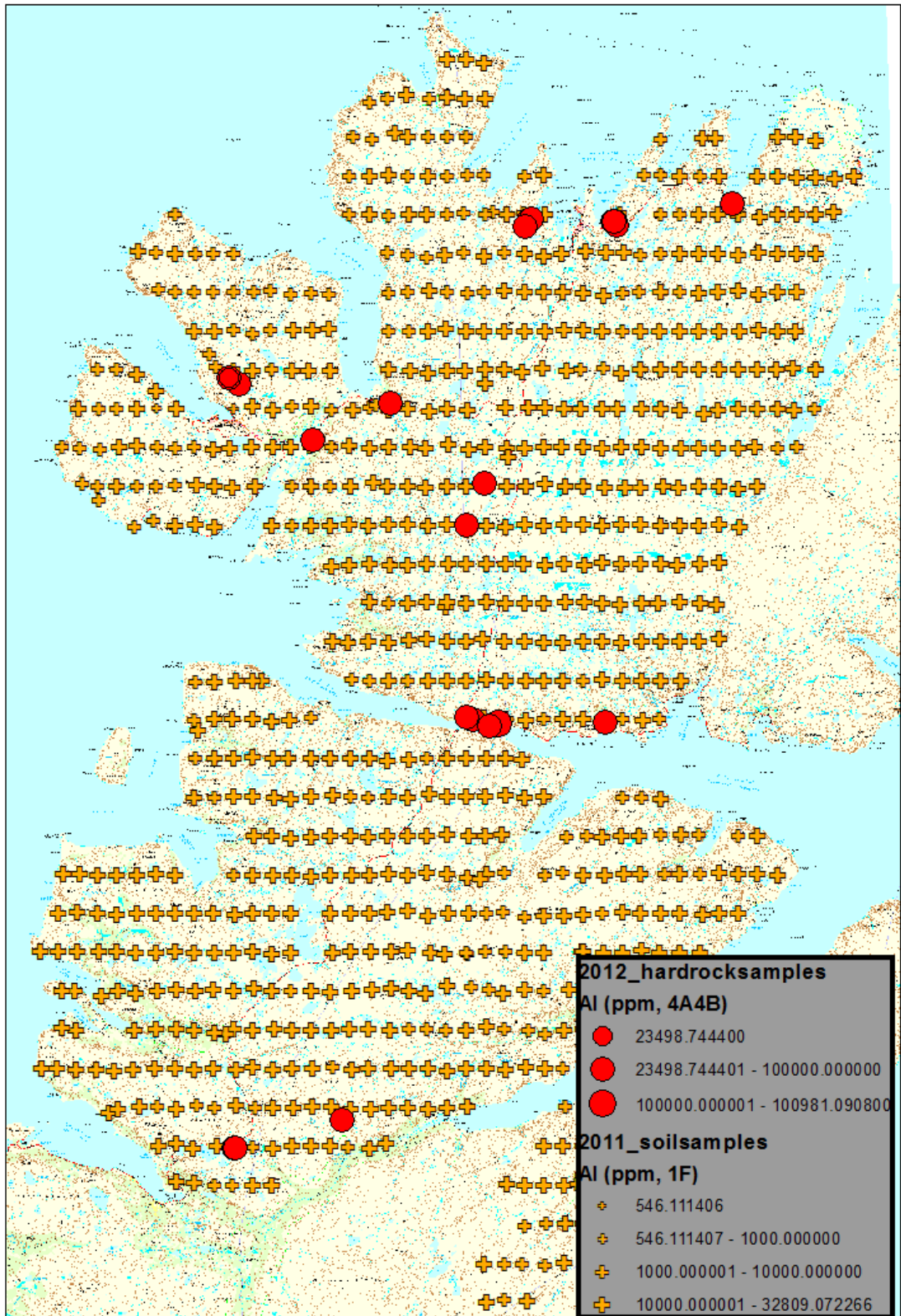
4.1 Major elements

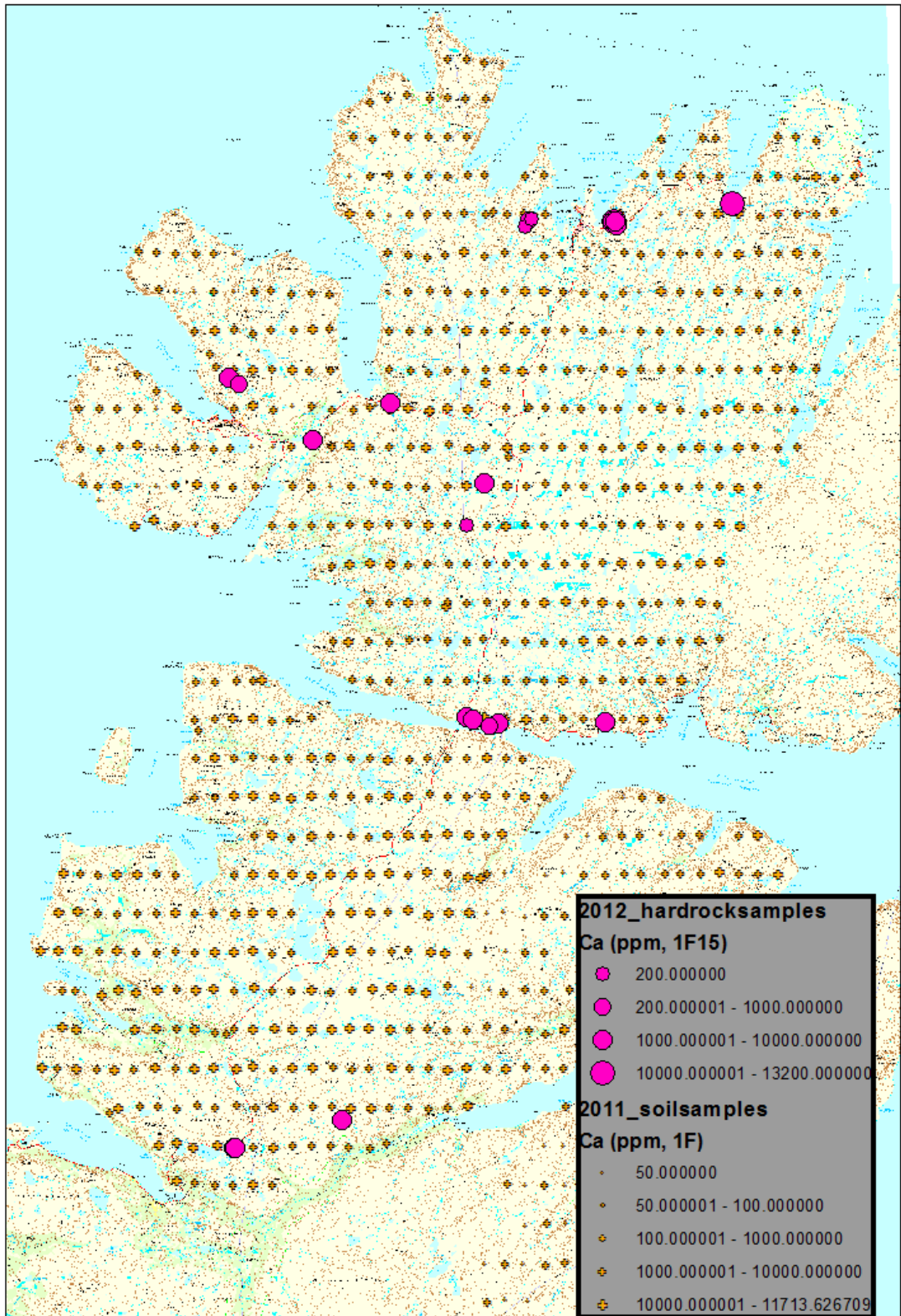
The compositions of the major elements Al, Fe, Mg, Mn, Ca, Na, K and P are visualised as symbols with sizes proportional to their respective element concentrations (Fig. 6). Such map visualisations were done for all of the above sample preparation techniques with pink-filled circles for the AR digestion, blue-filled circles for 4-Acid digestion and red-filled circles for Li borate fusion/decomposition. Major elements analysed in soil samples are those given by Reimann et al. (2012) and are shown as orange crosses with symbol sizes proportional to the concentration of the respective element.

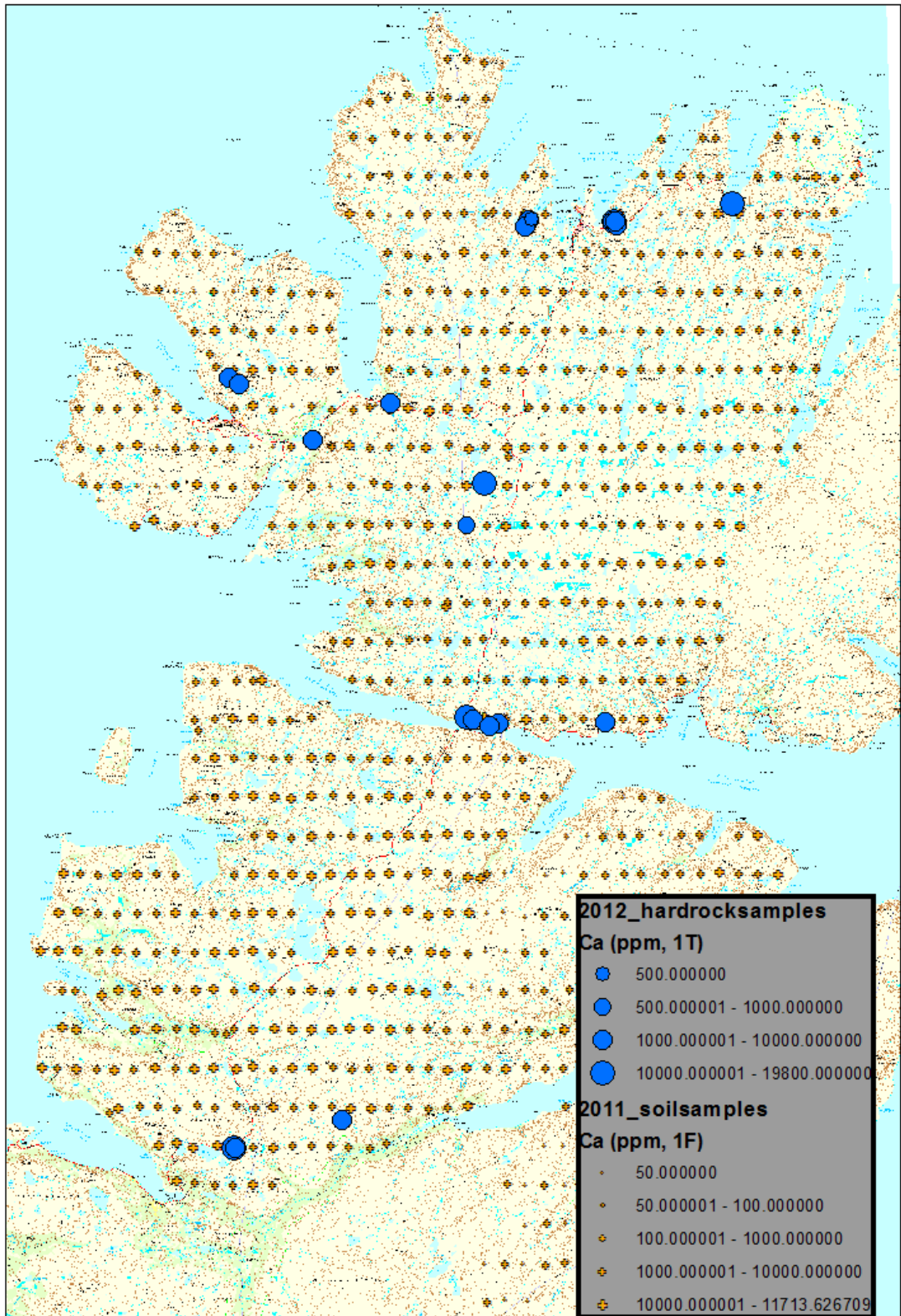
With the exception of Fe, all of the above major elements fall into the same concentration level in both bedrock samples analysed by ICP-MS subsequent to AR digestion and AR-treated soil samples. The lowest values for Al, Ca, Fe, K, Mg and Na were detected in soil samples whereas P is lowest in one of the bedrock samples prepared by AR digestion (for comparability of the two datasets, see discussion).

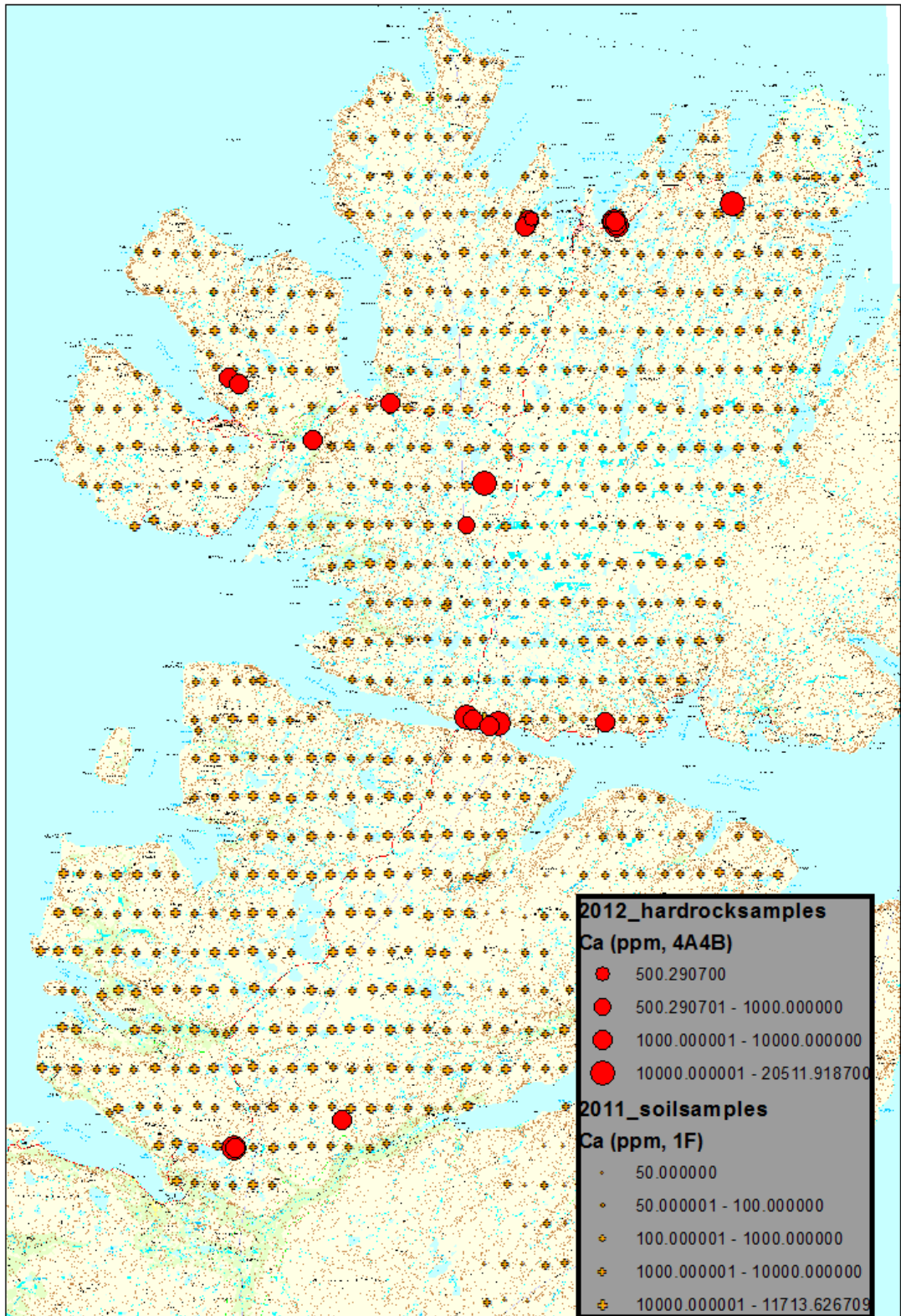


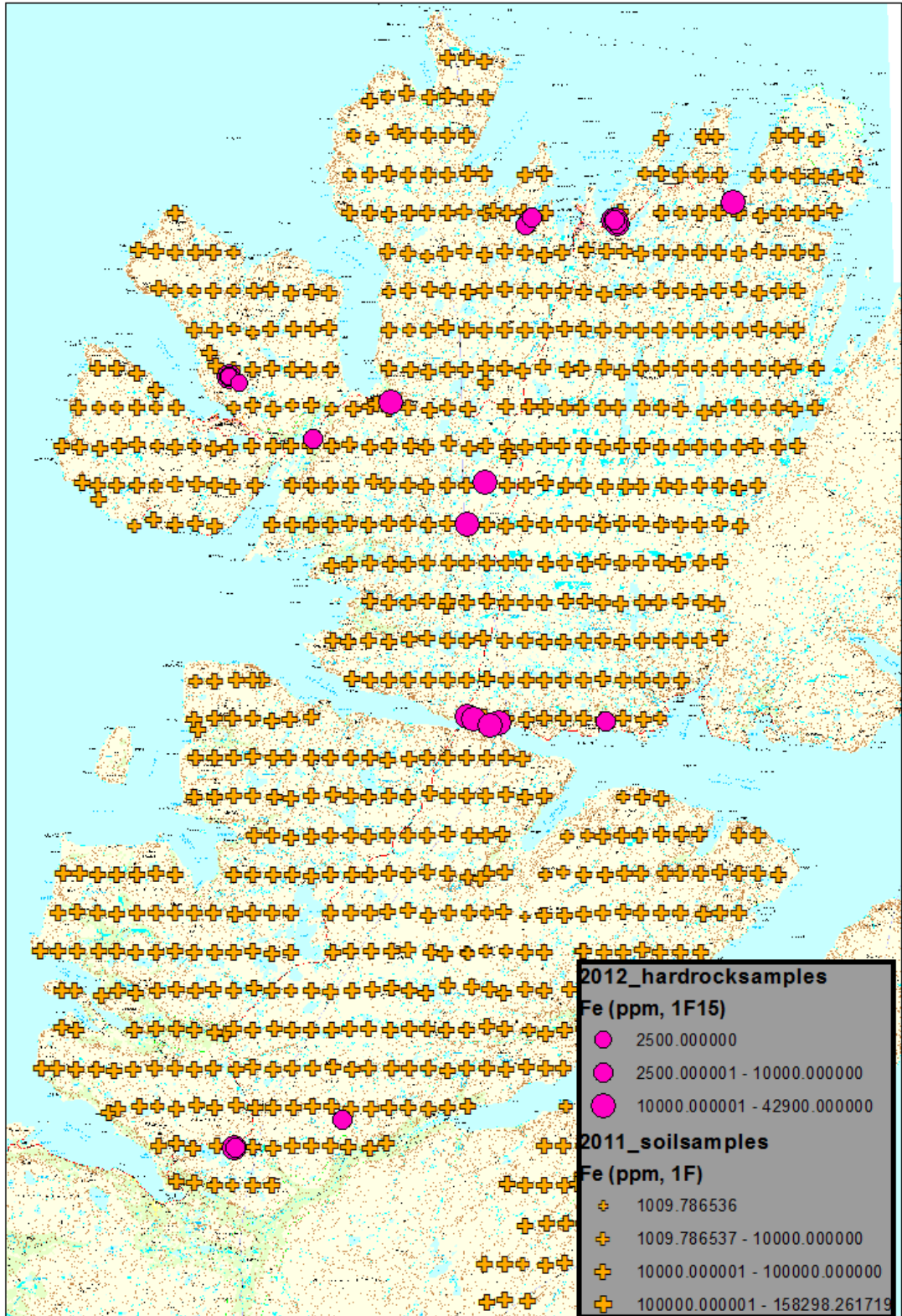


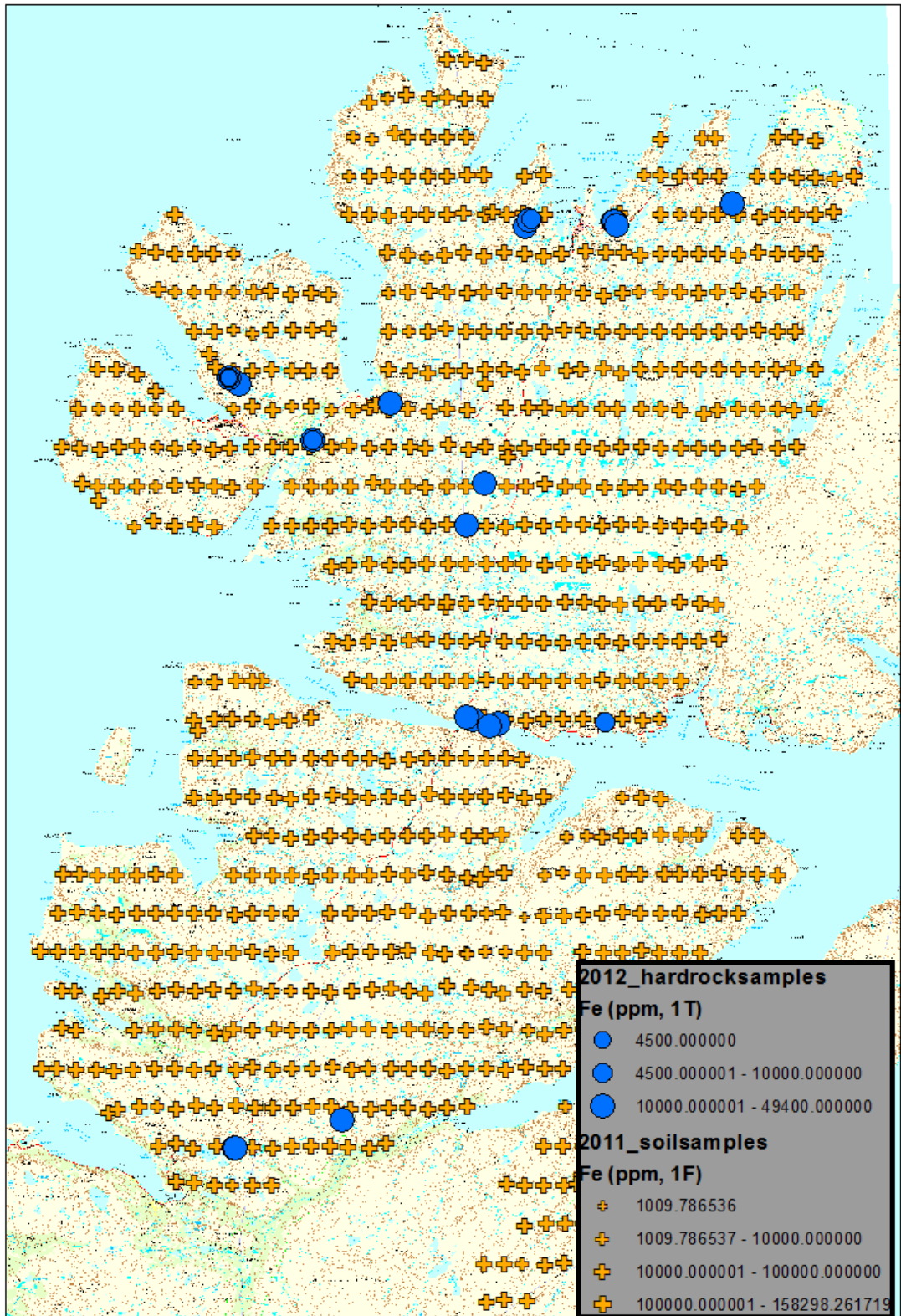


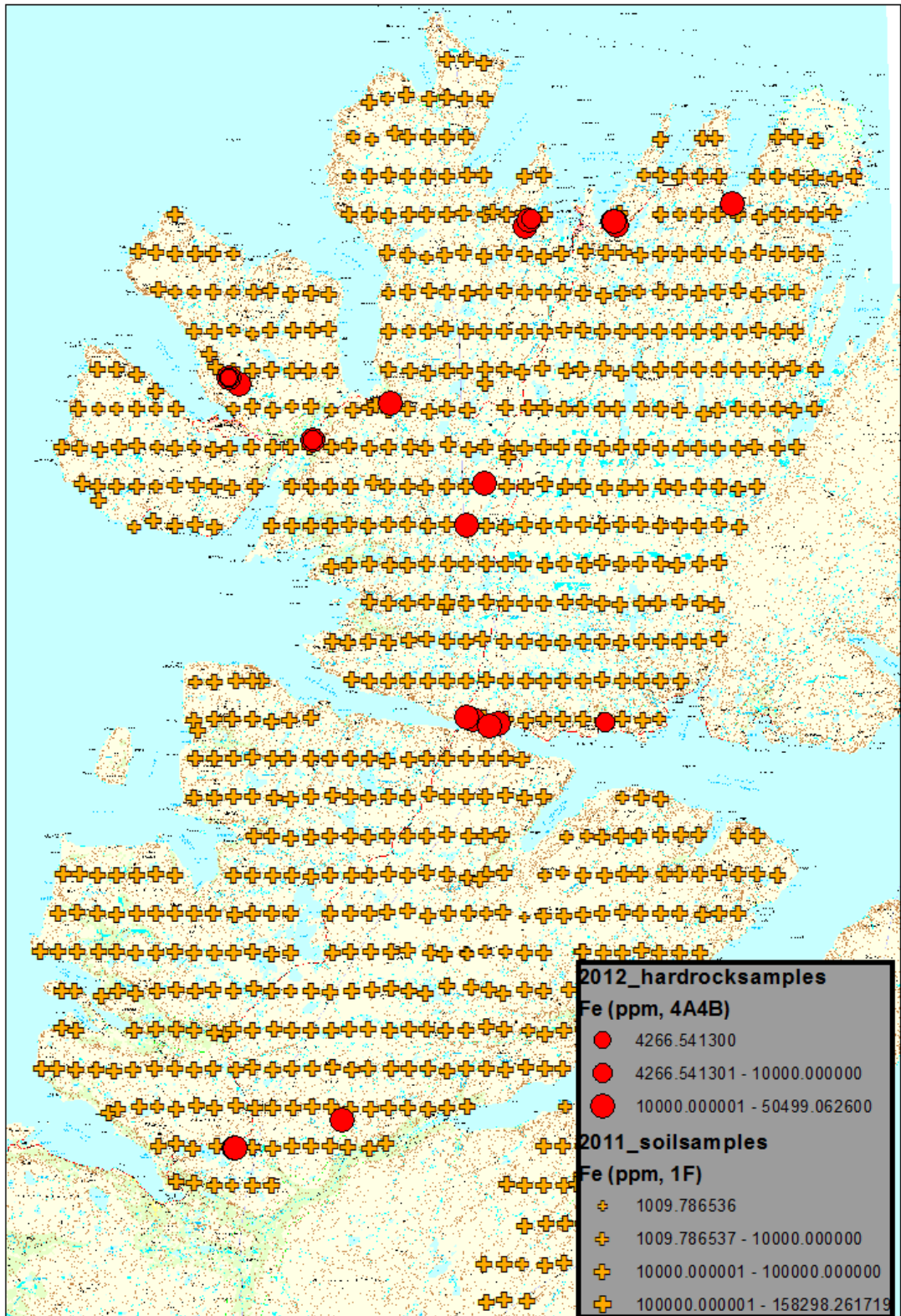


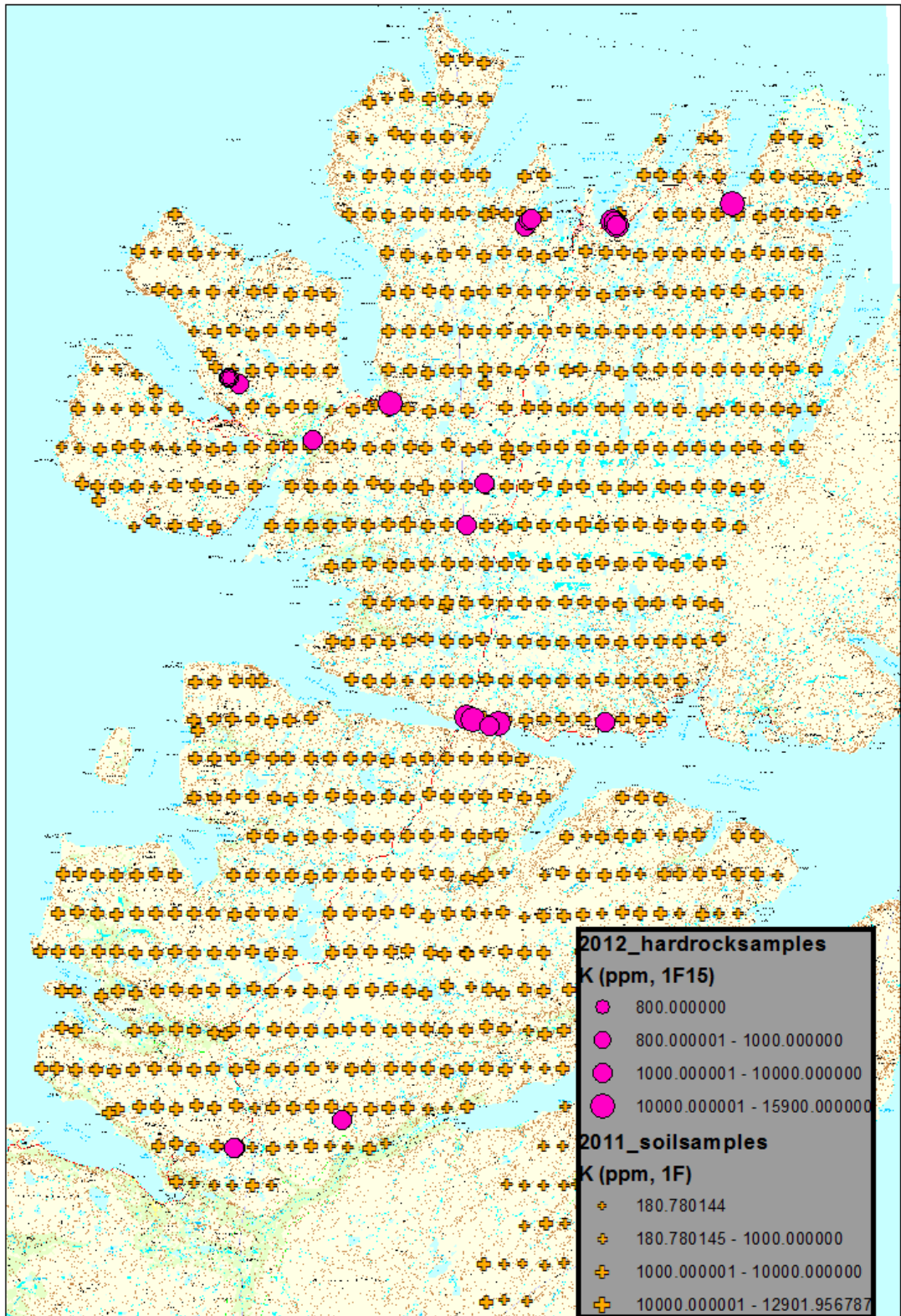


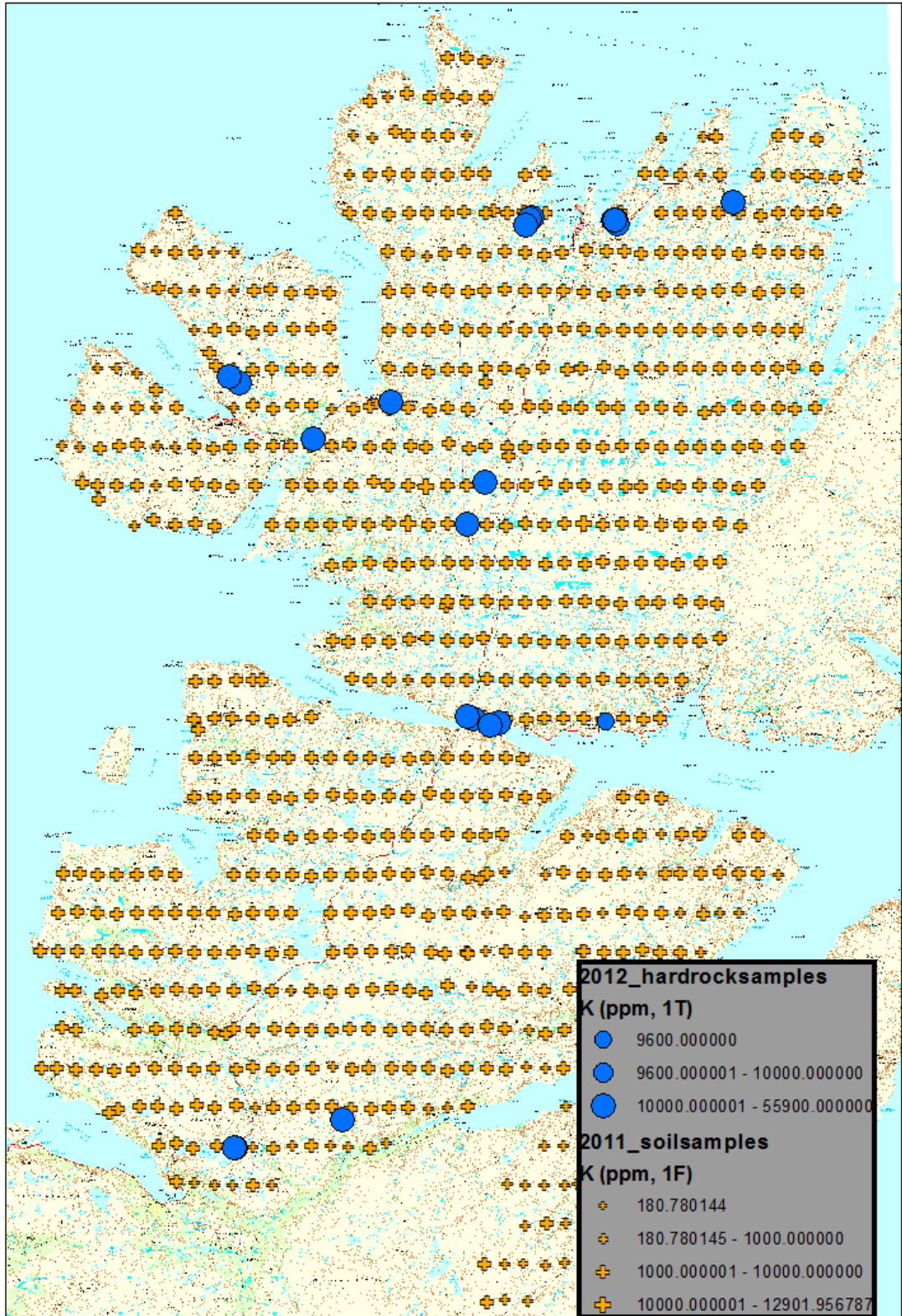


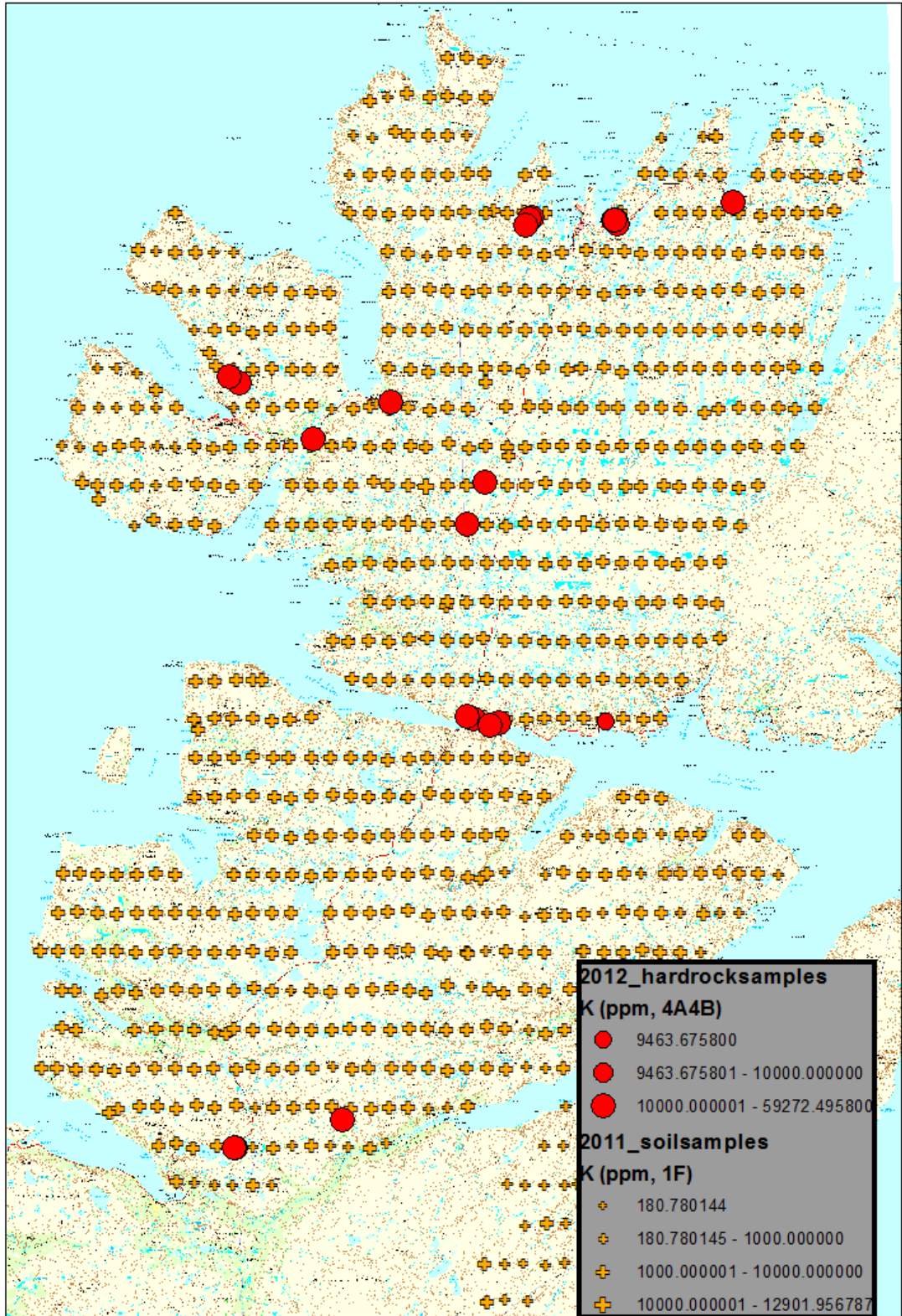


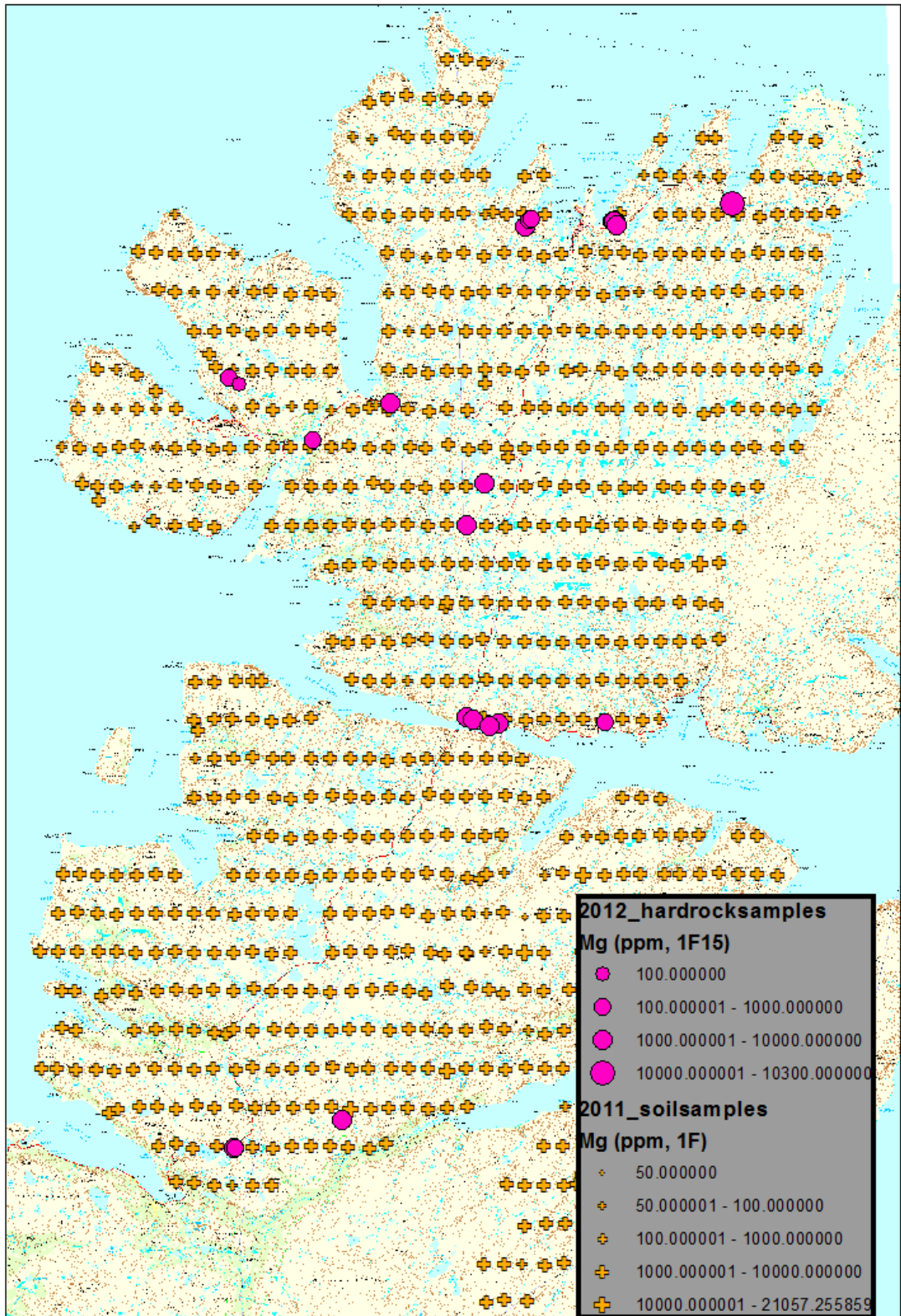


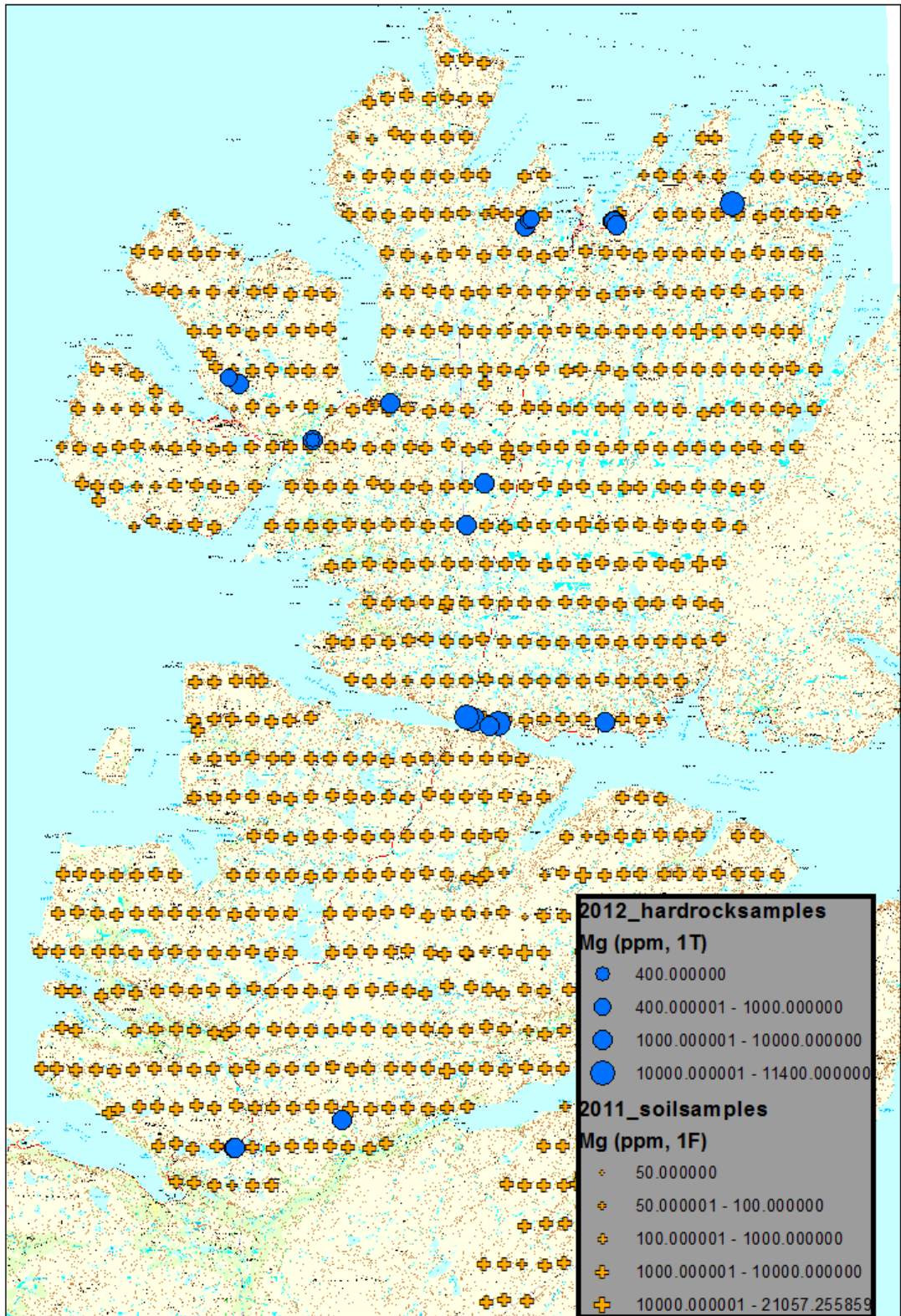


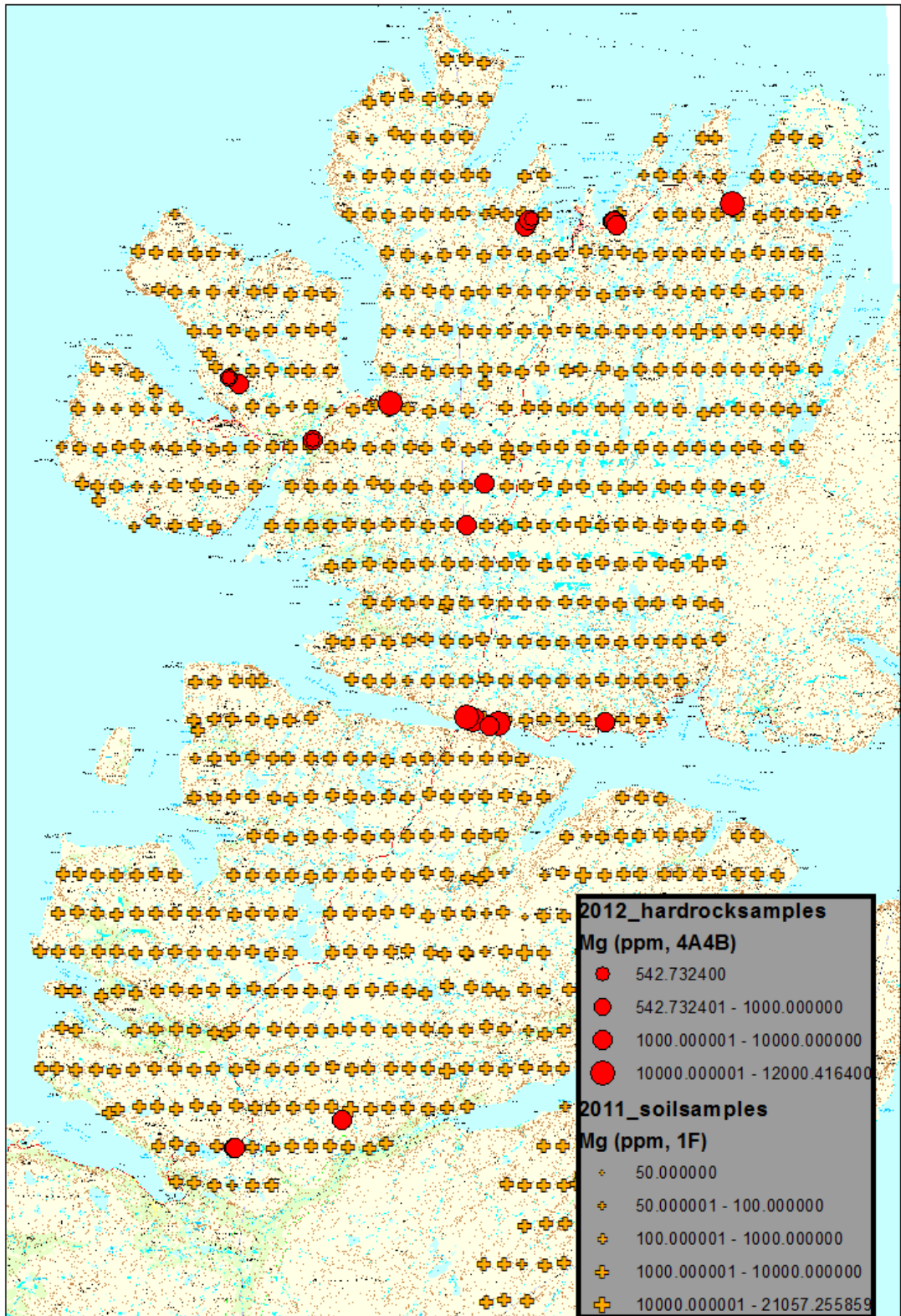


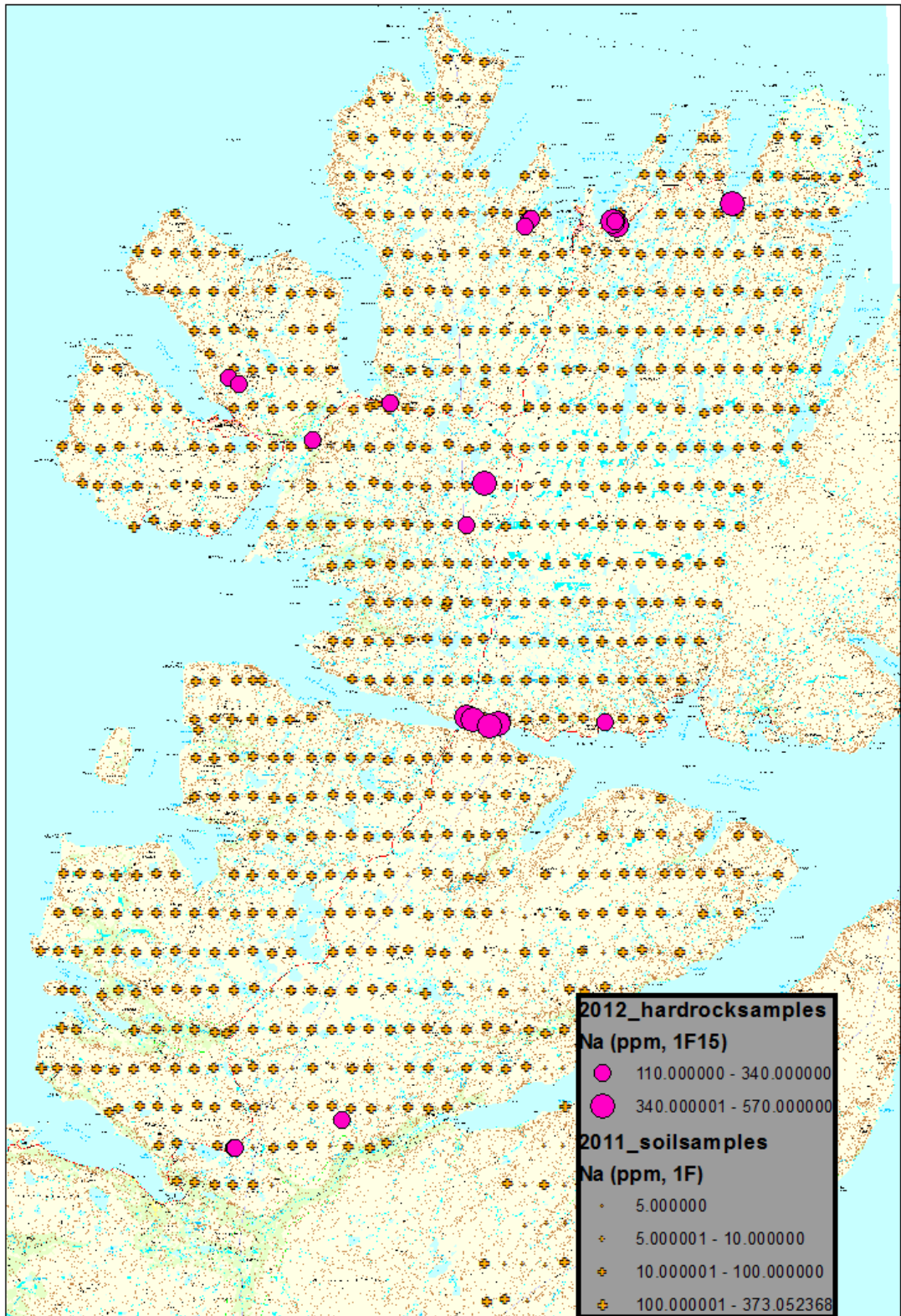


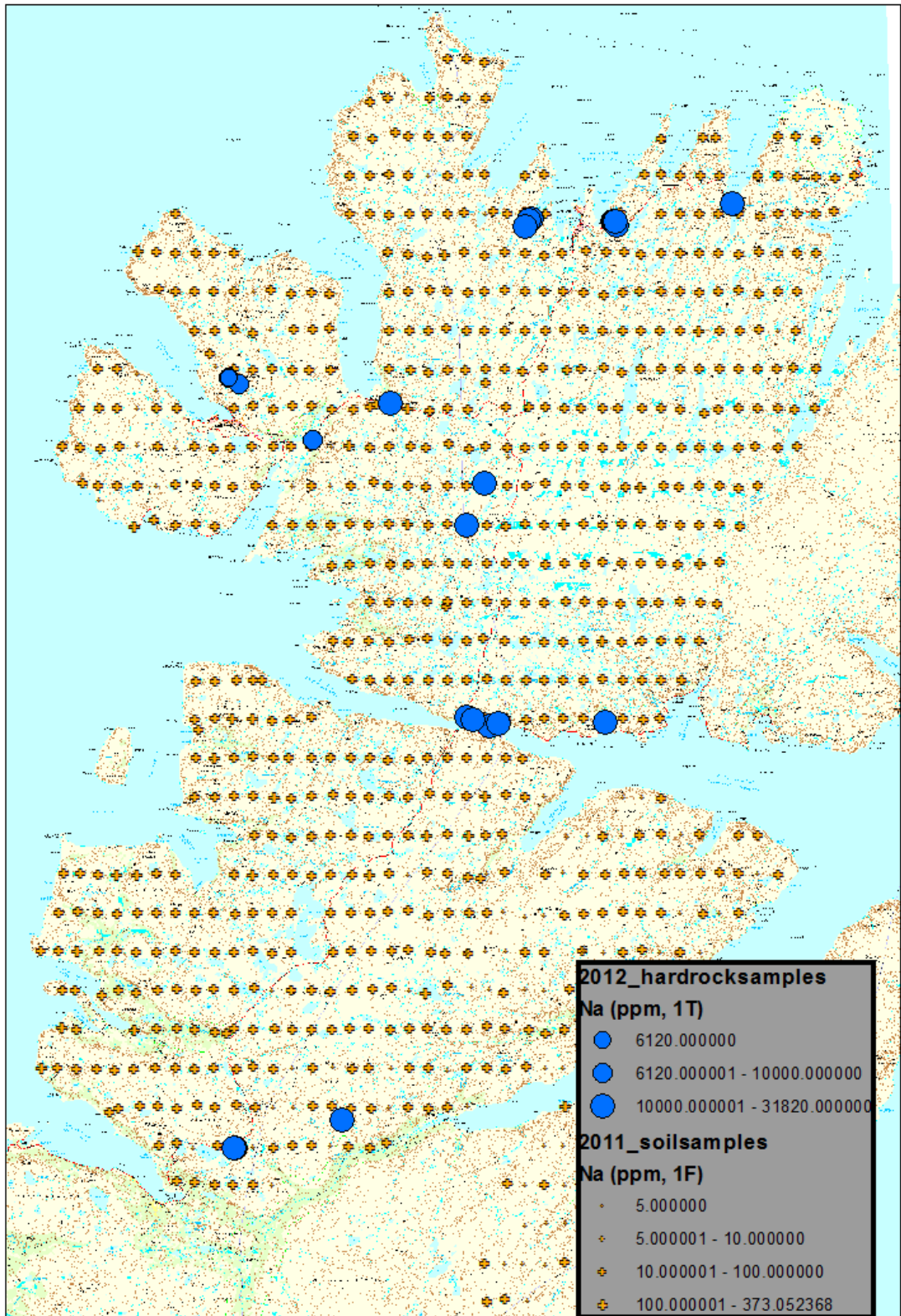


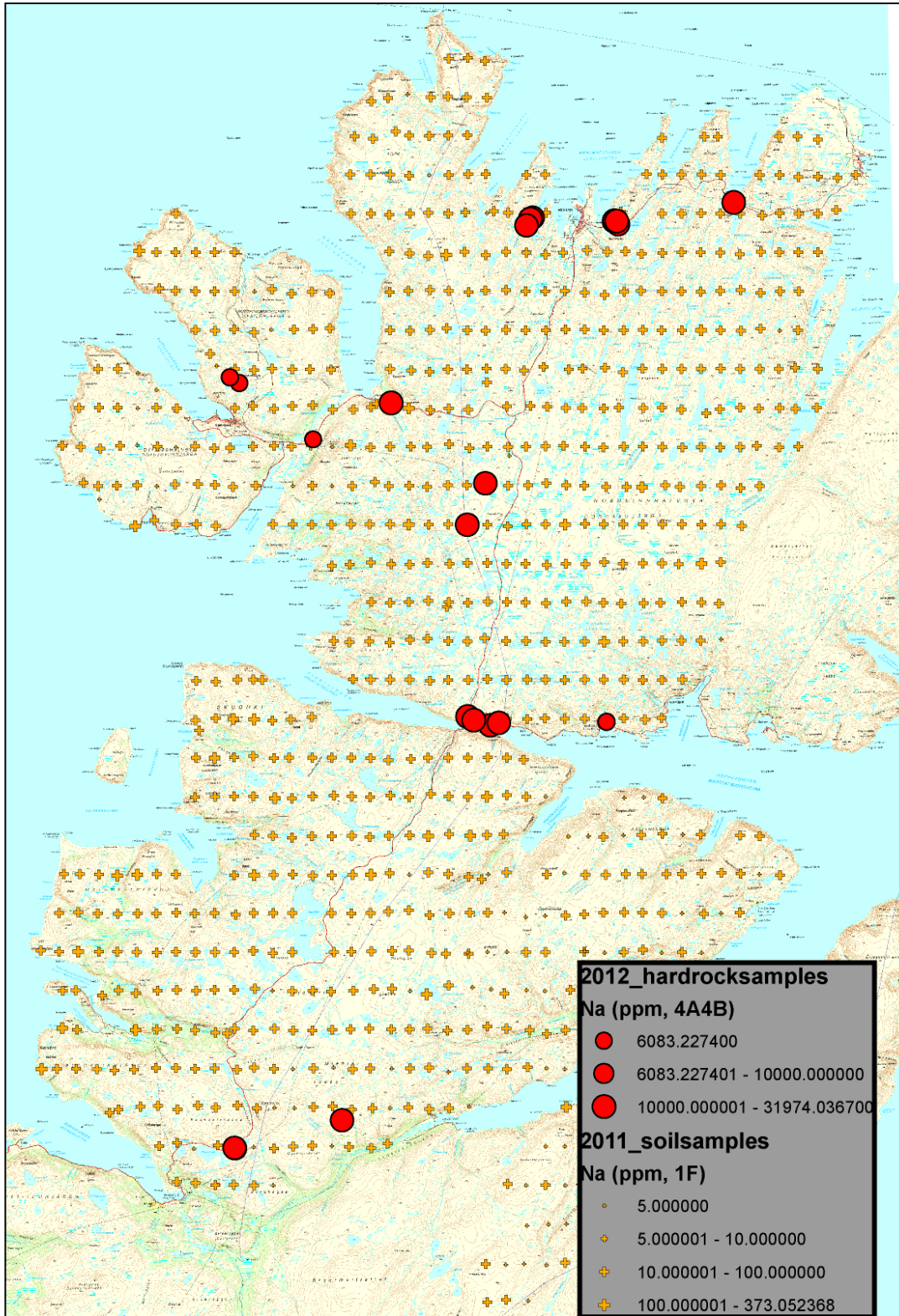


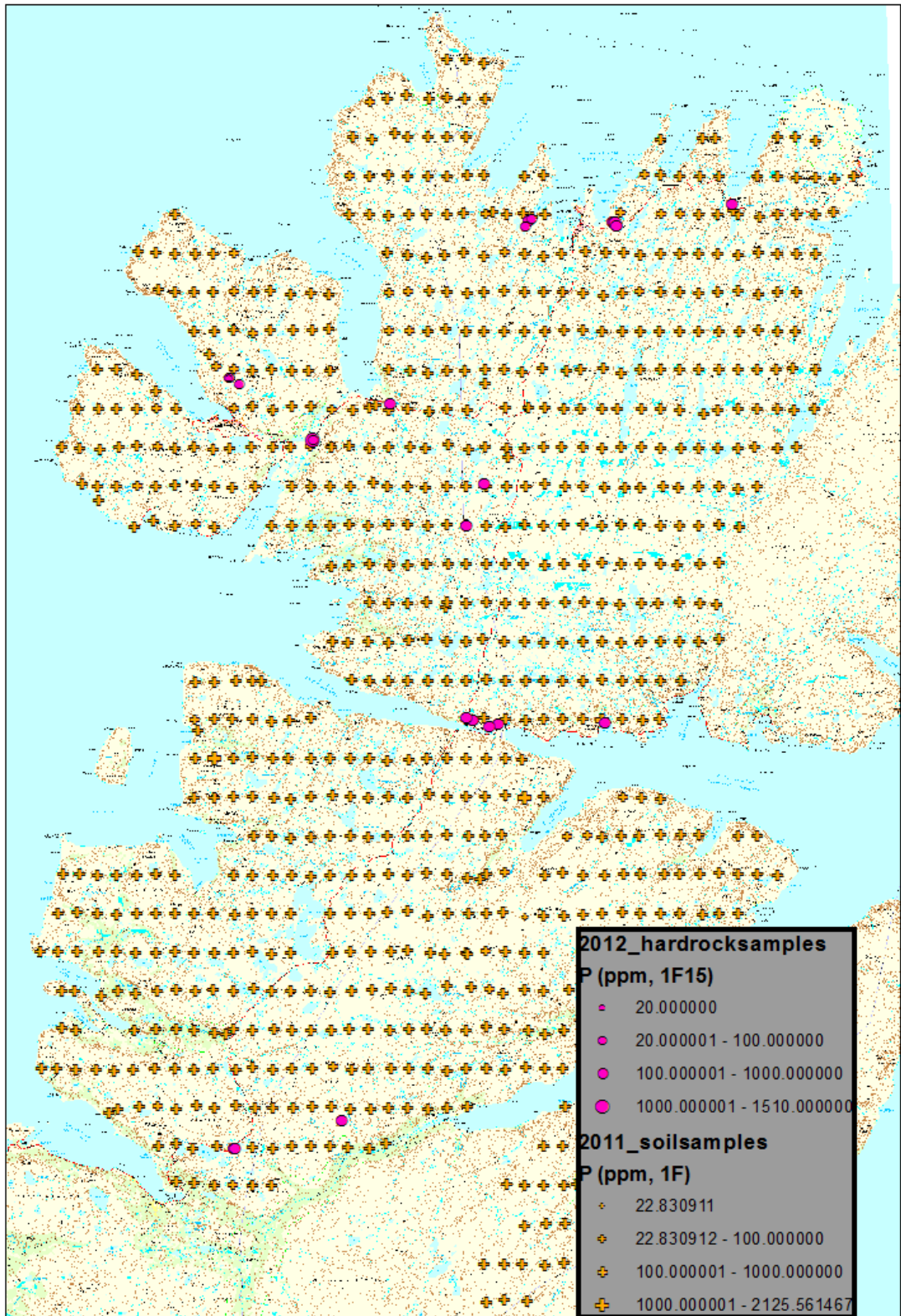


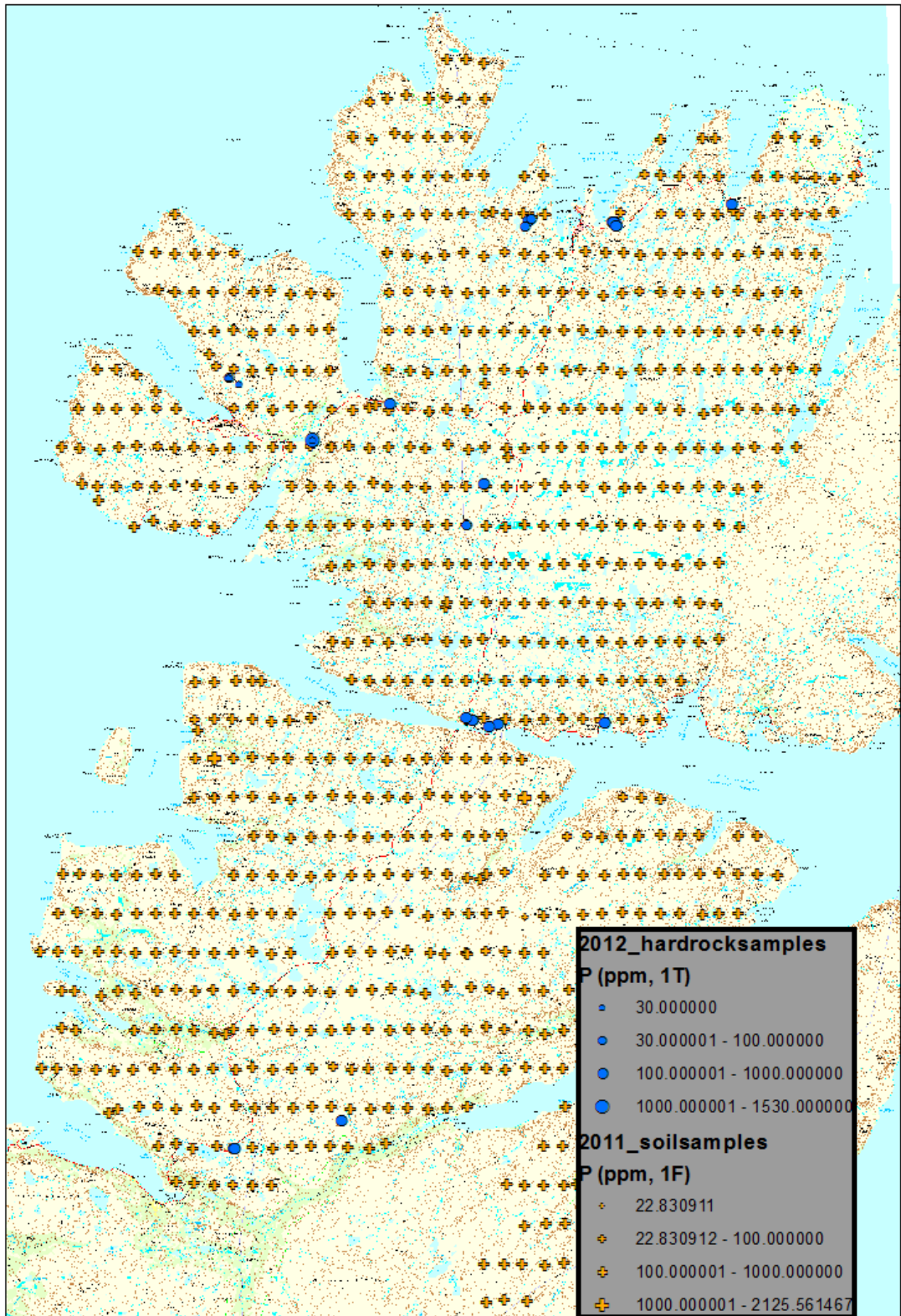












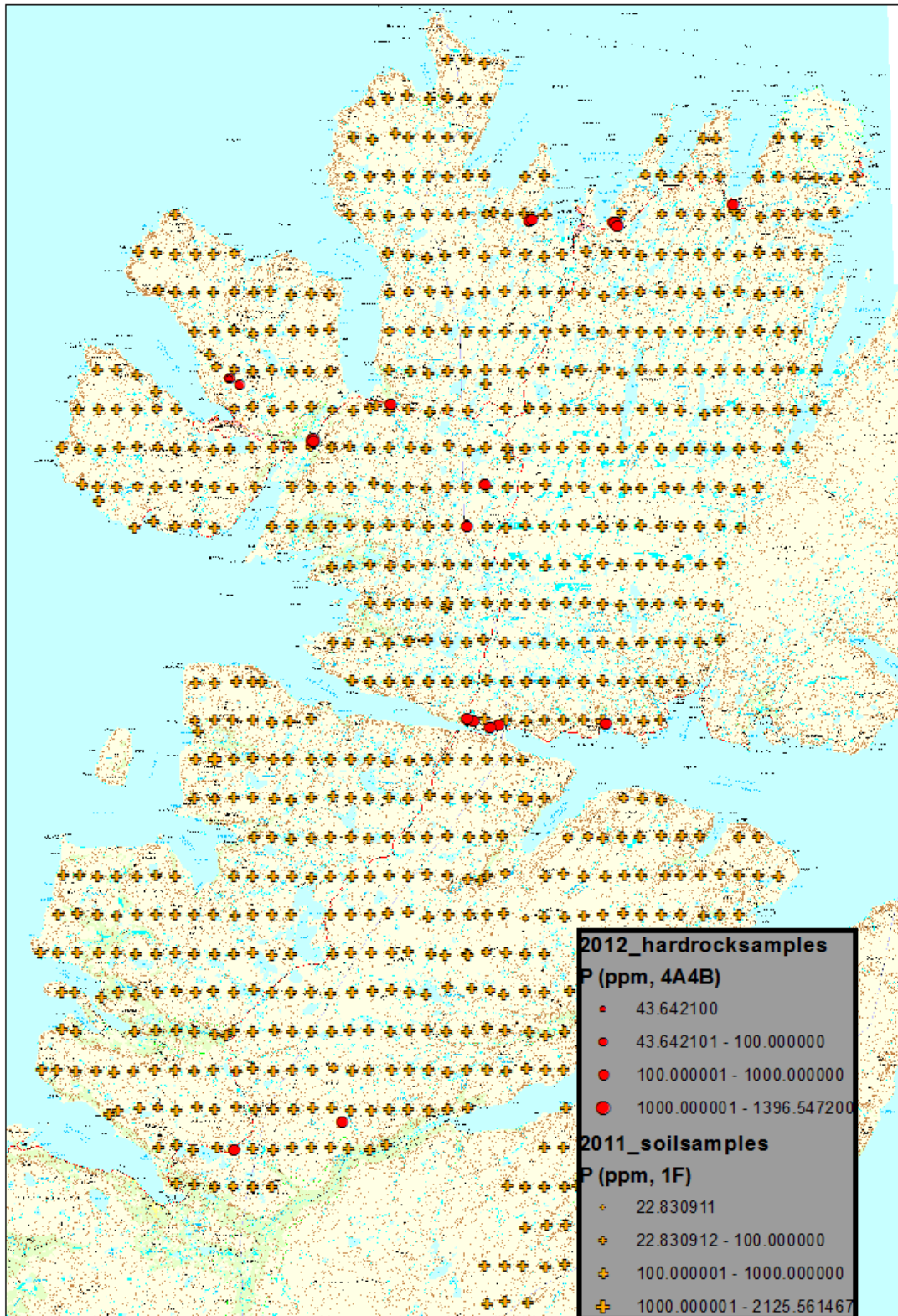


Figure 6: Spatially resolved concentrations of the major elements Al, Ca, Fe, K, Mg, Na and P analysed after AR digestion (pink-filled circles, 1F15), 4-Acid digestion (blue-filled circles, 1T) and Li-borate fusion/decomposition (red-filled circles, 4A4B, see legend). For comparison, the concentrations of the respective elements in the soil samples determined

subsequent to AR digestion (Reimann et al., 2012) are shown as filled orange crosses (1F). Symbol sizes vary with the concentration range as given in the legend.

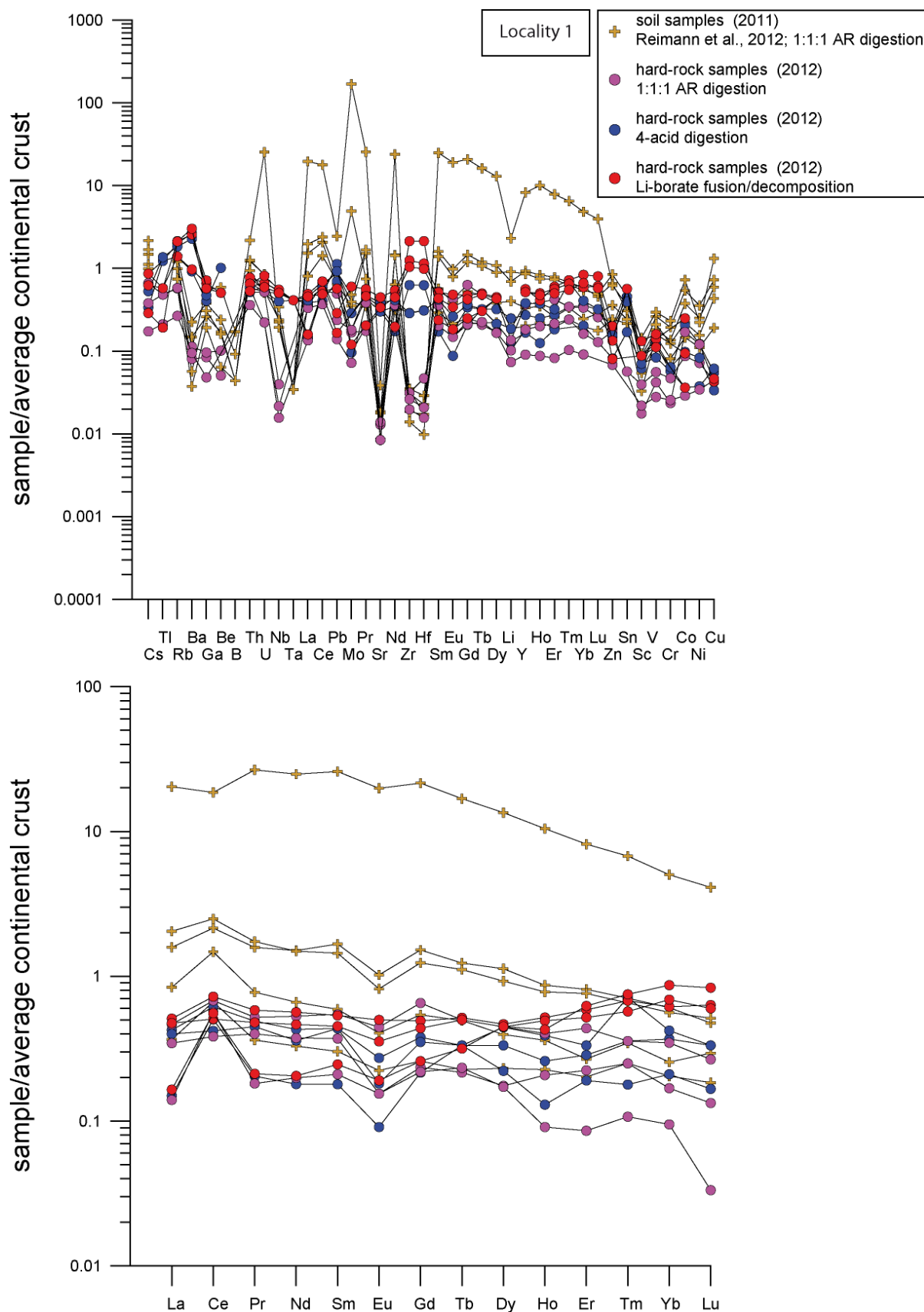
Considering samples prepared by AR digestion, maximum concentrations for Al, Fe, Mg and P were detected in soil samples, whereas the highest concentrations of Ca, K and Na were found in hard-rock samples. Even though the concentrations of the above major elements fall in the same order of magnitude for AR digested hard-rock and soil samples, Al, Mg and Fe are more elevated in the soil samples and compared to the maximum Fe contents found for AR-digested hard rocks, the soil samples display almost a 4-fold enrichment.

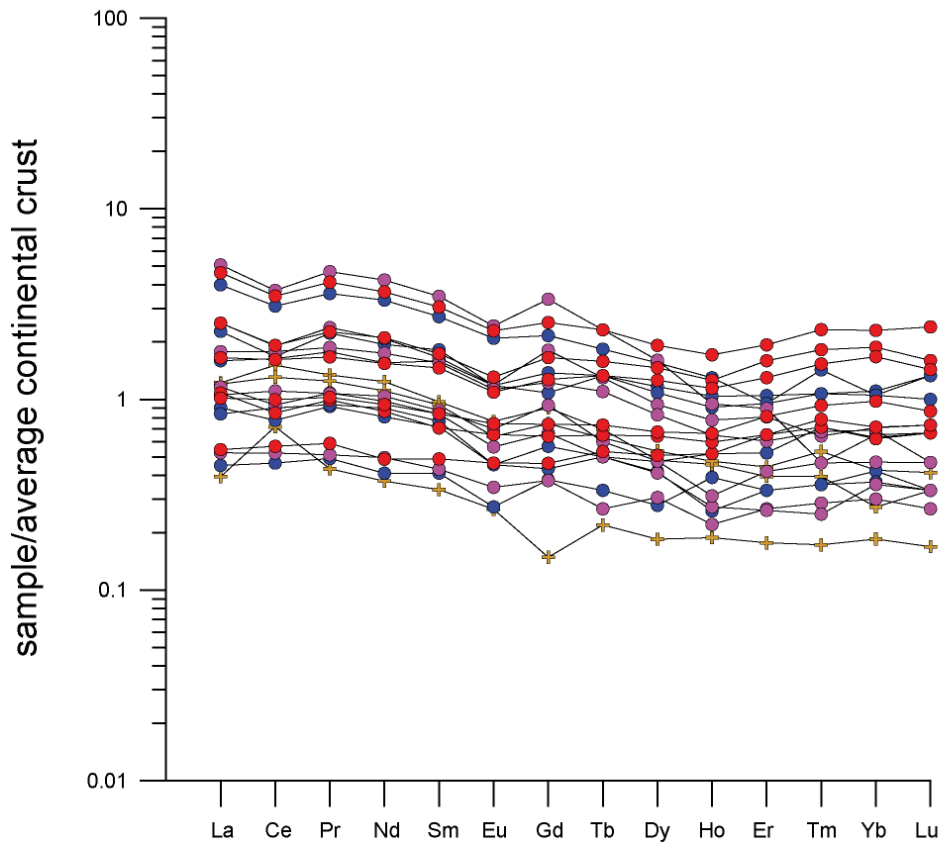
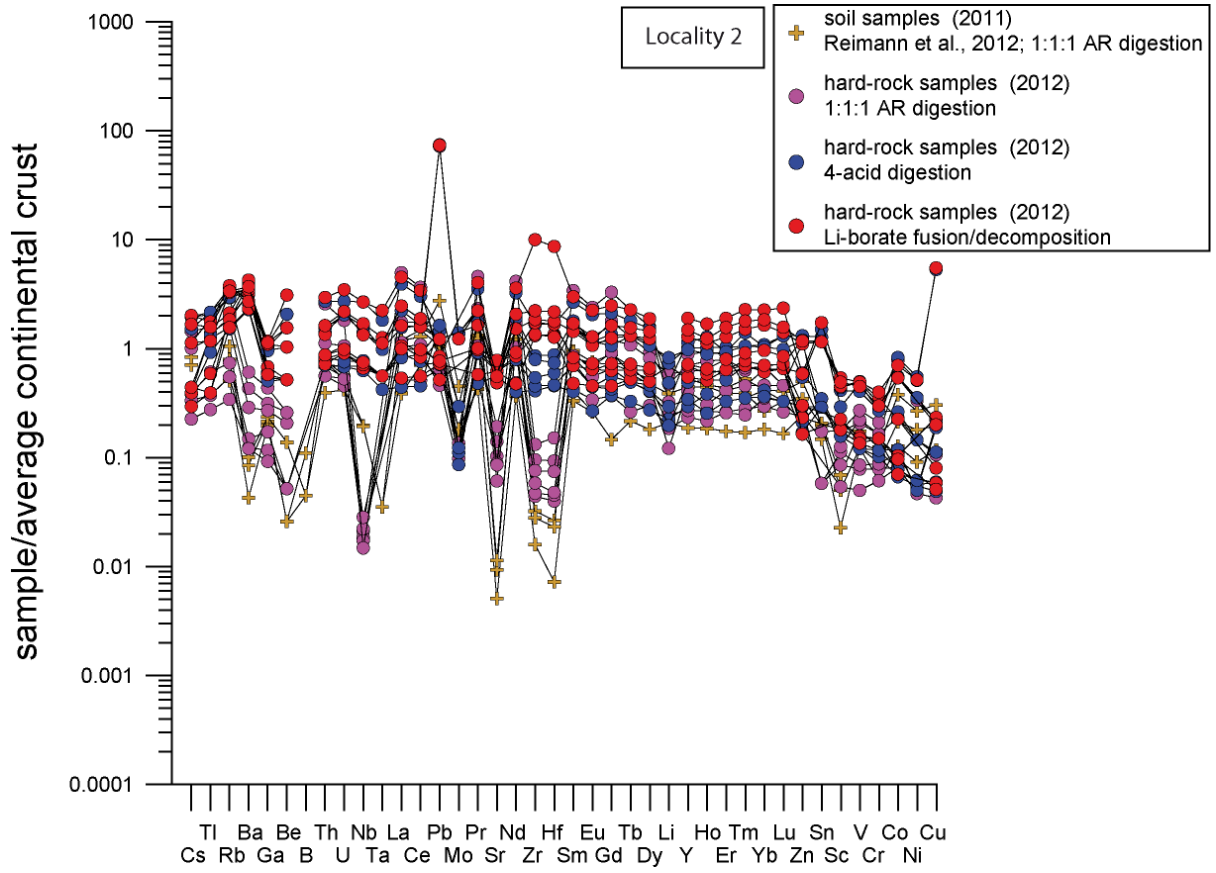
Systematic variations in the hard-rock major element compositions are observed with the sample preparation methods. Contents of Al, Ca, Fe, Mg, K and Na increase for each sample with the sample preparation in the order AR digestion < 4-Acid digestion < Li-borate fusion/digestion. Relative to the contents of Al analysed subsequent to AR digestion, analyses following 4-Acid and Li-borate fusion/digestion reveal up to 4- and 5-fold higher concentrations, respectively. The differences for Ca, Fe and Mg in the hard rocks between the different digestion methods are less pronounced than for Al and concentrations are about 35 % (Ca), 15 % (Fe and Mg) higher in Li-borate fusion/digested samples than for AR digestion prepared samples. Relative to the highest concentrations found for K in AR-digested hard-rock samples, 4-Acid digested and Li-borate fusion/digestion prepared samples are as high as 4-fold enriched. The largest differences were found in the determination of Na, for which 4-Acid digestion and Li-borate fusion/digestion gave results two orders of magnitude higher than for the AR extraction.

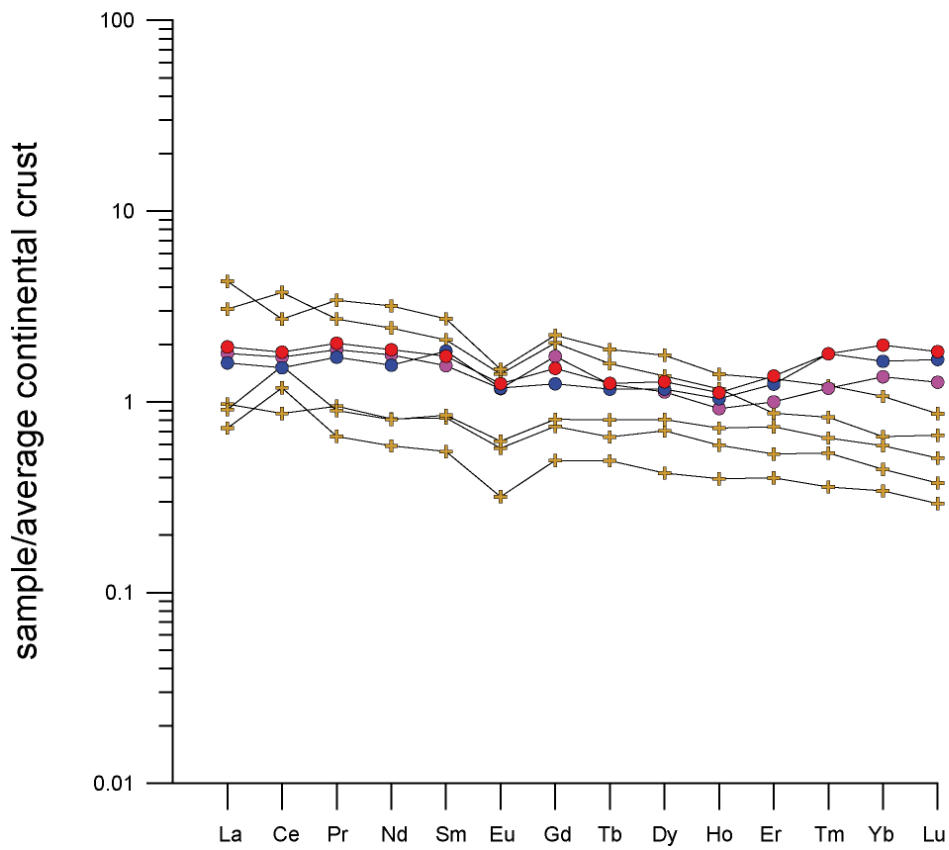
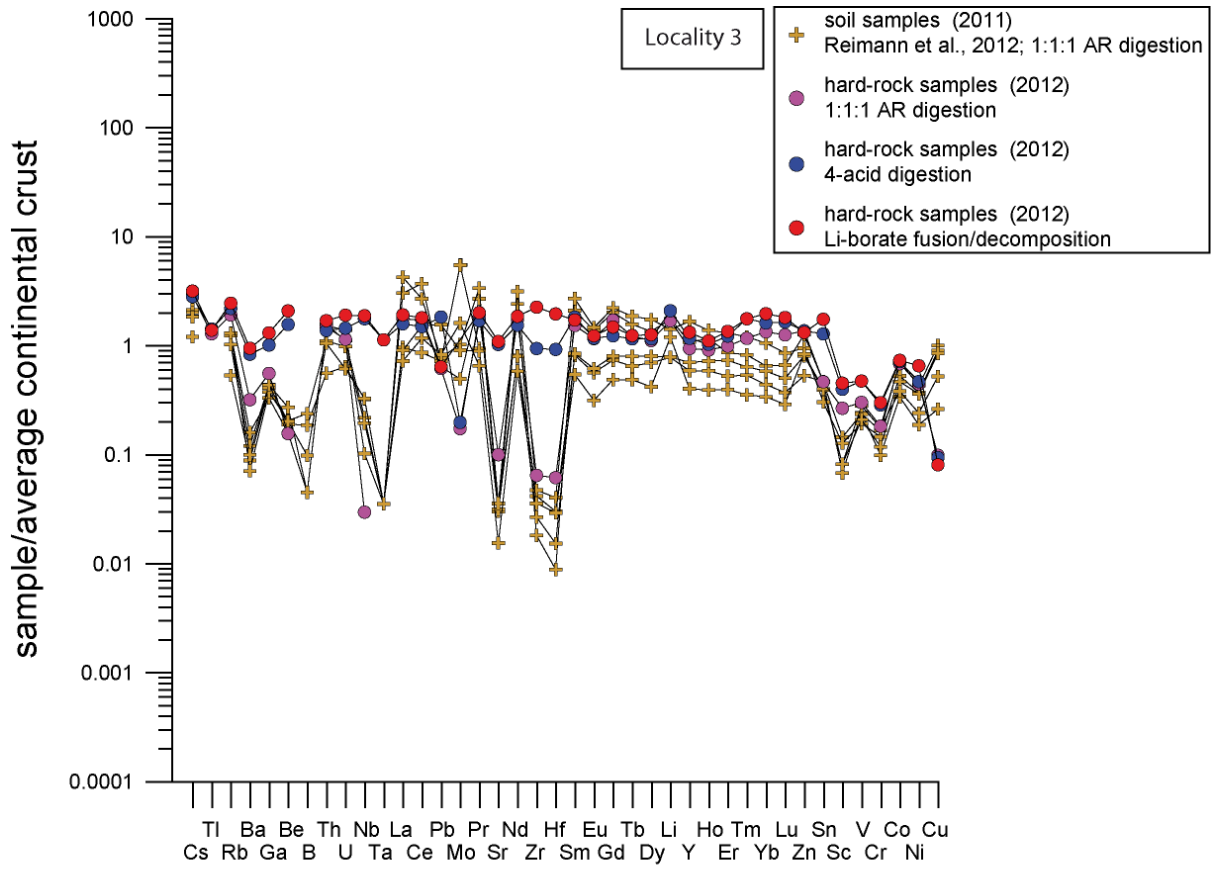
4.2 Trace elements

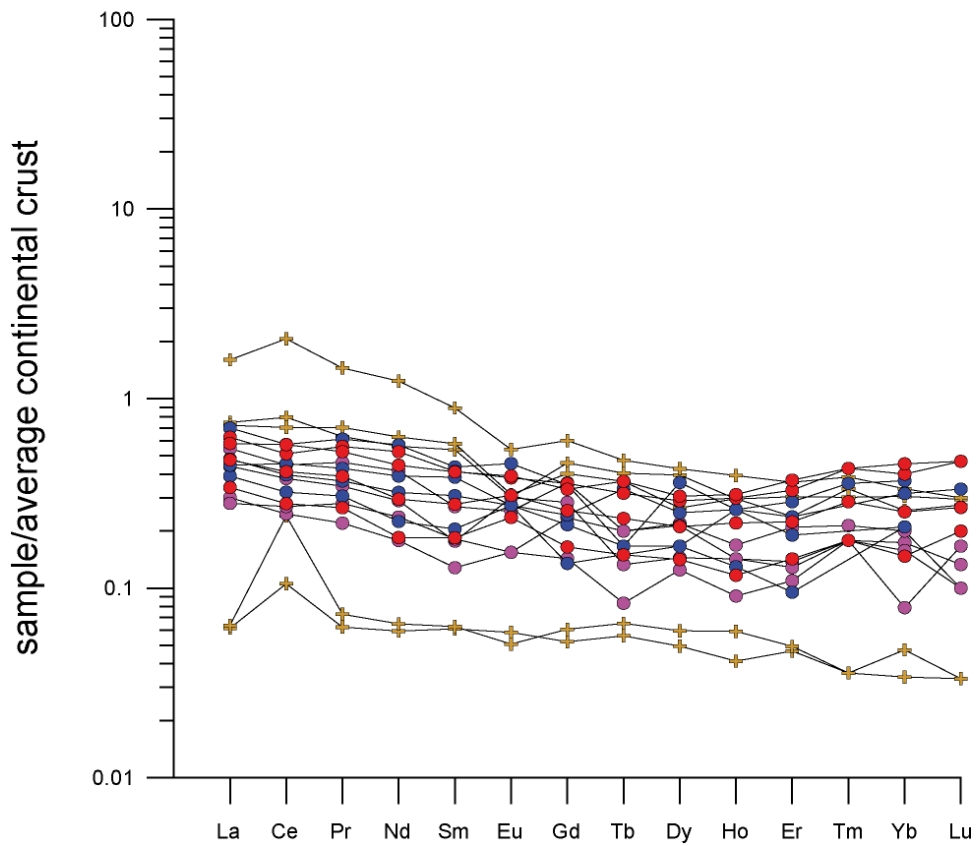
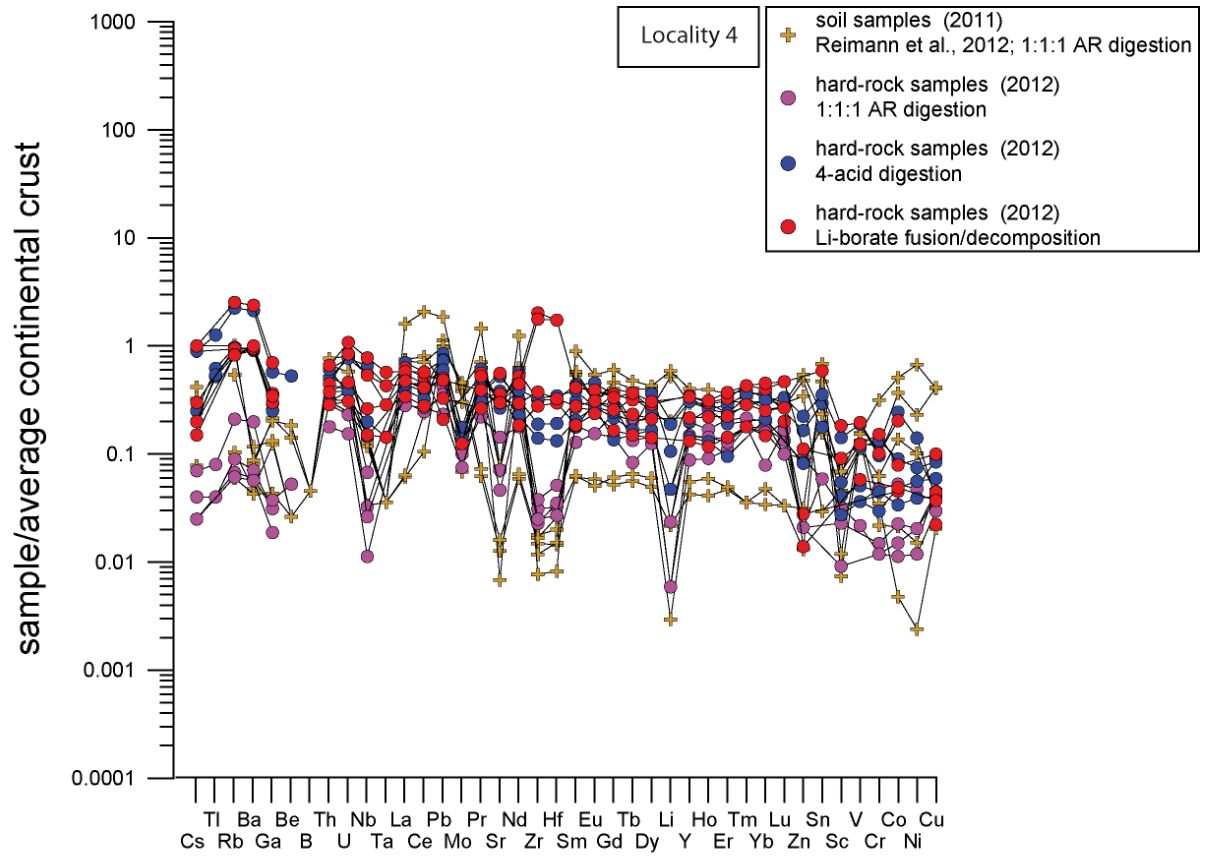
Trace-element variation diagrams shown in Fig. show that most trace elements are similar in terms of concentration in the hard-rock and the soil samples. In each of the variation ('spider') diagrams, the trace-element compositions of samples from the different above-defined localities 1 - 12 are shown. Orange crosses represent the soil sample sites directly adjacent to the hard rocks, while each of the hard-rock samples is shown three times, prepared by AR digestion (pink-filled circles), 4-Acid digestion (blue-filled circles) and Li-borate fusion/decomposition (red-filled circles). The levels of concentration of the trace elements shown mostly agree between hard-rock samples analysed after AR digestion and soil samples (also analysed subsequent to AR digestion), and in some localities the hard rocks show higher degrees of enrichment than the soil samples, whereas in other localities it is vice versa. Most trace elements range between 5-fold enrichment and 100-fold depletion relative to average continental crust in hard-rock samples analysed subsequent to AR digestion. Trace elements in soil samples spatially related to the hard rocks show a wider spread and vary between 10-fold enrichment (one single sample shows even 30-fold enrichment of some of the REE, and 110-fold enrichment of Mo) and 1000-fold depletion. Negative spikes, i.e. lower concentrations than the preceding and successive elements, are found for Ba, B, Sr, Nb and Ta, as well as for Zr and Hf in both hard-rock and soil samples. The LREE are more enriched than the HREE, resulting in a slightly dipping REE pattern. A weak Eu anomaly is observed

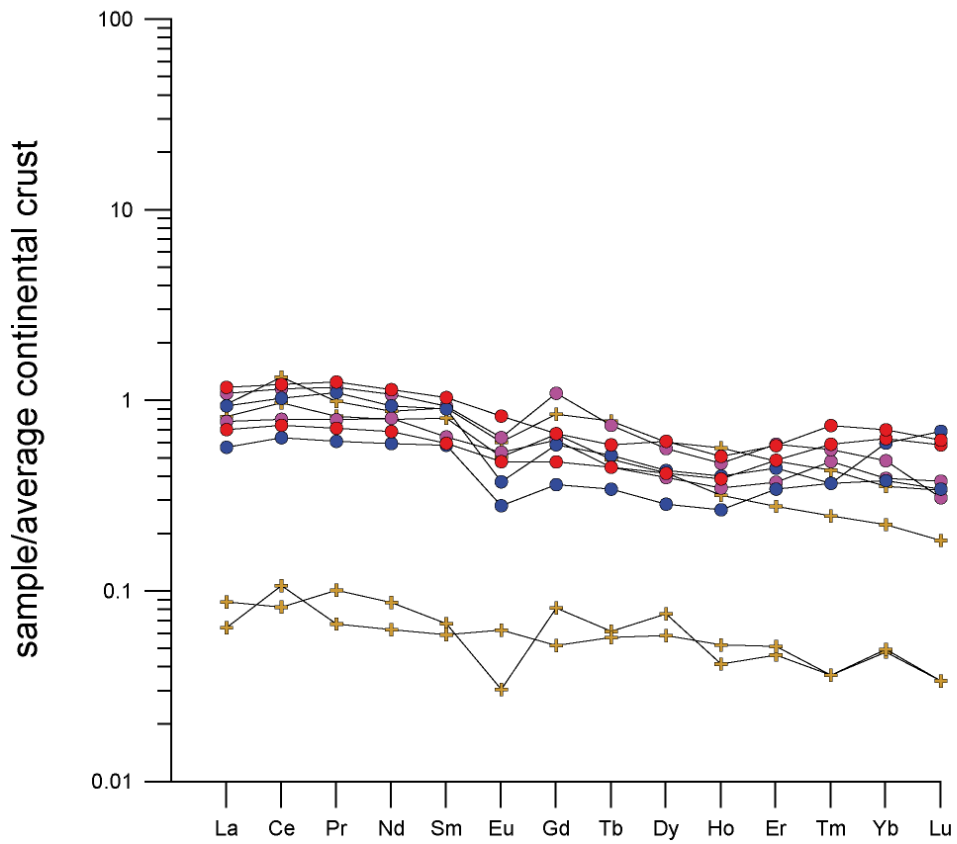
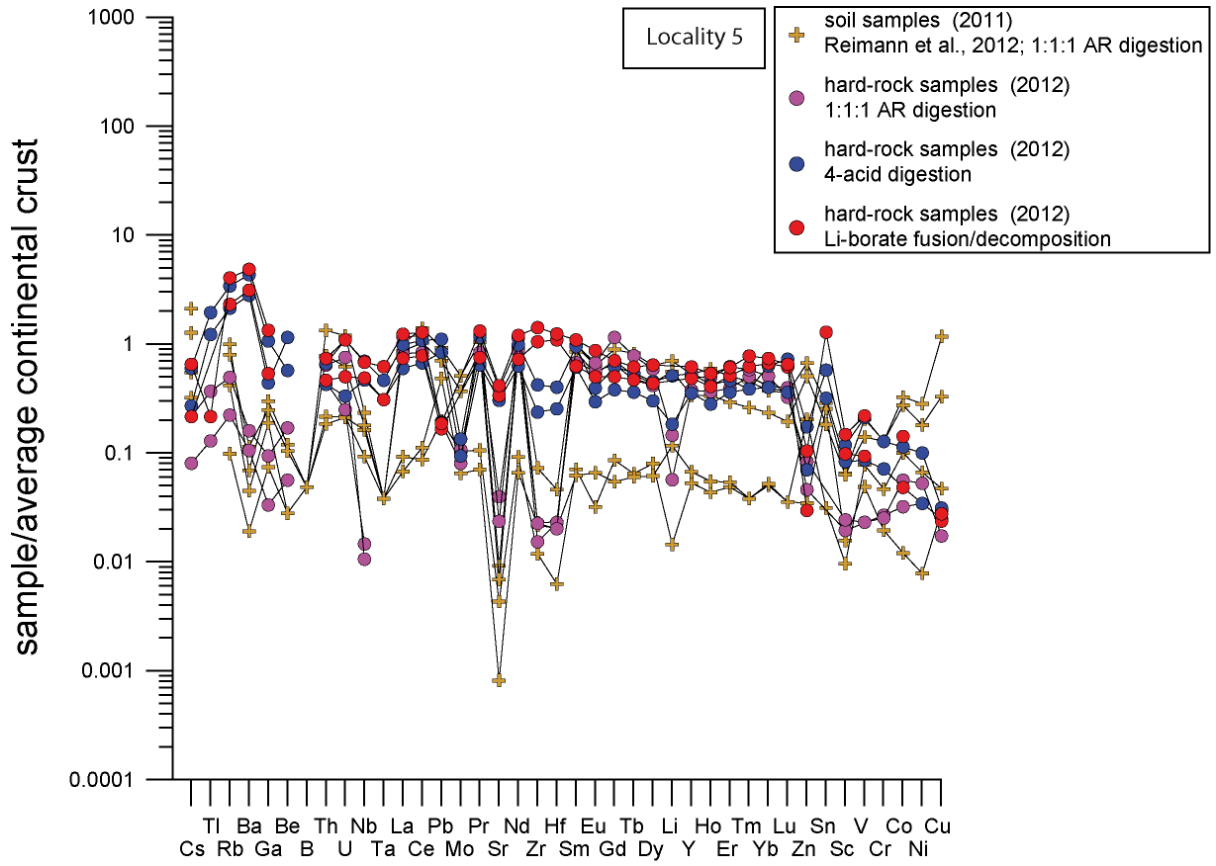
in both hard-rock and soil samples, while Ce anomalies are slightly positive in most soil samples and slightly negative or, more rarely, positive or absent in the hard rocks.

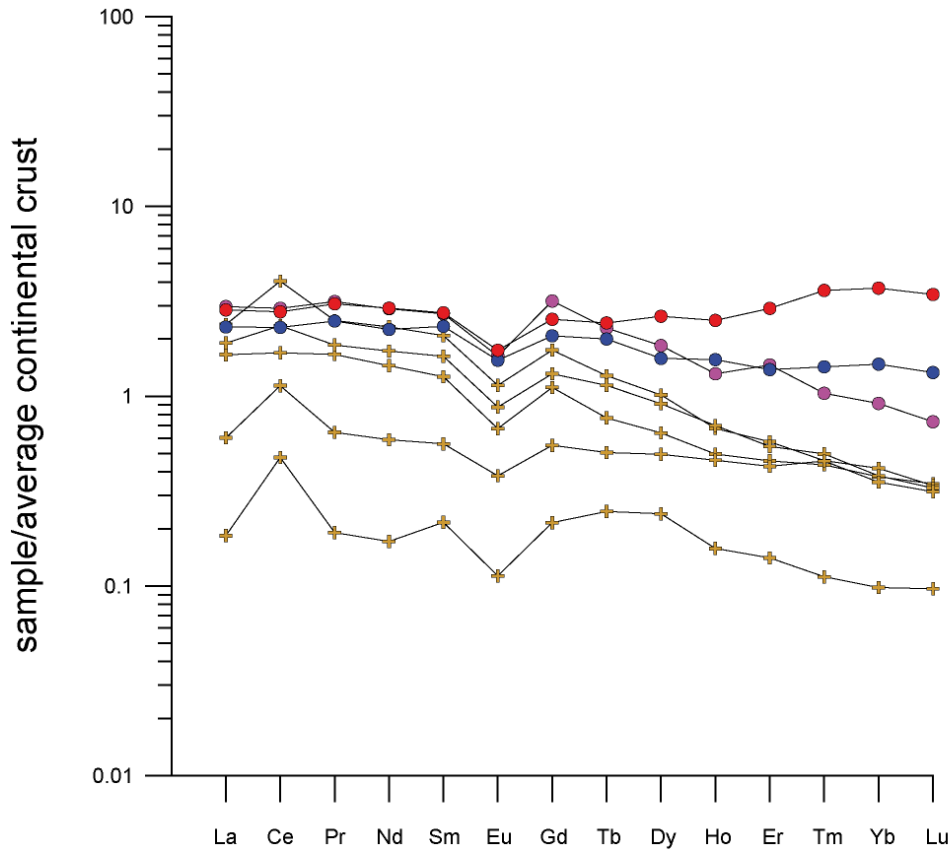
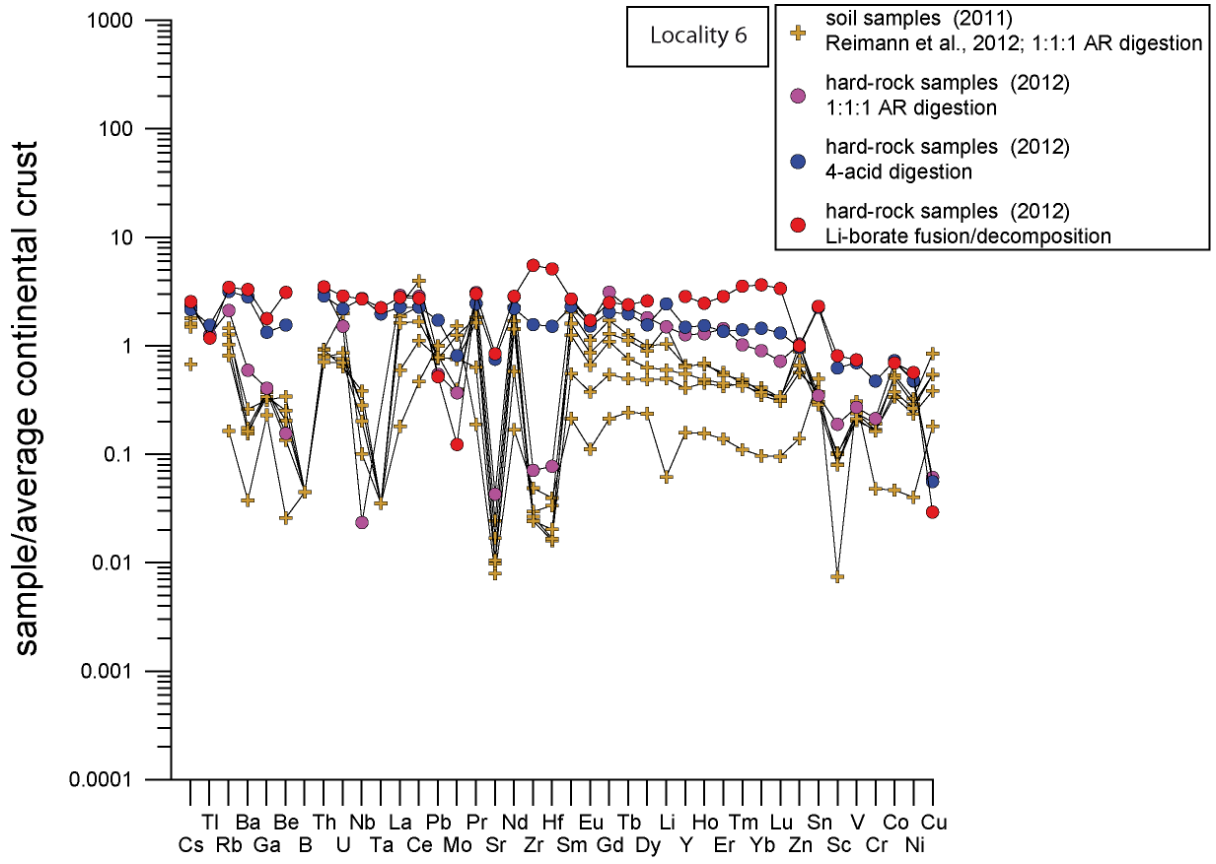


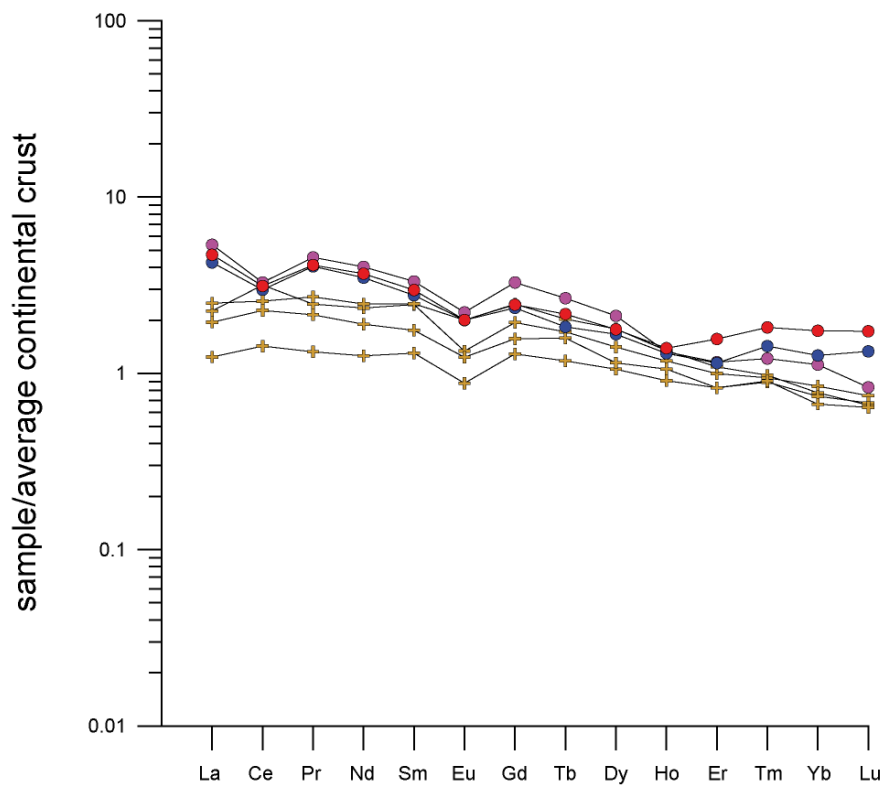
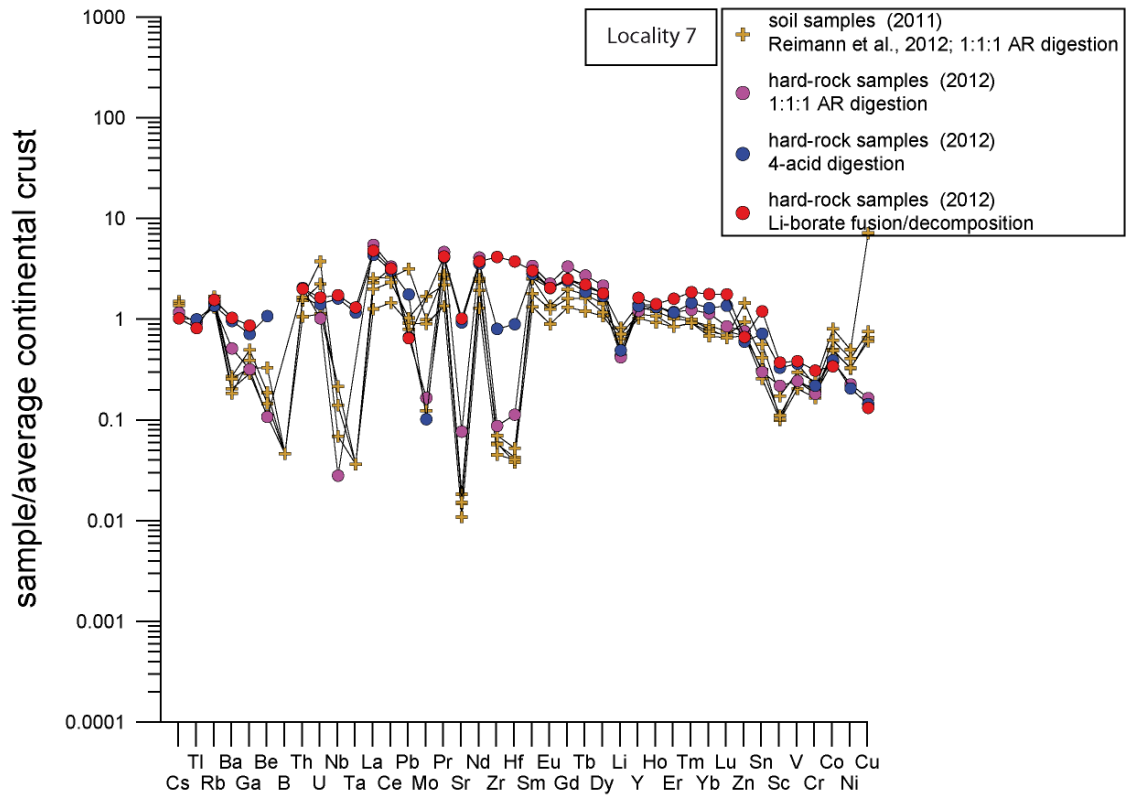


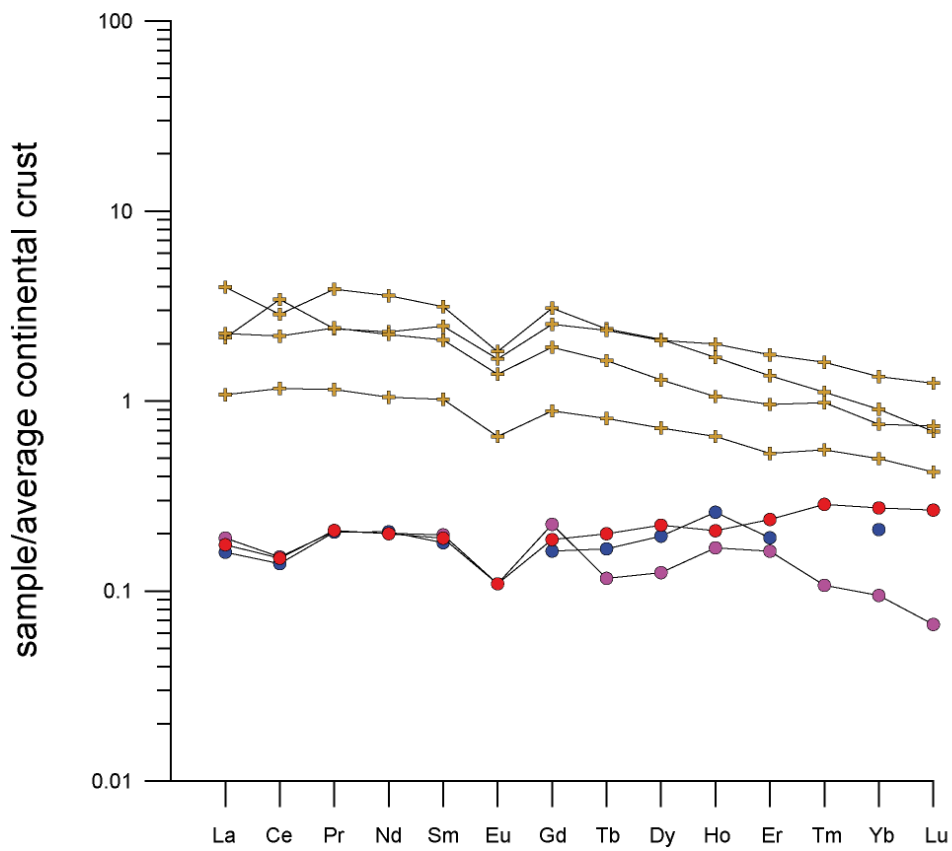
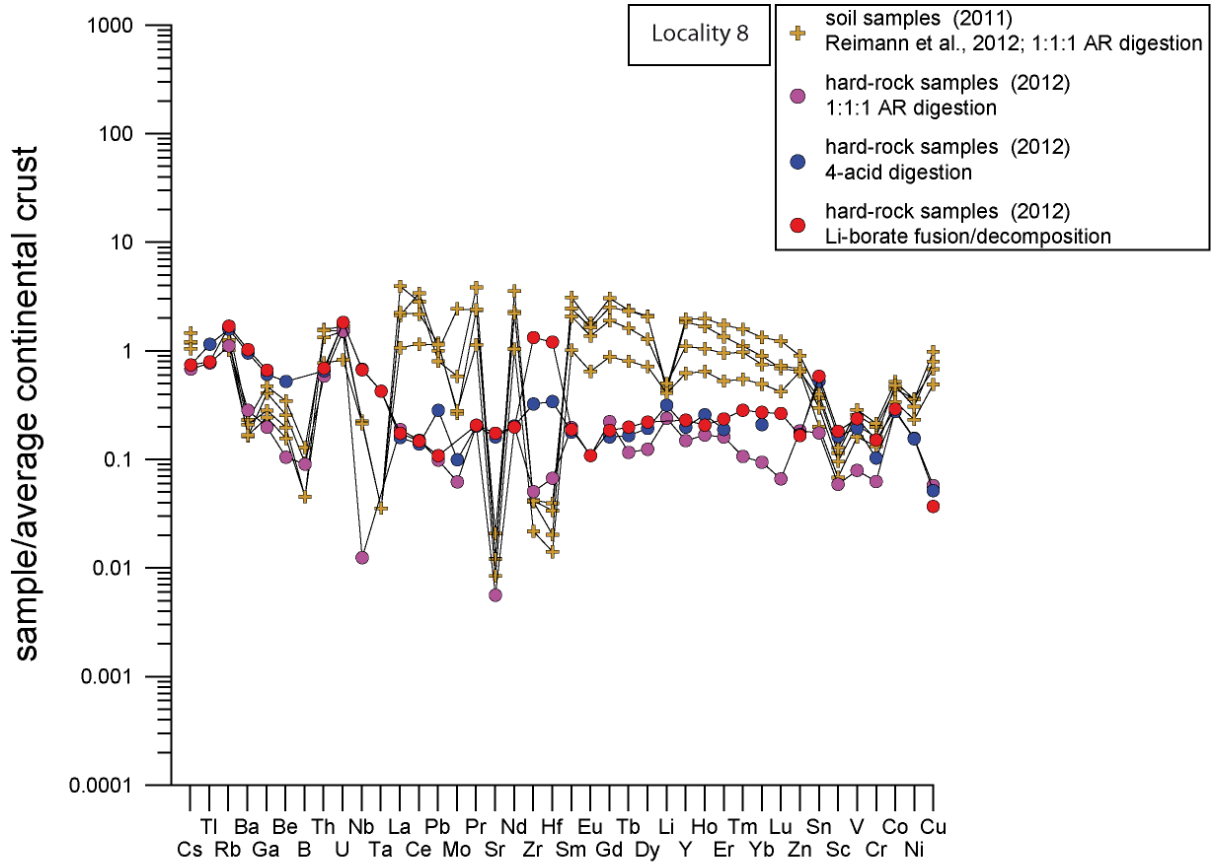


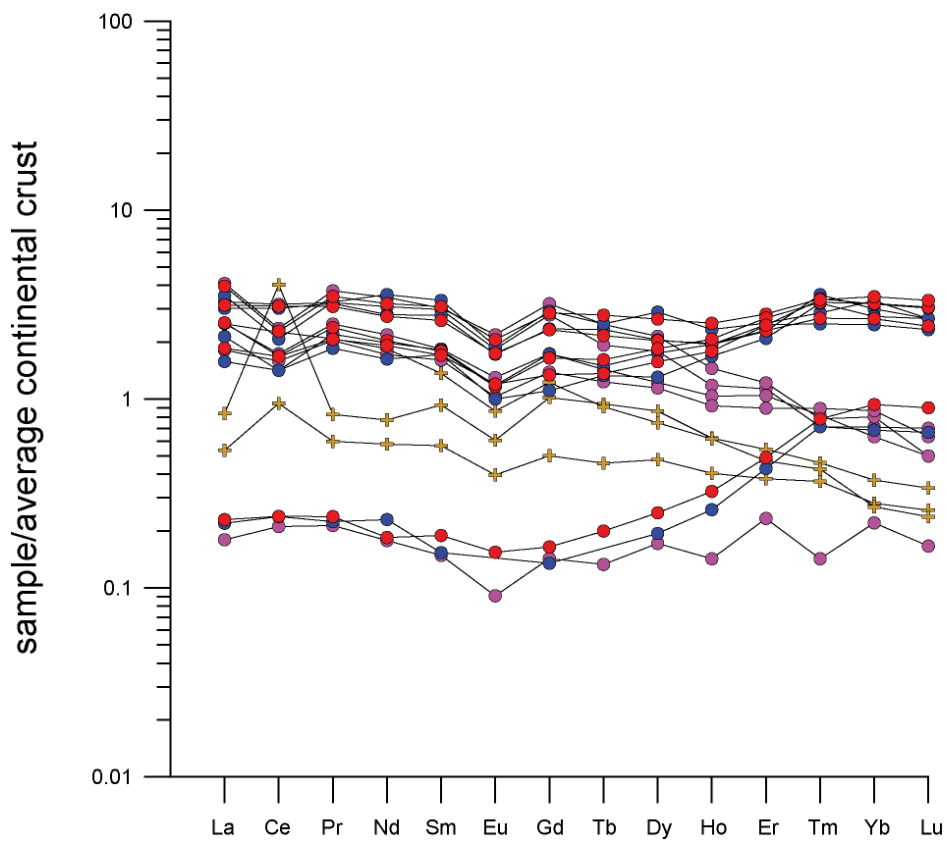
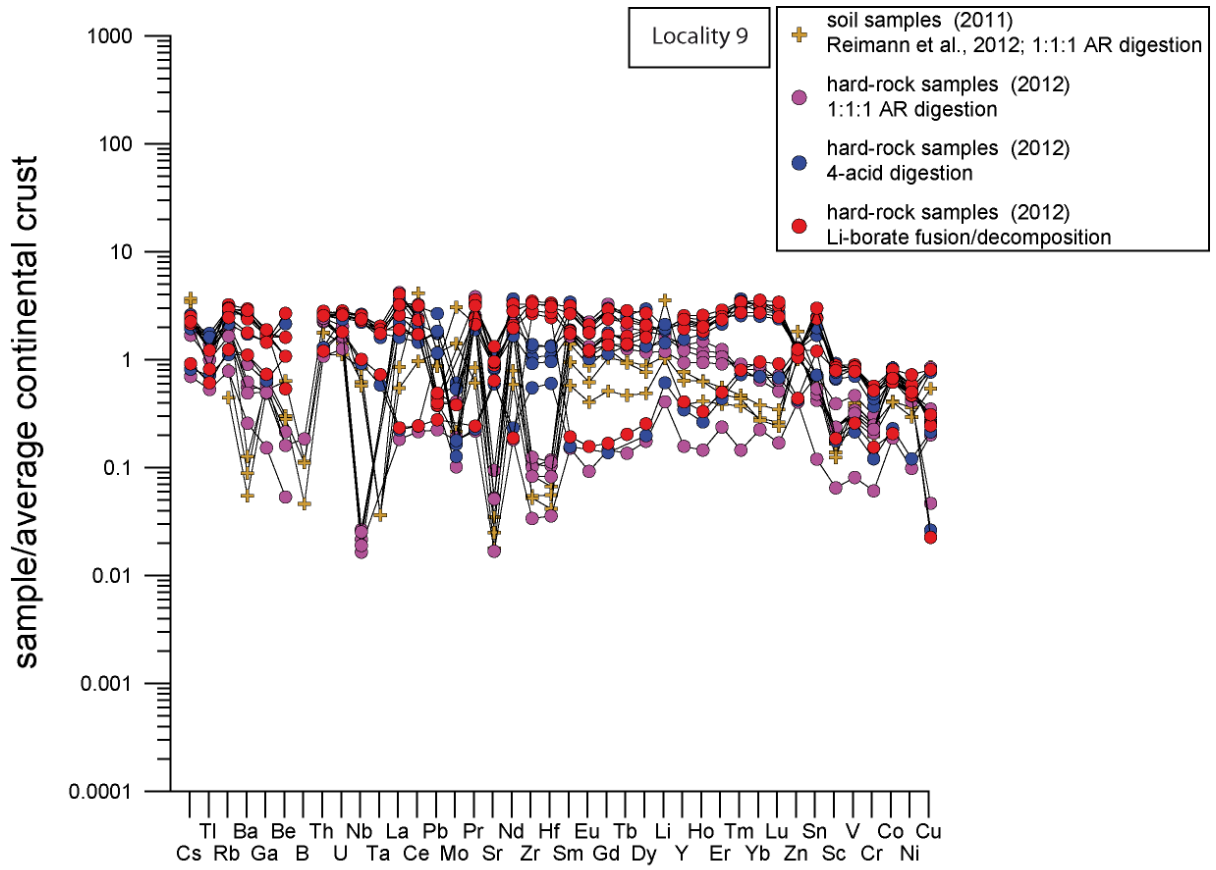


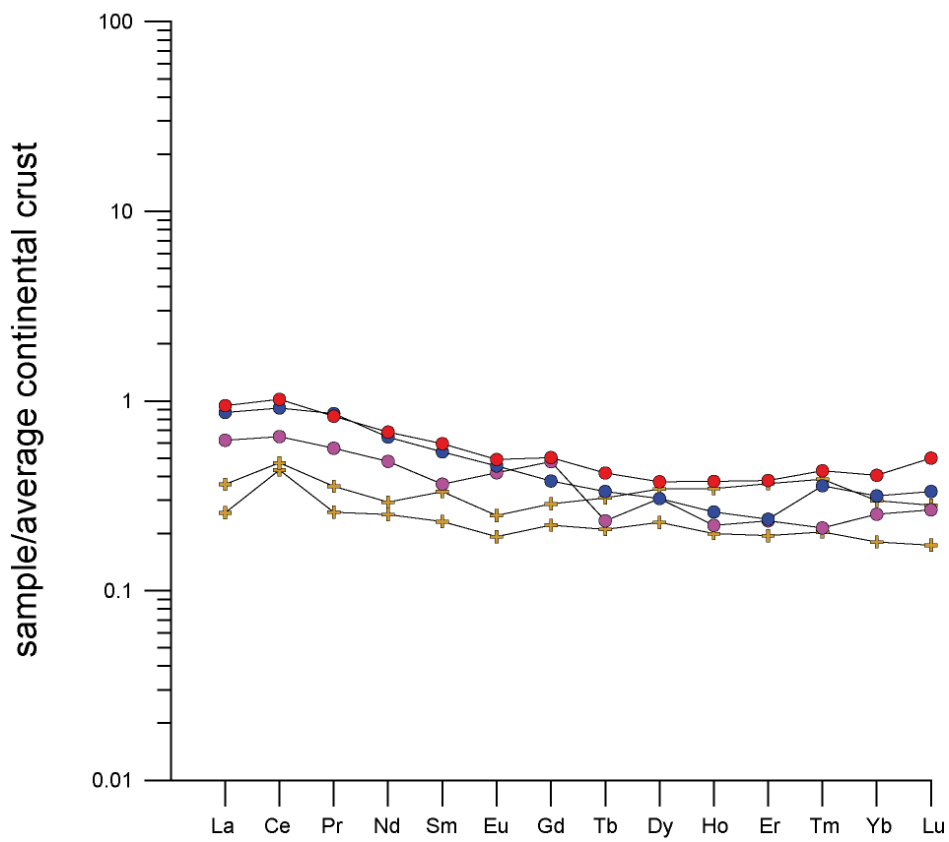
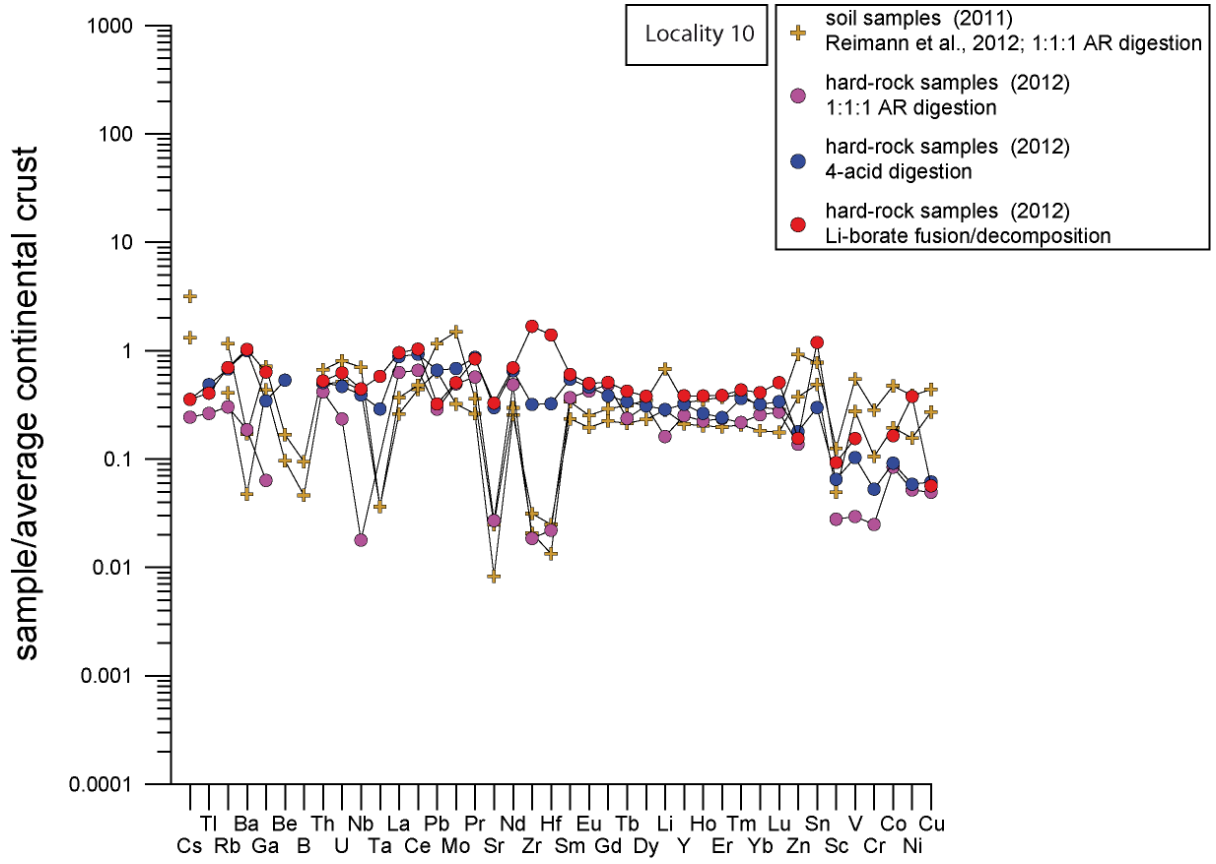


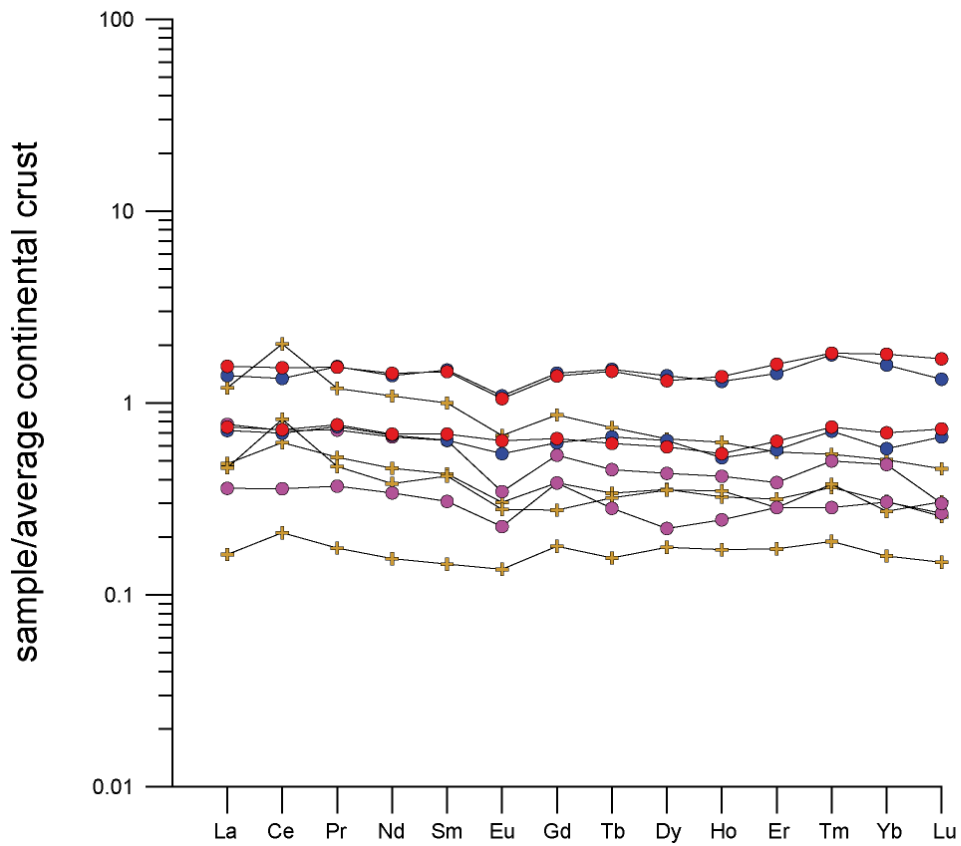
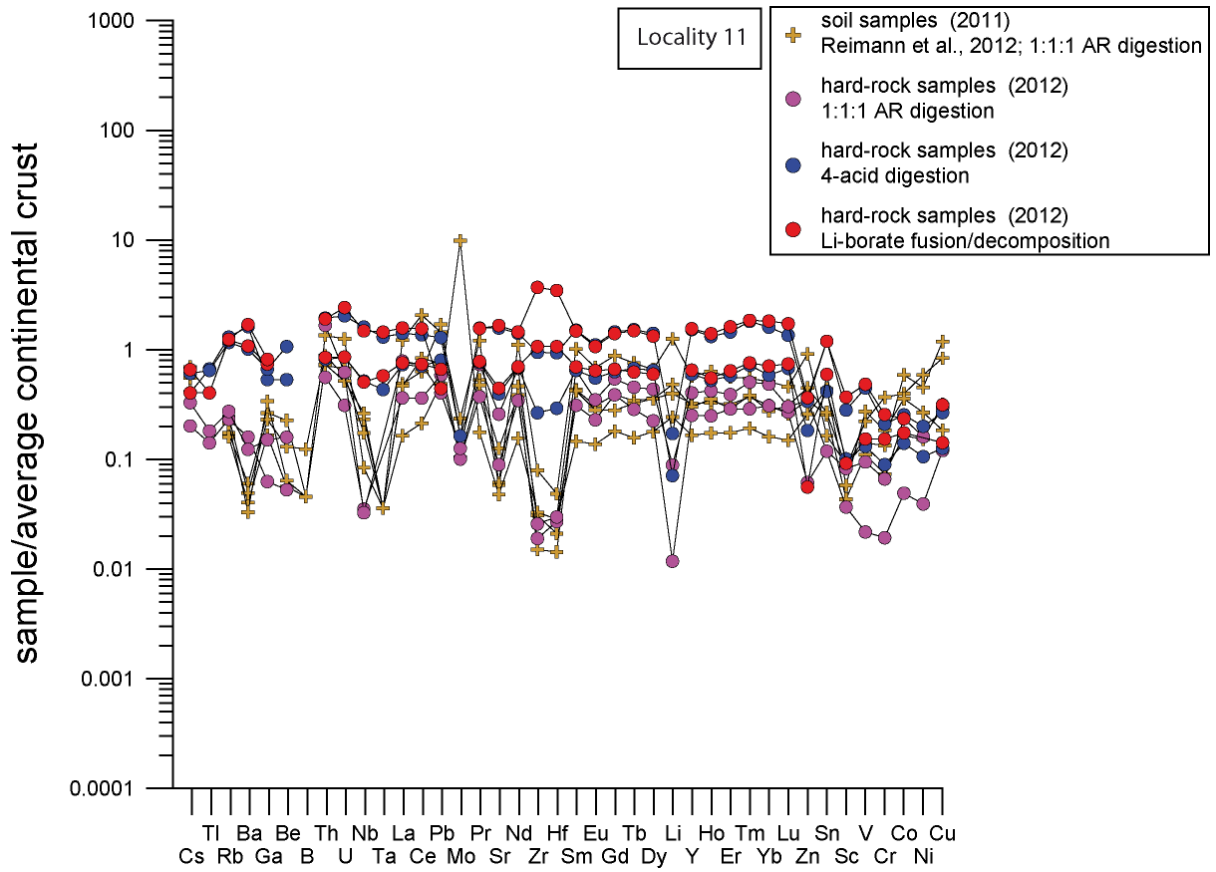












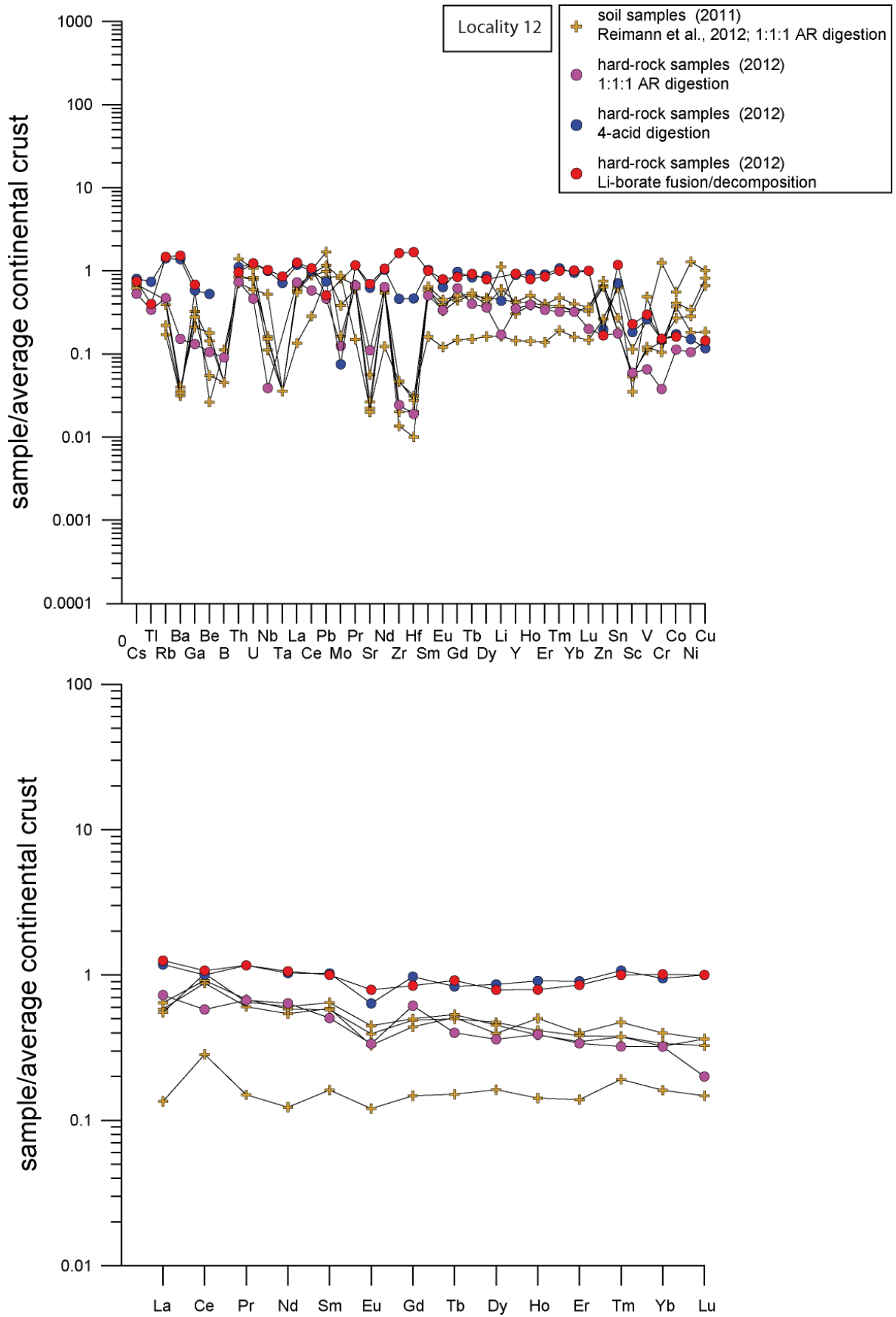


Figure 7: Trace-element variation diagrams for the 12 localities defined in Fig. 1. Average continental crust concentration values are those from Gao and Rudnick (2003).

Hard-rock samples analysed subsequent to the more potent 4-Acid and Li-borate fusion/decomposition digestions resulted in indistinguishable results for the LREE, but revealed systematically higher concentrations for the HREE with the highest concentrations invariably observed in samples treated with Li-borate fusion/digestion. Thus, the REE patterns change from slightly dipping (AR digestion) to flat and for some samples even inclining (4-Acid digestion and Li-borate fusion/decomposition). Total REE contents determined after AR leaching, 4-Acid digestion and Li-borate fusion/decomposition range from 22 to 429, 19-379 and 25 to 371 ppm, respectively. For Zr and Hf, the Li-borate fusion/digestion approach results in the determination of distinctly higher concentrations, leading to positive anomalies. Depending on the sample preparation technique, Zr and Hf vary by up to three orders of magnitude in concentration and were found to be present in the ppm-level in AR digested samples and in the 100- to 1000 ppm range in the samples prepared by Li-borate fusion/decomposition.

5. Discussion

As noted earlier, comparability with respect to the major- and trace-element compositions between the hard-rock and soil sample sets is restricted for the following reasons: (i) hard-rock and soil samples have formed through different processes and are not the same category of samples, i.e. Neoproterozoic metasedimentary rocks are compared with respect to their compositions to their weathering products; (ii) the sample sets are of different size and the major-element composition of a total of 28 hard rock samples is compared to 808 soil samples; (iii) the soil samples were taken in a pre-defined grid whereas the hard-rock samples were mostly taken from outcropping bedrock in approximate positions spatially related to element anomalies found in the soil samples. However, bedrock and soil samples that are spatially related were compared and the mineralogical and compositional comparison between hard-rock and soil samples combined with field observations sheds light on the question as to whether in-situ weathering is an important process in the working area. Furthermore, the present study has compared different whole-rock preparation methods and, taking into account the condition of the REE minerals in the bedrock, draws conclusions on the enhanced REE contents found in the soil samples reported by Reimann et al. (2012).

5.1 Weathering

Comparable concentration levels are to be expected if the major mineral(s) incorporating the respective element is present in equal proportions in both the hard rock and the overlying soil. As the results from the AR digested hard rock and spatially related soil samples are in the same range for most elements, this appears to be the case on the Nordkinn Peninsula. Thus, in-situ weathering is likely to have been an operative process. Similar trace-element patterns, e.g. of the REE, and similar concentration levels for most elements, indicate an in-situ formation of the soil layers and rule out major transport processes. The conclusion that most of the material forming the soil horizon is a product of in-situ weathering is in accordance with the mineralogical investigation of the soil material, which was found to be similar to the

hard rocks in terms of mineralogy. Furthermore, field observations showed that rocks found in the blockfields are lithologically identical to the bedrock. Disagreement with respect to the mineralogical composition is seen only in the higher relative frequency of biotite and magnetite in soil samples, which is possibly a consequence of the higher contents of K, Al, Fe and Mg in the soil samples. As the degree of enrichment in the soil relative to bedrock is higher for Fe than for K, Mg and Al, the soil is possibly also rich in a second Fe phase, which is most likely magnetite based on SEM investigations.

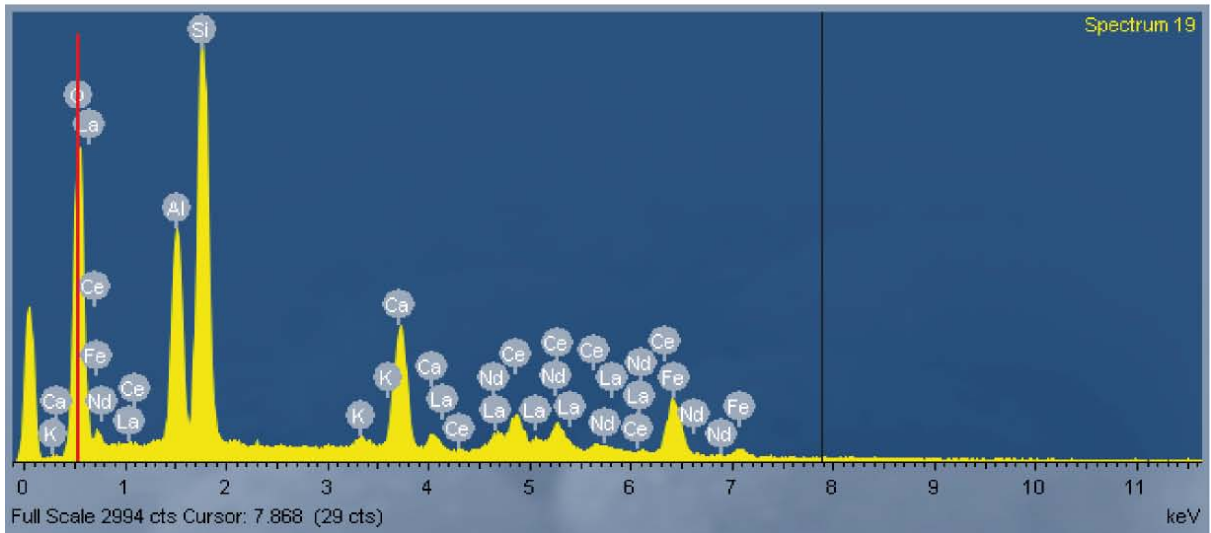
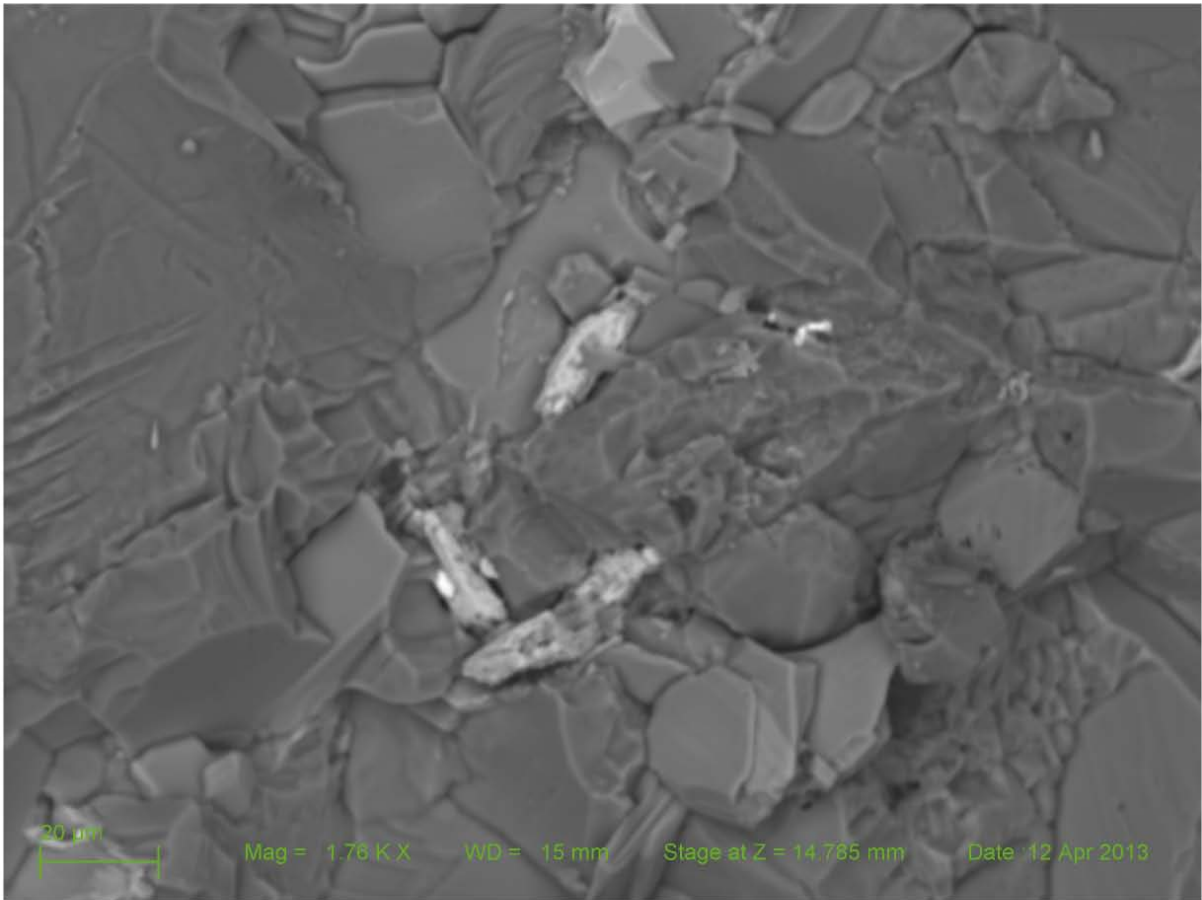
In addition to the variation observed with respect to major-element composition, a positive Ce anomaly is recorded in most soil samples. For rare bedrock samples characterised by the absence of a positive Ce anomaly, the alteration and the variable degree of decomposition of the primary REE minerals probably took place prior to weathering and was possibly caused by (metamorphic?) fluids that had a low oxidation potential. This interpretation is based on the fact that fluids with a potential to alter Ce from the three- to the four-valent oxidation state acting mostly as meteoric, superficial fluids are responsible for Ce anomalies in minerals that underwent interaction with such fluids or precipitated from these (e.g. Mongelli, 1997; Goeb et al., 2011). The majority of bedrock samples, however, show slightly negative Ce anomalies, possibly indicating an alteration (weathering?) process and it appears that the positive Ce anomaly displayed by soil samples is outbalanced by negative Ce anomalies in the bedrock. The process linking the opposed Ce anomalies is most likely weathering: while a superficial, oxidising fluid altered the REE minerals in the bedrock, causing a negative Ce anomaly, the REE minerals forming the overlying soil are characterised by positive Ce anomalies. The fact that the REE concentration level and REE distribution (i.e. the shape of the REE patterns) does not change from bedrock to soil provides further evidence that the outcropping bedrock underwent in-situ weathering with or without minor removal or enrichment of the REE.

5.2 REE mineralogy and economic potential

REE mineralogy

The REE minerals have been identified by means of qualitative EDS and the spectra obtained do not allow for a definite identification of the various minerals. However, LREE silicates predominate over LREE carbonates and phosphates in all samples investigated and compositionally different REE minerals may be texturally associated (cf. Fig. 4h). Back-scatter electron images and point spectra of slightly and strongly altered REE phases are shown in Figs. 8a and b, respectively. Both spectra (and other spectra not presented here) are compatible with and therefore possibly point to allanite, a REE-incorporating epidote-group mineral with the formula $A_2M_3Si_3O_{11}(O,F)(OH)$ with $A = Ca, Sr, Pb^{2+}, Mn^{2+}, Th, REE^{3+}, U$ and $M = Al, Fe^{3+}, Fe^{2+}, Mn^{3+}, Mn^{2+}, Mg, Cr^{3+},$ and V^{3+} and a density ranging from 3.5 to 4.2. (Deer et al., 1986; Giere and Sorensen, 2004). Allanite forms by coupled substitution of Ca^{2+}, Fe^{3+} and/or Al^{3+} by REE^{3+} and Fe^{2+} from epidote and clinozoisite. Some authors have reported REE-bearing epidote-group minerals to be locally important constituents of heavy-mineral layers in clastic sediments such as sandstones (e. g. Sevastjanova et al., 2012; Morton, 1991).

a



b

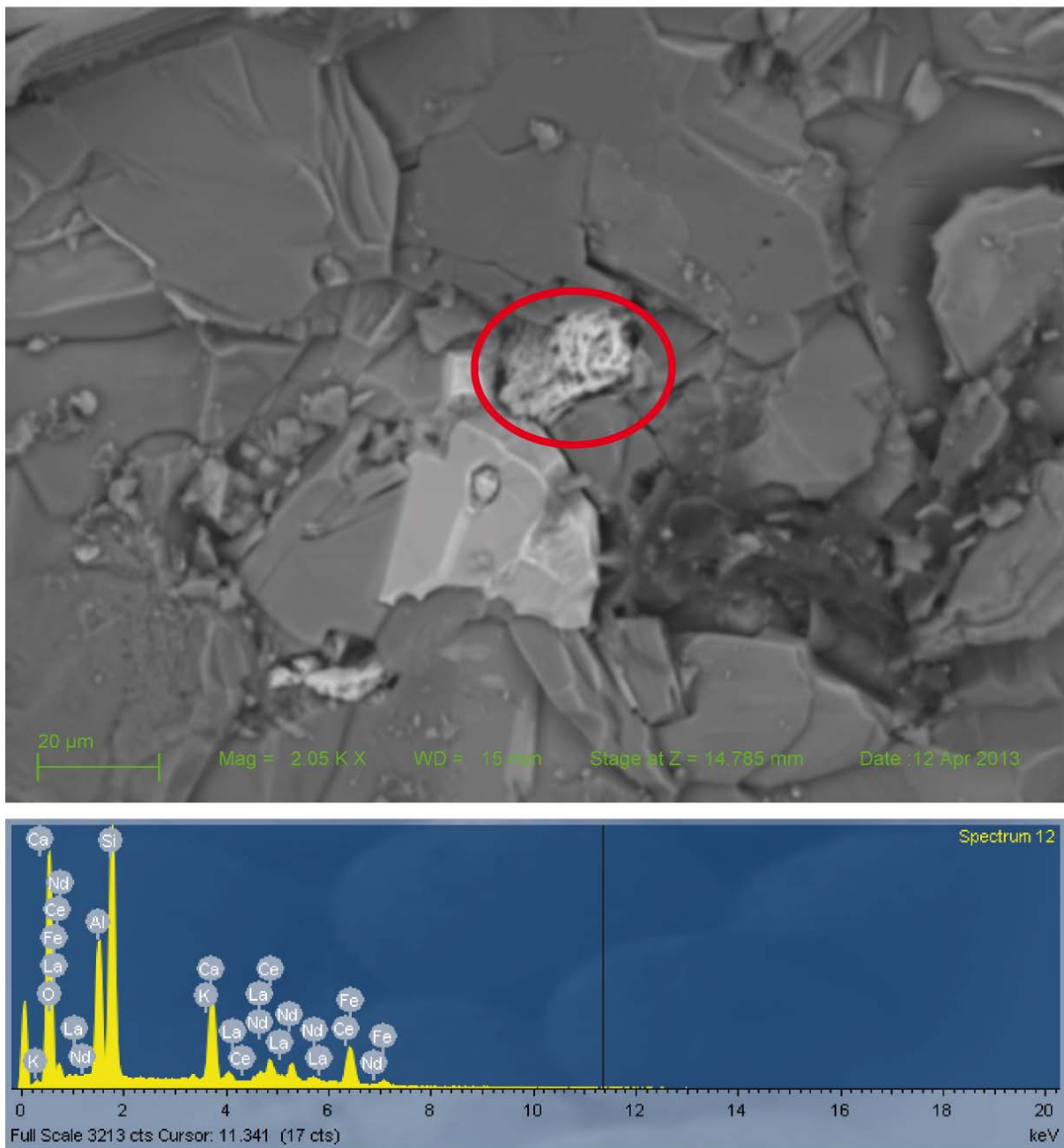


Figure 8: EDS spectra of in-situ point analyses performed on REE phases in sample chips. The three brightest minerals in the centre of (a) are relatively intact and most likely allanite, based on the EDS spectra obtained; (b) shows a stronger decomposed REE mineral (circle) which, based on the obtained EDS spectrum, is indistinguishable from allanite. The ED spectra obtained for relatively intact REE minerals (Fig. 8a) and decomposed REE minerals (Fig. 8b) are indistinguishable from each other. Given the degree of decomposition of the REE minerals in some samples, it cannot be ruled out that new minerals replaced the primary REE silicates and subordinate REE phosphates and carbonates. However, newly formed fine-grained mineral aggregates would be indistinguishable from more intact REE minerals by means of EDS.

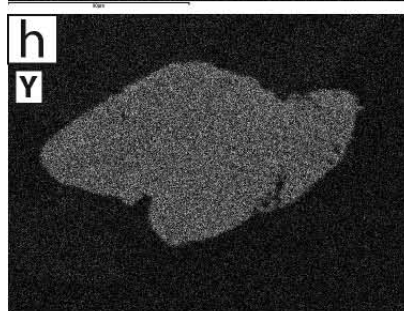
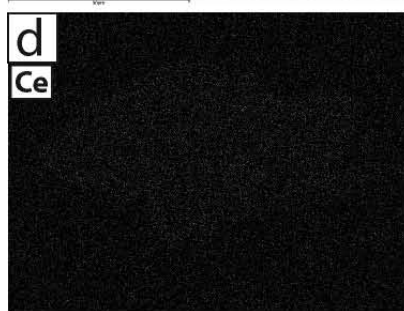
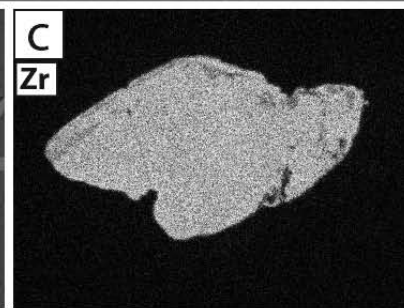
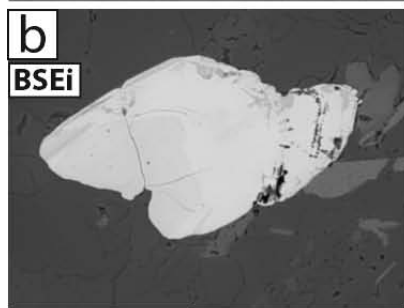
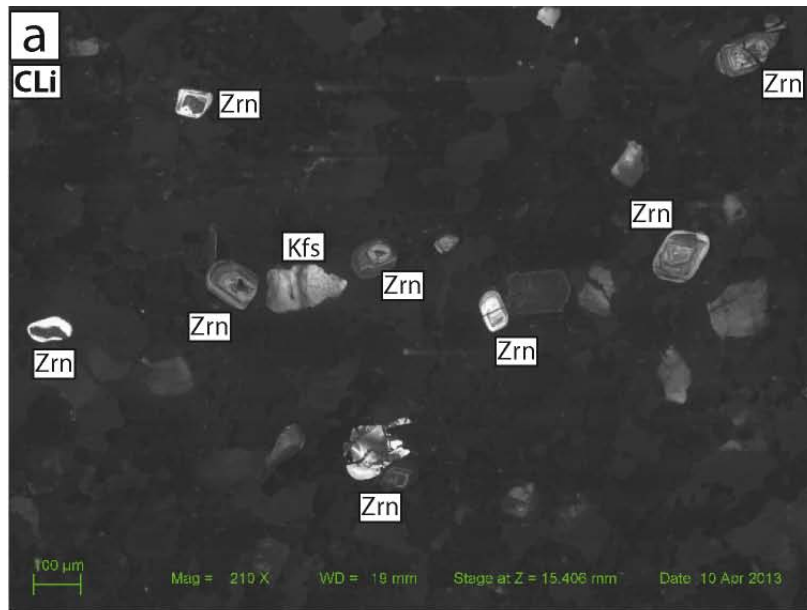


Figure 9: Zircon grains in a heavy-mineral rich zone display bright margins in CL image (a); (b) is a BSEi of a zircon grain showing bright margins in CLi; (c), (d), (e), (f), (g), (h) and (i) are element maps obtained in ED mode showing the elements Zr, Ce, Nd, Eu, Yb, Y and Th, respectively. No compositional differences with respect to the REE are observed in zircon in ED element mapping.

As redistribution and transport of the REE may be an important process occurring during decomposition of the presumably primary allanite, the samples were checked for possible REE sinks. Zircon is the only mineral present in the bedrock to have partition coefficients (Kd-values) greater than 1 and, thus, may incorporate REE to higher degrees than a coexisting fluid (e.g. Bea et al., 1994; Watson, 1980; Fujimaki, 1986). Checking for REE in zircon was, as a first approach, done by applying CL imaging where most zircon grains show bright margins (Fig. 9 a). Most likely, these represent seams that grew during upper greenschist-facies conditions, which are the peak metamorphic conditions based on the presence of garnet and biotite porphyroblasts in metapelitic horizons and epidote-calcite joint fillings in all lithologies. As shown by Dempster et al. (2004), zircon may be stabilised under greenschist-facies conditions in metasedimentary rocks and can even grow at temperatures as low as 350°C. Following CL imaging, grains with bright rims visible in CL image were investigated with ED element mapping (Fig. 9 b – i, where b shows the BSE image of the same grain), but none of the grains displayed elevated contents for the REE in the seams and, e.g., Y is evenly distributed over the whole grain shown in Fig. 9 and in the other grains investigated. Thus, the only viable sink for the REE after a possible mobilisation from the primary REE minerals was found not to contain detectable amounts of the REE. Given the scarcity of newly formed REE minerals and the common observation of in-situ replacement of primary REE minerals by fine-grained mineral aggregates, it is concluded that the REE have not been mobilised during decomposition of the primary REE minerals and that alteration of the REE phases is mostly an in-situ alteration phenomena.

Economic potential

In addition to the identification of the REE minerals, the economic potential is assessed through whole-rock analyses. For this purpose, three different preparation methods were employed, all followed by ICP MS analysis at the ACME lab in Vancouver, Canada. Whole-rock results retrieved by digestion with an AR mixture can be best compared to the soil sample composition results; however, it must be kept in mind that AR digestion is a relatively weak extraction method often providing incomplete dissolution if resistant minerals are subject to the leaching (e. g. Chao, 1984; Church et al., 1987). Based on the higher concentrations retrieved for Zr, Hf, Nb and Ta by 4-Acid leaching and Li-borate fusion/digestion than for AR leaching, it is indicated that zircon (which was identified in the soil samples, see Fig. 5 f) and possibly pyrochlore (or different Nb/Ta phases) are not dissolved during AR leaching. Interestingly, Zr, Hf, Nb and Ta behave differently from the REE: for the latter group of elements, only minor compositional differences are observed between the weaker AR leaching and the more potent 4-Acid and Li-borate fusion/decomposition methods. This finding allows for drawing the conclusion that the AR extraction technique leached the REE nearly completely in both soil and bedrock. Given the marginal compositional differences especially for the LREE, the AR leaching provided the

same degree of extraction as the 4-Acid and Li-borate fusion/digestion methods. The reason for the susceptibility of the REE towards treatment with AR is related to the state of the REE-incorporating minerals. As described above, the REE minerals display partly strong alteration and even in-situ decomposition to fine-grained mineral aggregates. Being incorporated in texturally unstable allanite and, to minor degrees, xenotime, the altered minerals are interpreted to be easily dissolved when treated with different extraction methods such as AR, 4-Acid leaching and Li-borate fusion/decomposition. Experimental work showed that the Ca incorporated in intact epidote-group minerals is dissolved to only 18 % during treatment with an AR solvent (Snäll and Liljefors, 2000). Our results contrast the experimental work and lead us to the conclusion that the presence of altered and locally decomposed REE mineral aggregates at Nordkinn lead to a more or less complete dissolution of the REE minerals in the soils. The REE anomaly associated with the soil consequently rather reflects the alteration state of the REE phases than ore-grade REE concentration in the bedrock. It is furthermore concluded that, based on the higher contents of HREE analysed after 4-Acid leaching and Li-borate fusion/digestion than for AR digestion, the HREE are incorporated in more resistant (or less altered) minerals that are less susceptible to treatment by AR digestion.

Given the maximum degree of 6-fold enrichment relative to average continental crust of the REE found in the bedrock relative to average continental crust, the economic potential for REE in the metasedimentary rocks of the Kalak Nappe Complex appears to be somewhat limited. The maximum totals for the REE detected by ICP MS following AR leaching, 4-Acid leaching and Li-borate fusion/digestion are 429, 371 and 379 ppm, respectively, based on a total of 28 samples of bedrock. The lowest values found with AR- and 4-Acid leaching and Li-borate fusion/decomposition are 22, 25 and 19 ppm, respectively. Such REE contents are even lower than the values of 0.05 to 0.2 wt % REE₂O₃ determined for Chinese ion-adsorption clays (Kanazawa and Kamitani, 2006), which themselves are considered to be low compared to other high-grade deposits. It is known that the outcrop area of the Neoproterozoic metasedimentary rocks of the Kalak Nappe Complex is relatively large but as the concentration of the REE is underneath that of spatial variation (possibly as a function of the distribution of primary REE minerals) and does not exceed 429 ppm, the economic potential is rated to be rather low.

7. Acknowledgements

Clemens Reimann and David Roberts are thanked for their continuous interest in the progress of the work, their help during numerous discussions and for providing data and sample material. Karl Fabian and Maarten Broekmans are thanked for insightful discussions. Financial support from the MINN programme is gratefully acknowledged. The research leading to these results has received funding from the European Community's Seventh Framework Programme ([FP7/2007-2013]) under grant agreement n°309373. This publication reflects only the author's view, exempting the Community from any liability. Project web site: www.bgs.ac.uk/eurare/.

8. References

Bea, F., Pereira, M.D. and Stroh, A. (1994) Mineral/leucosome trace-element partitioning in a peraluminous migmatite (a laser ablation-ICP-MS study). *Chemical Geology* 117: 291-312.

Bryan, K.R., Robinson, A. and Briggs, R.M. (2007) Spatial and temporal variability of titanomagnetite placer deposits on a predominantly black sand beach. *Marine Geology* 236: 45-59.

Bølviken, B., Bergström, B., Björklund, A., Konti, M., Lehmuspelto, P., Lindholm, T., Magnusson, J., Ottesen, R.T., Steenfelt, A. and Volden, T. (1986) *Geochemical Atlas of Northern Fennoscandia, Scale 1:4,000,000*. Geological Survey of Norway.

Chao, T.T. (1984) Use of partial dissolution techniques in geochemical exploration. *Journal of Geochemical Exploration* 20: 101–135.

Church, S.E., Mosier, E.L. and Motooka, J.M. (1987) Mineralogical basis for the interpretation of multi-element (ICP-AES), oxalic acid, and aqua regia partial digestions of stream sediments for reconnaissance exploration geochemistry. *Journal of Geochemical Exploration* 29: 207–233.

Deer, W.A., Howie, R.A. and Zussman, J. (1986) *Rock forming minerals, Vol. 1B: Disilicates and ringsilicates (2nd edition)*, Longman.

Dill, H.G. (2007) Grain morphology of heavy minerals from marine and continental placer deposits, with special reference to Fe–Ti oxides. *Sedimentary Geology* 198: 1-27.

Fujimaki, H. (1986) Partition-Coefficients of Hf, Zr, and REE between Zircon, Apatite, and Liquid. *Contributions to Mineralogy and Petrology* 94: 42-45.

Gao, S. and Rudnick, R.L. (2003) Composition of the continental crust. *Treatise on geochemistry, Vol.3: 1-64*, Elsevier.

Giere, R. and Sorensen, S.S. (2004) Allanite and other REE-rich epidote-group minerals. *Reviews in Mineralogy and Geochemistry*, 56: 431-493.

Giusti, L. (1986) The morphology, mineralogy, and behavior of ‘fine-grained’ gold from placer deposits of Alberta: sampling and implications for mineral exploration. *Canadian Journal of Earth Sciences*, 23: 1662-1672.

Göb, S., Wenzel, T., Bau, M., Jacob, D. E. Loges, A. and Markl, G. (2011) The redistribution of rare earth elements in secondary minerals of hydrothermal veins, Schwarzwald, SW Germany, *The Canadian Mineralogist* 49: 1305-1333.

- Kanazawa, Y. and Kamitani, M. (2006) Rare earth minerals and resources in the world. *Journal of Alloys and Compounds*, 408: 1339-1343.
- Kirkland, C. L., Daly, J. S. and Whitehouse, M. J. (2007) Provenance and terrane evolution of the Kalak Nappe Complex, Norwegian Caledonides: Implications for Neoproterozoic Paleogeography and Tectonics. *Journal of Geology*, 115, pp. 21-41.
- Minter, W.E.L. (1993) Ancient placer gold deposits. *Gold Metallogeny and Exploration*, 283-308. Chapman and Hall.
- Mongelli, G. (1997) Ce-anomalies in the textural components of Upper Cretaceous karst bauxites from the Apulian carbonate platform (southern Italy). *Chemical Geology*, 140: 69–79.
- Moore, J.M. and Moore, A.E. (2004) The roles of primary kimberlitic and secondary Dwyka glacial sources in the development of alluvial and marine diamond deposits in Southern Africa. *Journal of African Earth Sciences*, 38: 115-134.
- Morton, A.C. (1991) Geochemical studies of detrital heavy minerals and their application to provenance research. In: *Developments in sedimentary provenance studies*, Geological Society Special Publications 57: 31-45.
- Patyk-Kara, N.G. (1999) Cenozoic placer deposits and fluvial channel systems on the Arctic shelf of Siberia. *Economic Geology* 94: 707-720.
- Reimann, C., Finne, T.E. and Filzmoser, P. (2012) Soil geochemical data from the Nordkinn peninsula, Finnmark. NGU Report 2012.016.
- Reimann, C., Finne, T.E. and Filzmoser, P. (2011) New geochemical data from a collection of till samples from Nordland, Troms and Finnmark. NGU Report 2011.45.
- Rice, A.H.N. and Roberts, D. (1988) Multi-textured garnets from a single growth event: an example from northern Norway. *Journal of Metamorphic Geology* 6: 159-172.
- Roberts, D. (2007) Palaeocurrent data from the Kalak Nappe Complex, northern Norway: a key element in models of terrane affiliation. *Norwegian Journal of Geology* 87: 319-328.
- Roberts, D. (2006) Berggrunnskart Skjøtningberg 2237 III, Scale 1:50,000, Norges geologiske undersøkelse.
- Roberts, D. (2006) Berggrunnskart Mehamn 2237 II, Scale 1:50000. Norges geologiske undersøkelse.

- Roberts, D. (2000) Reverse-slip offsets and axial fractures in road-cut boreholes from the Caledonides in Finnmark, northern Norway: neotectonic stress orientation indicators. *Quaternary Science Reviews* 19: 1437-1445.
- Roberts, D. (1998) Berggrunnskart Honningsvåg, Scale 1:250,000. Norges geologiske undersøkelse.
- Roberts, D., (1985) The Caledonian fold belt in Finnmark: a synopsis. *Norges geologiske undersøkelse Bulletin* 403: 161-177.
- Roberts, D. (1981) Berggrunnskart Nordkapp, Scale 1:250,000. Norges geologiske undersøkelse.
- Roberts, D. and Andersen, T.B. (1985) Nordkapp. Beskrivelse til det berggrunnsgeologiske kartbladet Scale 1:250,000. *Norges geologiske undersøkelse Skrifter* 61, 49 pp.
- Roberts, D. and Siedlecka, A. (2011) Berggrunnskart Finnkongkeila 2336-4, Scale 1:50000, revidert foreløpig utgave. Norges geologiske undersøkelse.
- Roberts, D. and Siedlecka, A. (2012) Provenance and sediment routing of Neoproterozoic formations on the Varanger, Nordkinn, Rybachi and Sredni peninsulas, North Norway and Northwest Russia: a review. *Norges geologiske undersøkelse Bulletin* 452: 1-19.
- Roy, P.S. (1999): Heavy mineral beach placers in southeastern Australia; their nature and genesis. *Economic Geology*, 94: 567-588.
- Sevastjanova, I., Hall, R. and Alderton, D. (2012) A detrital heavy mineral viewpoint on sediment provenance and tropical weathering in SE Asia. *Sedimentary Geology* 280: 179-194.
- Siedlecka, A., (2009) Berggrunnsgeologisk kart Trollfjorden 2336 3, M=1:50000, foreløpig utgave 2, revidert. Norges geologiske undersøkelse.
- Siedlecka, A., Reading, H.G., Williams, G.D. and Roberts, D. (2006) Berggrunnsgeologisk kart Langfjorden 2236 2, Scale 1:50,000 foreløpig utgave. Norges geologiske undersøkelse.
- Sircombe, K.N. and Freeman, K.J. (1999) Provenance of detrital zircons on the Western Australia coastline—Implications for the geologic history of the Perth basin and denudation of the Yilgarn craton. *Geology* 27: 879–882.
- Snäll, S., and Liljefors, T. (2000) Leachability of major elements from minerals in strong acids. *Journal of Geochemical Exploration* 71: 1-12.
- Van Emden, B., Thornber, M.R., Graham, J. and Lincoln, F. J. (1997) The incorporation of actinides in monazite and xenotime from placer deposits in Western Australia. *Canadian Mineralogist* 35: 95-104.

Watson, E.B. (1980) Some experimentally determined Zircon-liquid partition-coefficients for the Rare-Earth Elements. *Geochimica et Cosmochimica Acta* 44: 895-897.

Whitney, D.L. and Evans, B.W. (2010) Abbreviations for names of rock-forming minerals. *American Mineralogist* 95: 185–18.

9. Appendices

Appendix 1: Whole-rock data analysed subsequent to AR-digestion, 4-Acid leaching and Li-borate fusion/decomposition.

Bedrock samples		Method	WGHT	4A4B	4A4B	4A4B
		Analyte	Wgt	SiO ₂	Al ₂ O ₃	Fe ₂ O ₃
		Unit	KG	%	%	%
		MDL	0.01	0.01	0.01	0.04
name	coordinates	Type				
JS-NK2	35 W 528034 7881368	Rock	0.5	85.81	7.39	1.69
JS-NK3	35 W 528229 7881705	Rock	0.51	79.52	10.65	1.58
JS-NK7	35 W 528359 7881769	Rock	0.47	80.73	10.25	0.87
JS-NK12	35 W 524993 7865959	Rock	0.79	81.48	8.92	3.41
JS-NK17	35 W 525925 7868101	Rock	0.58	73.74	11.55	4.13
JS-NK20	35 W 525005 7856097	Rock	0.56	62.57	17.03	6.62
JS-NK22	35 W 525316 7855918	Rock	0.65	62.33	17.51	6.85
JS-NK23	35 W 525316 7855918	Rock	0.42	60	18.83	6.98
JS-NK26	35 W 526176 7855644	Rock	0.62	80.66	9.9	2.56
JS-NK27	36 W 526620 7855763	Rock	0.63	59.54	19.08	7.08
JS-NK30	35 W 532149 7855834	Rock	0.37	88.78	5.71	1.23
JS-NK36	35 W 532749 7881448	Rock	0.42	73.98	12.26	1.64
JS-NK37	35 W 532749 7881448	Rock	0.52	73.84	12.27	1.92
JS-NK38	35 W 532749 7881448	Rock	0.68	67.27	15.19	4.75
JS-NK39	35 W 532671 7881587	Rock	0.66	71.13	12.66	5.09
JS-NK41	35 W 532569 7881608	Rock	0.74	75.42	11.03	1.61
JS-NK42	35 W 532531 7881601	Rock	0.61	64.78	15	6.94
JS-NK49	35 W 538691 7882555	Rock	0.48	65.13	13.8	7.22
JS-NK55	35 W 513050 7833886	Rock	0.47	82.94	8.58	1.53
JS-NK56	35 W 513038 7833909	Rock	0.49	77.99	9.39	3.7
JS-NK57	35 W 518570 7835328	Rock	0.52	79.66	9.93	2.37
JS-NK61	35 W 512781 7873561	Rock	0.59	88.24	4.95	0.81
JS-NK62	35 W 512781 7873561	Rock	0.61	89.03	4.51	1.92
JS-NK64	35 W 512781 7873561	Rock	0.65	90.4	4.44	0.61
JS-NK65	35 W 513255 7873267	Rock	0.45	78.48	10.98	2.44
JS-NK67	35 W 517075 7870362	Rock	0.44	81.49	8.79	0.9
JS-NK68	35 W 517075 7870362	Rock	0.55	72.11	15.02	1.84
JS-NK69	35 W 521063 7872244	Rock	0.48	60.64	18.58	6.47

	4A4B	4A4B	4A4B	4A4B	4A4B	4A4B	4A4B
	MgO	CaO	Na2O	K2O	TiO2	P2O5	MnO
	%	%	%	%	%	%	%
	0.01	0.01	0.01	0.01	0.01	0.01	0.01
name							
JS-NK2	0.28	0.17	1.7	2.31	0.21	<0.01	0.02
JS-NK3	0.2	0.27	2.49	4.27	0.23	0.12	0.01
JS-NK7	0.09	0.07	2.54	4.66	0.18	0.03	<0.01
JS-NK12	0.78	0.12	1.75	2.27	0.28	0.03	0.04
JS-NK17	0.94	1.86	3.28	2.01	0.79	0.09	0.08
JS-NK20	1.84	2.28	3.97	2.79	1.14	0.17	0.14
JS-NK22	1.98	1.32	2.44	4.11	1.23	0.2	0.15
JS-NK23	1.97	1.2	2.17	4.74	1.24	0.21	0.14
JS-NK26	0.66	0.69	2.42	1.81	0.41	0.04	0.07
JS-NK27	1.99	1.47	2.14	4.49	1.18	0.13	0.22
JS-NK30	0.25	0.48	1.28	1.14	0.16	0.03	0.02
JS-NK36	0.26	1.33	3.54	4.88	0.29	0.04	0.05
JS-NK37	0.35	1.45	3.9	4.32	0.31	0.04	0.07
JS-NK38	0.92	0.79	4.31	4.2	0.73	0.13	0.1
JS-NK39	0.53	0.26	2.17	5.38	1.37	0.05	0.06
JS-NK41	0.32	1.95	3.5	3.53	0.35	0.05	0.11
JS-NK42	1.37	1.1	3.59	4.14	0.79	0.14	0.11
JS-NK49	1.93	2.87	2.51	2.54	0.78	0.09	0.18
JS-NK55	0.36	0.77	1.73	2.8	0.19	<0.01	0.02
JS-NK56	0.72	2.45	1.7	1.73	0.82	0.09	0.06
JS-NK57	0.39	1.08	2.32	2.66	0.4	0.05	0.04
JS-NK61	0.1	1.34	1.13	2.26	0.08	0.02	0.05
JS-NK62	0.15	0.49	0.82	2.18	0.35	0.02	0.03
JS-NK64	0.09	0.59	0.91	2.14	0.04	0.01	0.03
JS-NK65	0.5	0.31	0.95	4.44	0.34	0.02	0.03
JS-NK67	0.09	1.13	1.14	4.6	0.14	0.03	0.03
JS-NK68	0.21	0.65	1.06	7.14	0.19	0.32	0.02
JS-NK69	1.7	1.15	2.36	5.39	1.43	0.12	0.14

	4A4B	4A4B	4A4B	4A4B	4A4B	4A4B	4A4B
	Cr2O3	Ni	Sc	LOI	Sum	Ba	Be
	%	PPM	PPM	%	%	PPM	PPM
	0.002	20	1	-5.1	0.01	1	1
name							
JS-NK2	<0.002	<20	2	0.3	99.9	460	1
JS-NK3	<0.002	<20	3	0.5	99.83	1215	<1
JS-NK7	<0.002	<20	2	0.4	99.82	1429	1
JS-NK12	0.003	<20	4	0.8	99.92	473	<1
JS-NK17	0.006	<20	8	1.3	99.78	461	<1
JS-NK20	0.01	29	17	1.1	99.71	795	5
JS-NK22	0.01	27	18	1.6	99.69	1063	3
JS-NK23	0.01	34	19	2.2	99.67	1318	2
JS-NK26	0.003	<20	4	0.7	99.87	493	<1
JS-NK27	0.011	42	18	2.3	99.67	1278	1
JS-NK30	<0.002	22	2	0.8	99.89	463	<1
JS-NK36	0.003	<20	4	1.5	99.73	1979	<1
JS-NK37	0.003	<20	5	1.3	99.78	1503	1
JS-NK38	0.006	<20	11	1.2	99.59	1719	3
JS-NK39	0.007	<20	10	0.9	99.55	1614	2
JS-NK41	0.003	<20	5	1.9	99.82	1080	1
JS-NK42	0.008	31	12	1.8	99.73	1260	6
JS-NK49	0.006	39	10	2.7	99.79	436	4
JS-NK55	0.003	<20	2	0.9	99.87	760	<1
JS-NK56	0.005	<20	8	1.1	99.79	486	<1
JS-NK57	0.003	<20	5	1	99.86	694	<1
JS-NK61	<0.002	<20	<1	1	99.95	457	<1
JS-NK62	0.003	<20	2	0.4	99.92	440	<1
JS-NK64	<0.002	<20	<1	0.7	99.96	433	<1
JS-NK65	0.002	<20	4	1.3	99.84	1085	<1
JS-NK67	<0.002	<20	2	1.5	99.83	1298	<1
JS-NK68	<0.002	<20	3	1.2	99.71	2009	<1
JS-NK69	0.011	34	18	1.6	99.58	1535	6

	4A4B	4A4B	4A4B	4A4B	4A4B	4A4B	4A4B
	Co	Cs	Ga	Hf	Nb	Rb	Sn
	PPM	PPM	PPM	PPM	PPM	PPM	PPM
	0.2	0.1	0.5	0.1	0.1	0.1	1
name							
JS-NK2	6.9	1.8	10.9	8.2	4.5	71.1	1
JS-NK3	2.6	1.3	11.9	4.4	4.6	108.9	1
JS-NK7	1	0.6	9.5	3.8	4.2	107.9	<1
JS-NK12	7.8	1.5	10.7	4.5	5.4	83.5	1
JS-NK17	8.9	2	13.6	13.6	13.6	74.7	2
JS-NK20	17.5	4.4	22.7	11.2	18.6	117.8	2
JS-NK22	16.1	4.9	25.9	11.6	20.1	144.5	4
JS-NK23	20.8	4.8	28	12.1	19.8	155.1	5
JS-NK26	5.4	1.8	11.5	8.9	7.9	59.6	2
JS-NK27	21.1	4.2	29.6	9.9	18	141.9	5
JS-NK30	4.3	0.7	10	5.1	3.5	33.8	2
JS-NK36	1.9	0.6	10.9	5.1	5.4	106	<1
JS-NK37	2.8	0.8	11.1	4.8	5.8	92.3	<1
JS-NK38	14.6	3.4	18.5	8.2	10.9	168.1	2
JS-NK39	6.1	2.3	17.9	32.7	21.8	163.9	3
JS-NK41	2.6	0.9	9.4	6.3	6.1	78.1	<1
JS-NK42	19	4.1	19.1	6.7	13.8	189.1	2
JS-NK49	19.7	6.4	21.2	7.3	15.2	121.4	3
JS-NK55	4.6	0.8	12.9	3.9	4	60	1
JS-NK56	6.2	1.3	11.7	12.6	11.7	59.2	2
JS-NK57	4.3	1.5	10.9	6.2	8.2	72	2
JS-NK61	1.3	0.4	5.5	1.2	2.1	40.4	<1
JS-NK62	2.1	0.6	5.8	6.4	4.3	46.4	<1
JS-NK64	1.2	0.3	4.8	1.1	1.2	40.8	<1
JS-NK65	5.4	2	11.2	6.4	6.2	123.9	1
JS-NK67	1.2	0.4	7.9	3.7	3.6	103.9	<1
JS-NK68	3.5	1.2	19.6	4.2	5	180.3	2
JS-NK69	18.8	5.2	29	19.3	22	172.5	4

	4A4B	4A4B	4A4B	4A4B	4A4B	4A4B	4A4B
	Sr	Ta	Th	U	V	W	Zr
	PPM	PPM	PPM	PPM	PPM	PPM	PPM
	0.5	0.1	0.2	0.1	8	0.5	0.1
name							
JS-NK2	112.4	0.3	4.5	0.9	20	0.7	292.4
JS-NK3	148.7	0.3	3.8	1.1	23	0.6	171.1
JS-NK7	112.1	0.3	3.1	0.8	16	<0.5	143
JS-NK12	56.2	0.3	3.9	2.4	33	0.5	176.6
JS-NK17	319.2	0.9	11	2.1	52	0.6	537.8
JS-NK20	415.2	1.2	14	3.3	105	0.9	431.4
JS-NK22	296.6	1.4	14.6	3.6	116	1.8	419.3
JS-NK23	280.4	1.4	14.9	3.4	121	2.3	449.9
JS-NK26	200.7	0.5	6.6	2.3	35	0.6	343.6
JS-NK27	301.5	1.3	15.4	3.4	115	2.1	365.1
JS-NK30	103.7	0.4	2.9	0.8	21	0.5	218.9
JS-NK36	199	0.4	4.6	1.2	22	<0.5	176.7
JS-NK37	203.8	0.4	4.1	1.2	21	<0.5	182.1
JS-NK38	181	0.8	9.3	2.9	63	<0.5	300
JS-NK39	179.1	1.6	16.8	4.6	70	0.8	1344.6
JS-NK41	254.7	0.4	5	1.3	19	<0.5	232.7
JS-NK42	158.4	0.9	7.7	2.9	69	0.8	249
JS-NK49	353.9	0.8	9.6	2.5	66	4.2	300.9
JS-NK55	140.8	0.4	4.7	1.1	21	0.6	138.9
JS-NK56	523.8	1	10.5	3.1	66	0.7	480.2
JS-NK57	223	0.6	5.4	1.6	41	0.7	215.2
JS-NK61	178.4	0.2	2.1	0.6	8	<0.5	49.4
JS-NK62	95.2	0.3	2.5	1.1	17	<0.5	267.5
JS-NK64	114.9	0.1	1.6	0.4	<8	<0.5	36.7
JS-NK65	95.6	0.4	3.7	1.4	27	0.5	233.7
JS-NK67	99.7	0.2	2.4	0.6	12	<0.5	127.2
JS-NK68	122.9	0.4	3.8	1.3	28	0.7	171.2
JS-NK69	275.1	1.6	19.9	3.8	104	2.2	741.5

	4A4B	4A4B	4A4B	4A4B	4A4B	4A4B	4A4B
	Y	La	Ce	Pr	Nd	Sm	Eu
	PPM	PPM	PPM	PPM	PPM	PPM	PPM
	0.1	0.1	0.1	0.02	0.3	0.05	0.02
name							
JS-NK2	11.1	3.3	23.9	1.04	4.1	0.96	0.21
JS-NK3	10.2	10.2	31.1	2.86	11.3	2.09	0.55
JS-NK7	10.2	9.5	21.8	2.35	9.3	1.76	0.39
JS-NK12	4.4	3.5	6.4	1.02	4	0.74	0.12
JS-NK17	30.4	94.1	134.6	20.14	73.5	11.58	2.21
JS-NK20	43.9	63	133.4	15.15	54.8	10.17	1.92
JS-NK22	47.5	79.2	98.3	17.16	64	12.03	2.27
JS-NK23	44.3	50.7	72.6	11.71	40.8	6.99	1.28
JS-NK26	7.6	4.6	10.3	1.17	3.7	0.74	0.17
JS-NK27	36	37.2	72.4	10.16	38.4	6.65	1.32
JS-NK30	7.2	18.9	43.9	4.07	13.7	2.32	0.54
JS-NK36	10.6	10.9	24.4	2.88	9.7	1.9	0.51
JS-NK37	13.4	21.6	36.5	4.86	17.3	2.76	0.72
JS-NK38	28.7	50.2	82.6	11.09	42.1	6.77	1.44
JS-NK39	36.7	92.4	149.8	20.18	73.3	11.91	2.52
JS-NK41	13.9	20.3	42.9	5.02	18.8	3.28	0.82
JS-NK42	24.9	33.1	69.5	8.18	30.9	5.71	1.2
JS-NK49	25.5	38.8	78.4	9.94	37.5	6.77	1.37
JS-NK55	12.2	15	31.3	3.78	13.8	2.69	0.7
JS-NK56	29.1	31.1	65.8	7.54	28.6	5.69	1.16
JS-NK57	17.5	25.1	46.1	5.7	21.2	3.9	0.87
JS-NK61	4.1	9.5	17.7	1.91	5.9	1.08	0.34
JS-NK62	6.6	12.5	22	2.74	10.5	1.61	0.42
JS-NK64	2.5	6.8	12	1.3	3.7	0.72	0.26
JS-NK65	6.4	11.6	24.6	2.57	8.9	1.6	0.43
JS-NK67	8.5	13.6	30.8	3.39	13.3	2.25	0.51
JS-NK68	10.8	22.6	50.4	5.91	22	3.9	0.88
JS-NK69	55.1	57	119.8	15.02	58.2	10.73	1.92

	4A4B	4A4B	4A4B	4A4B	4A4B	4A4B	4A4B
	Gd	Tb	Dy	Ho	Er	Tm	Yb
	PPM	PPM	PPM	PPM	PPM	PPM	PPM
	0.05	0.01	0.05	0.02	0.03	0.01	0.05
name							
JS-NK2	0.96	0.19	1.62	0.33	1.31	0.21	1.65
JS-NK3	1.82	0.31	1.68	0.4	1.23	0.19	1.17
JS-NK7	1.62	0.3	1.61	0.38	1.09	0.16	1.31
JS-NK12	0.69	0.12	0.8	0.16	0.5	0.08	0.52
JS-NK17	9.07	1.3	6.39	1.07	3.29	0.51	3.31
JS-NK20	8.61	1.3	7.34	1.52	4.84	0.75	5.06
JS-NK22	10.58	1.67	9.54	1.94	5.92	0.95	6.05
JS-NK23	6.1	0.97	6.65	1.6	5.64	0.91	6.09
JS-NK26	0.61	0.12	0.9	0.25	1.03	0.22	1.78
JS-NK27	4.97	0.82	5.67	1.38	5.16	0.94	6.62
JS-NK30	1.86	0.25	1.35	0.29	0.8	0.12	0.77
JS-NK36	1.71	0.32	1.83	0.4	1.37	0.2	1.18
JS-NK37	2.37	0.39	2.31	0.46	1.37	0.22	1.36
JS-NK38	6.13	0.95	5.28	0.97	3.35	0.51	3.57
JS-NK39	9.37	1.39	6.91	1.32	4.06	0.65	4.37
JS-NK41	2.74	0.44	2.43	0.51	1.71	0.26	1.86
JS-NK42	4.71	0.8	4.53	0.88	2.73	0.43	3.18
JS-NK49	5.54	0.75	4.59	0.86	2.87	0.5	3.77
JS-NK55	2.42	0.37	2.13	0.42	1.33	0.21	1.33
JS-NK56	5.12	0.88	4.71	1.06	3.35	0.51	3.42
JS-NK57	3.12	0.55	2.84	0.61	1.79	0.28	1.92
JS-NK61	0.95	0.14	0.76	0.17	0.47	0.08	0.48
JS-NK62	1.32	0.19	1.04	0.23	0.69	0.12	0.76
JS-NK64	0.61	0.09	0.51	0.09	0.3	0.05	0.28
JS-NK65	1.23	0.22	1.1	0.24	0.78	0.12	0.86
JS-NK67	1.71	0.26	1.45	0.29	0.99	0.16	1.16
JS-NK68	2.4	0.34	2.13	0.38	1.18	0.2	1.29
JS-NK69	9.41	1.46	9.5	1.93	6.09	1.01	7.05

	4A4B	1DX	1DX	1DX	1DX	1DX	1DX
	Lu	Mo	Cu	Pb	Zn	Ag	Ni
	PPM	PPM	PPM	PPM	PPM	PPM	PPM
	0.01	0.1	0.1	0.1	1	0.1	0.1
name							
JS-NK2	0.25	0.1	1.2	6.5	15	<0.1	9.4
JS-NK3	0.19	0.5	1.3	3.3	10	<0.1	7.7
JS-NK7	0.18	<0.1	1.3	1.9	6	<0.1	2.5
JS-NK12	0.08	<0.1	1	1.2	12	<0.1	9.2
JS-NK17	0.52	<0.1	3.5	7	47	<0.1	12.7
JS-NK20	0.73	0.3	8.2	5.3	88	<0.1	30.5
JS-NK22	0.91	<0.1	0.6	4.7	89	<0.1	25
JS-NK23	0.92	<0.1	6.7	4.1	81	<0.1	30.8
JS-NK26	0.27	<0.1	6.5	3	31	<0.1	6.9
JS-NK27	1	0.3	21.4	4.3	74	<0.1	32.2
JS-NK30	0.15	0.4	1.5	3.5	11	<0.1	3.5
JS-NK36	0.2	<0.1	1.6	8.1	17	<0.1	2.9
JS-NK37	0.22	<0.1	6.4	5.8	22	<0.1	3.2
JS-NK38	0.48	1	5.5	828.8	86	0.8	19.7
JS-NK39	0.72	<0.1	2.2	9.5	43	<0.1	9.4
JS-NK41	0.26	<0.1	1.4	8.6	12	<0.1	3.5
JS-NK42	0.43	<0.1	151.7	13.7	81	0.3	30.7
JS-NK49	0.55	<0.1	2.2	7.1	96	<0.1	26.3
JS-NK55	0.22	<0.1	3.8	7.2	4	<0.1	2.3
JS-NK56	0.51	<0.1	8.4	4.8	26	<0.1	10.9
JS-NK57	0.3	<0.1	3.9	5.6	12	<0.1	6.6
JS-NK61	0.08	<0.1	1	5.3	1	<0.1	1
JS-NK62	0.14	0.1	2.7	5.5	8	<0.1	3.1
JS-NK64	0.06	<0.1	1.2	3.6	2	<0.1	1.1
JS-NK65	0.14	<0.1	0.6	2.3	<1	<0.1	0.6
JS-NK67	0.17	<0.1	0.6	1.7	2	<0.1	1.4
JS-NK68	0.18	<0.1	0.7	1.9	7	<0.1	3
JS-NK69	1.03	0.1	0.8	5.8	73	<0.1	26.8

	1DX	1DX	1DX	1DX	1DX	1DX	1DX
	As	Au	Cd	Sb	Bi	Hg	Tl
	PPM	PPB	PPM	PPM	PPM	PPM	PPM
	0.5	0.5	0.1	0.1	0.1	0.01	0.1
name							
JS-NK2	<0.5	4.4	<0.1	<0.1	<0.1	<0.01	0.3
JS-NK3	<0.5	2.4	<0.1	<0.1	<0.1	<0.01	0.3
JS-NK7	<0.5	<0.5	<0.1	<0.1	<0.1	<0.01	0.1
JS-NK12	<0.5	2.1	<0.1	<0.1	<0.1	<0.01	0.4
JS-NK17	2.1	<0.5	0.1	<0.1	<0.1	<0.01	0.4
JS-NK20	1.5	1.1	<0.1	<0.1	<0.1	<0.01	0.6
JS-NK22	<0.5	1.6	<0.1	<0.1	<0.1	<0.01	0.6
JS-NK23	1.6	<0.5	<0.1	<0.1	<0.1	<0.01	0.6
JS-NK26	<0.5	<0.5	<0.1	<0.1	<0.1	<0.01	0.3
JS-NK27	1.7	1.9	<0.1	<0.1	<0.1	<0.01	0.4
JS-NK30	<0.5	2.7	<0.1	<0.1	0.1	<0.01	0.2
JS-NK36	<0.5	<0.5	<0.1	<0.1	<0.1	<0.01	0.2
JS-NK37	<0.5	2.2	<0.1	<0.1	<0.1	<0.01	0.3
JS-NK38	7.3	1.6	0.2	0.3	0.5	<0.01	0.8
JS-NK39	0.6	2.5	<0.1	<0.1	<0.1	<0.01	0.6
JS-NK41	<0.5	1.8	<0.1	<0.1	<0.1	<0.01	0.2
JS-NK42	12	<0.5	0.1	<0.1	<0.1	<0.01	0.9
JS-NK49	1	1.1	<0.1	<0.1	<0.1	<0.01	0.7
JS-NK55	<0.5	3	<0.1	<0.1	<0.1	<0.01	0.2
JS-NK56	<0.5	2.9	<0.1	<0.1	<0.1	<0.01	0.2
JS-NK57	<0.5	2.7	<0.1	<0.1	<0.1	<0.01	0.2
JS-NK61	<0.5	<0.5	<0.1	<0.1	<0.1	<0.01	<0.1
JS-NK62	<0.5	2.2	<0.1	0.2	<0.1	<0.01	<0.1
JS-NK64	<0.5	<0.5	<0.1	<0.1	<0.1	<0.01	<0.1
JS-NK65	<0.5	2	<0.1	<0.1	<0.1	<0.01	<0.1
JS-NK67	<0.5	1.6	<0.1	<0.1	<0.1	<0.01	<0.1
JS-NK68	<0.5	3	<0.1	<0.1	<0.1	<0.01	0.1
JS-NK69	1.4	0.8	<0.1	<0.1	<0.1	<0.01	0.6

	1DX	1T	1T	1T	1T	1T	1T
	Se	Mo	Cu	Pb	Zn	Ag	Ni
	PPM	PPM	PPM	PPM	PPM	PPB	PPM
	0.5	0.01	0.01	0.01	0.1	2	0.1
name							
JS-NK2	<0.5	0.14	1.19	5.66	12.9	4	7.4
JS-NK3	<0.5	0.15	1.22	2.71	11.3	11	4.4
JS-NK7	<0.5	0.06	1.25	1.59	5.1	2	2.1
JS-NK12	<0.5	0.05	1.56	1.09	13.3	7	9.3
JS-NK17	<0.5	0.13	4.37	7.13	53.6	21	13.1
JS-NK20	<0.5	0.45	9.26	5.06	91	24	28.6
JS-NK22	<0.5	0.15	1.24	4.37	90.1	12	23.8
JS-NK23	<0.5	0.08	7.1	4.05	85.7	23	33.5
JS-NK26	<0.5	0.14	5.34	2.42	28.6	6	5.7
JS-NK27	<0.5	0.32	22.29	4.29	77.5	12	31.9
JS-NK30	<0.5	0.39	1.31	3.12	9.7	25	3
JS-NK36	<0.5	0.1	1.17	7.28	17.4	16	2.8
JS-NK37	<0.5	0.07	5.58	5.15	21.5	18	3.1
JS-NK38	<0.5	1.12	6.05	810.4	89.2	899	20.1
JS-NK39	<0.5	0.11	2.91	8.2	44.1	26	8.7
JS-NK41	<0.5	0.08	1.61	7.98	12.1	25	3.4
JS-NK42	0.6	0.24	151.09	13.45	82.2	287	30.7
JS-NK49	<0.5	0.14	2.69	6.87	99.5	21	26.5
JS-NK55	<0.5	0.08	3.23	6.39	4.4	5	2.3
JS-NK56	<0.5	0.1	7.86	4.38	24.4	5	9.4
JS-NK57	<0.5	0.1	3.88	5.08	12.1	5	6.2
JS-NK61	<0.5	0.09	1.21	5.68	1.5	5	1.2
JS-NK62	<0.5	0.13	2.45	4.61	6.6	13	2.8
JS-NK64	<0.5	0.08	1.05	3.93	1.5	14	1.2
JS-NK65	<0.5	0.06	0.8	2.56	1.5	<2	0.7
JS-NK67	<0.5	0.08	0.63	1.97	3.1	3	1.9
JS-NK68	<0.5	0.06	0.44	1.93	5.6	3	2.9
JS-NK69	<0.5	0.3	1.67	6.1	75.5	12	28.4

	1T	1T	1T	1T	1T	1T	1T
	Co	Mn	Fe	As	U	Au	Th
	PPM	PPM	%	PPM	PPM	PPB	PPM
	0.1	1	0.01	0.1	0.1	0.2	0.1
name							
JS-NK2	4.7	114	0.86	<0.1	0.3	1.9	3.4
JS-NK3	2.4	70	0.9	0.5	0.7	2.4	3.4
JS-NK7	0.8	32	0.45	0.2	0.3	1.1	2.1
JS-NK12	7.6	276	2.13	<0.1	2	0.5	3.3
JS-NK17	9.9	467	2.54	1.7	1.3	0.3	11.1
JS-NK20	19.1	423	3.82	1.7	2	<0.2	12.3
JS-NK22	16.5	323	3.7	0.2	2.1	0.2	12.6
JS-NK23	20	367	3.63	1.5	2.1	1.3	13.2
JS-NK26	4.9	208	1.42	0.7	1.6	1	5.9
JS-NK27	19.5	446	3.8	1.4	2.6	0.3	13.3
JS-NK30	2.2	134	0.68	0.2	0.3	0.2	2.3
JS-NK36	2.2	367	0.92	0.2	0.7	<0.2	3.2
JS-NK37	3	567	1.19	0.4	0.6	<0.2	3.2
JS-NK38	14.8	601	2.82	6.5	1.4	1.3	6.4
JS-NK39	6.3	168	2.51	<0.1	2.4	<0.2	14.7
JS-NK41	2.2	795	0.88	0.2	0.7	0.4	4.3
JS-NK42	20.9	806	4.01	9.9	1.4	0.5	5
JS-NK49	18.4	1082	4.29	0.7	1.5	0.8	8.4
JS-NK55	1.3	132	0.38	<0.1	0.4	<0.2	3.1
JS-NK56	6.2	239	1.36	<0.1	0.8	<0.2	9.2
JS-NK57	3	187	0.96	<0.1	0.6	<0.2	4.1
JS-NK61	0.6	434	0.35	<0.1	0.3	<0.2	1.6
JS-NK62	1.4	196	1.02	0.7	0.5	<0.2	2.1
JS-NK64	0.4	203	0.25	<0.1	0.2	<0.2	1
JS-NK65	0.3	38	0.25	0.3	0.5	<0.2	2.5
JS-NK67	0.8	215	0.39	<0.1	0.3	0.6	2.3
JS-NK68	1.4	91	0.6	<0.1	0.9	0.4	3.3
JS-NK69	19.2	652	3.61	0.7	2	<0.2	19.2

	1T	1T	1T	1T	1T	1T	1T
	Sr	Cd	Sb	Bi	V	Ca	P
	PPM	PPM	PPM	PPM	PPM	%	%
	0.5	0.01	0.02	0.02	2	0.01	0.001
name							
JS-NK2	4.3	<0.01	<0.02	0.09	6	0.02	0.008
JS-NK3	4.6	<0.01	0.04	0.04	8	0.1	0.047
JS-NK7	2.8	<0.01	<0.02	<0.02	4	0.02	0.009
JS-NK12	1.8	<0.01	0.03	0.03	11	0.02	0.011
JS-NK17	24.1	0.07	0.05	0.09	33	0.79	0.038
JS-NK20	29.7	0.03	<0.02	0.3	63	0.27	0.073
JS-NK22	16.4	0.01	<0.02	0.16	46	0.24	0.081
JS-NK23	16.5	0.03	<0.02	0.16	41	0.22	0.092
JS-NK26	5.3	0.02	<0.02	0.09	11	0.04	0.012
JS-NK27	16.1	0.04	0.02	0.12	43	0.22	0.054
JS-NK30	8.5	<0.01	<0.02	0.13	4	0.25	0.015
JS-NK36	33.4	<0.01	<0.02	0.04	11	0.88	0.017
JS-NK37	45.6	0.05	0.04	0.03	12	0.96	0.012
JS-NK38	19.8	0.16	0.46	0.59	29	0.46	0.056
JS-NK39	28.8	<0.01	0.06	0.03	31	0.15	0.014
JS-NK41	62.6	0.01	0.03	0.05	7	1.31	0.015
JS-NK42	27.9	0.05	0.07	<0.02	38	0.68	0.057
JS-NK49	32.3	0.09	0.09	0.07	42	1.32	0.045
JS-NK55	28.5	<0.01	0.05	<0.02	3	0.32	0.015
JS-NK56	81.8	<0.01	0.14	<0.02	13	0.41	0.033
JS-NK57	35.4	<0.01	0.17	<0.02	9	0.25	0.018
JS-NK61	102.2	0.01	0.04	<0.02	<2	0.93	0.005
JS-NK62	22.7	<0.01	0.19	<0.02	5	0.26	0.002
JS-NK64	45.8	0.02	0.04	<0.02	<2	0.39	0.004
JS-NK65	14.8	<0.01	0.08	<0.02	3	0.06	0.003
JS-NK67	11.9	<0.01	<0.02	<0.02	<2	0.78	0.005
JS-NK68	7.1	<0.01	<0.02	<0.02	3	0.37	0.151
JS-NK69	13.9	<0.01	0.11	0.09	38	0.26	0.072

	1T	1T	1T	1T	1T	1T	1T
	La	Cr	Mg	Ba	Ti	B	Al
	PPM	PPM	%	PPM	%	PPM	%
	0.5	0.5	0.01	0.5	0.001	1	0.01
name							
JS-NK2	2.8	3.3	0.12	38	0.063	<1	0.43
JS-NK3	9.3	6.6	0.08	53.7	0.061	<1	0.43
JS-NK7	6.9	3.6	0.03	44.9	0.029	<1	0.24
JS-NK12	3.8	8.5	0.37	130.3	0.123	1	1.01
JS-NK17	107.2	24.1	0.5	229.3	0.2	<1	1.21
JS-NK20	65.5	40.2	0.99	405.5	0.231	<1	2.15
JS-NK22	81.9	32.8	0.98	247.2	0.191	<1	2.15
JS-NK23	50.2	27.7	0.94	276.8	0.194	<1	2.16
JS-NK26	3.6	8.1	0.3	115.3	0.108	<1	0.79
JS-NK27	36.4	30	0.97	220.1	0.206	2	2.11
JS-NK30	12.4	3.3	0.09	83.5	0.034	<1	0.38
JS-NK36	10.5	10.8	0.14	57.1	0.046	<1	0.44
JS-NK37	23.2	12	0.19	69.1	0.095	<1	0.5
JS-NK38	50.2	22.5	0.45	199.5	0.242	<1	1.28
JS-NK39	101.5	22.6	0.25	133.9	0.204	<1	0.99
JS-NK41	21.1	8.4	0.15	55.8	0.077	<1	0.47
JS-NK42	35.6	28.9	0.67	282.2	0.334	<1	1.83
JS-NK49	35.9	24.9	1.03	147	0.175	<1	2.37
JS-NK55	7.2	2.6	0.05	72.2	0.035	<1	0.35
JS-NK56	15.5	8.9	0.29	55.9	0.13	<1	0.74
JS-NK57	14.5	5.1	0.11	69	0.09	1	0.55
JS-NK61	8.8	2	0.02	27.2	0.019	<1	0.11
JS-NK62	10.9	6.4	0.02	32.3	0.093	<1	0.14
JS-NK64	6	1.6	<0.01	25.9	0.005	<1	0.1
JS-NK65	5.6	1.6	0.01	90.6	0.049	<1	0.33
JS-NK67	15	3.4	0.02	44.8	0.017	<1	0.25
JS-NK68	21	3.2	0.04	67.8	0.029	<1	0.45
JS-NK69	59.3	29.2	0.77	275.2	0.347	<1	1.84

	1T	1T	1T	1T	1T	1T	1T
	Na	K	W	Sc	Tl	S	Hg
	%	%	PPM	PPM	PPM	%	PPB
	0.001	0.01	0.1	0.1	0.02	0.02	5
name							
JS-NK2	0.025	0.35	<0.1	0.4	0.25	<0.02	<5
JS-NK3	0.032	0.35	<0.1	0.9	0.25	<0.02	7
JS-NK7	0.029	0.19	<0.1	0.5	0.11	<0.02	<5
JS-NK12	0.028	0.8	<0.1	1.3	0.39	<0.02	5
JS-NK17	0.044	0.95	<0.1	4.7	0.45	<0.02	13
JS-NK20	0.057	1.52	<0.1	8.4	0.68	<0.02	<5
JS-NK22	0.042	1.46	0.1	5.1	0.6	<0.02	<5
JS-NK23	0.039	1.48	0.1	5.1	0.6	<0.02	<5
JS-NK26	0.038	0.61	<0.1	1.4	0.26	<0.02	12
JS-NK27	0.043	1.21	0.1	5.1	0.49	<0.02	<5
JS-NK30	0.023	0.26	<0.1	0.6	0.13	<0.02	<5
JS-NK36	0.042	0.22	<0.1	1.9	0.14	<0.02	<5
JS-NK37	0.045	0.41	<0.1	2.5	0.31	<0.02	<5
JS-NK38	0.044	1.1	<0.1	3.9	0.8	<0.02	7
JS-NK39	0.027	0.87	<0.1	2.8	0.63	<0.02	7
JS-NK41	0.043	0.34	<0.1	1.2	0.19	<0.02	<5
JS-NK42	0.038	1.59	<0.1	3.9	1.05	<0.02	<5
JS-NK49	0.056	1.23	<0.1	5.9	0.65	<0.02	<5
JS-NK55	0.022	0.26	<0.1	0.8	0.07	<0.02	14
JS-NK56	0.03	0.23	<0.1	1.8	0.09	<0.02	<5
JS-NK57	0.027	0.41	0.1	1.3	0.17	<0.02	<5
JS-NK61	0.016	0.08	<0.1	0.5	<0.02	<0.02	<5
JS-NK62	0.015	0.12	<0.1	0.7	0.02	<0.02	<5
JS-NK64	0.014	0.09	<0.1	0.2	<0.02	<0.02	<5
JS-NK65	0.011	0.29	<0.1	0.7	0.04	<0.02	<5
JS-NK67	0.018	0.2	<0.1	0.4	0.06	<0.02	7
JS-NK68	0.015	0.38	<0.1	0.5	0.17	<0.02	<5
JS-NK69	0.024	1.51	<0.1	4.2	0.64	<0.02	5

	1T	1T	1T	1T	1T	1T	1T
	Se	Te	Ga	Cs	Ge	Hf	Nb
	PPM	PPM	PPM	PPM	PPM	PPM	PPM
	0.1	0.02	0.1	0.02	0.1	0.02	0.02
name							
JS-NK2	<0.1	<0.02	1.4	1.38	<0.1	0.18	0.13
JS-NK3	<0.1	<0.02	1.6	0.79	<0.1	0.06	0.33
JS-NK7	<0.1	<0.02	0.8	0.36	<0.1	0.08	0.18
JS-NK12	<0.1	<0.02	3.2	1.37	<0.1	0.25	0.1
JS-NK17	<0.1	<0.02	5	2.28	0.1	0.41	0.22
JS-NK20	<0.1	<0.02	9.7	4.74	0.2	0.38	0.17
JS-NK22	<0.1	0.03	8.4	4.36	0.2	0.43	0.13
JS-NK23	<0.1	<0.02	7.7	4.26	<0.1	0.41	0.21
JS-NK26	<0.1	<0.02	2.4	1.37	<0.1	0.13	0.15
JS-NK27	<0.1	<0.02	7.8	3.3	0.2	0.3	0.2
JS-NK30	<0.1	0.03	1	0.48	<0.1	0.08	0.14
JS-NK36	<0.1	<0.02	1.9	0.46	<0.1	0.15	0.17
JS-NK37	<0.1	<0.02	2.8	0.78	<0.1	0.17	0.15
JS-NK38	<0.1	<0.02	5.1	2.94	0.2	0.35	0.14
JS-NK39	<0.1	<0.02	4.4	2.05	<0.1	0.57	0.18
JS-NK41	<0.1	<0.02	1.5	0.68	<0.1	0.18	0.23
JS-NK42	<0.1	<0.02	7.1	3.96	0.2	0.28	0.12
JS-NK49	<0.1	<0.02	9	5.8	<0.1	0.23	0.24
JS-NK55	<0.1	<0.02	1	0.4	<0.1	0.1	0.28
JS-NK56	<0.1	<0.02	2.4	0.65	<0.1	0.11	0.26
JS-NK57	<0.1	0.03	2.1	1.06	<0.1	0.07	0.31
JS-NK61	<0.1	<0.02	0.5	0.05	<0.1	0.12	0.26
JS-NK62	<0.1	<0.02	0.5	0.08	0.1	0.19	0.54
JS-NK64	<0.1	<0.02	0.3	0.05	<0.1	0.13	0.09
JS-NK65	<0.1	<0.02	0.6	0.14	<0.1	0.1	0.21
JS-NK67	<0.1	<0.02	0.5	0.15	<0.1	0.08	0.11
JS-NK68	<0.1	<0.02	1.4	0.4	<0.1	0.07	0.08
JS-NK69	<0.1	<0.02	6.6	4.69	<0.1	0.29	0.19

	1T	1T	1T	1T	1T	1T	1T
	Rb	Sn	Ta	Zr	Y	Ce	In
	PPM	PPM	PPM	PPM	PPM	PPM	PPM
	0.1	0.1	0.05	0.1	0.01	0.1	0.02
name							
JS-NK2	29.1	<0.1	<0.05	4.3	3.6	24.3	<0.02
JS-NK3	29.5	0.1	<0.05	2.7	7.26	29.2	<0.02
JS-NK7	13.6	<0.1	<0.05	3.6	1.79	16.5	<0.02
JS-NK12	55.1	0.3	<0.05	6.7	2.85	6.5	<0.02
JS-NK17	65.1	0.5	<0.05	11.3	22.57	140.8	<0.02
JS-NK20	103.1	1.2	<0.05	13.7	24.88	136.4	0.05
JS-NK22	93.5	0.7	<0.05	13.1	25.3	101.8	0.05
JS-NK23	100.5	0.8	<0.05	16.2	22.7	74.7	0.03
JS-NK26	37.6	0.2	<0.05	4.4	2.94	9.1	<0.02
JS-NK27	79	0.9	<0.05	10.8	17.45	68.4	<0.02
JS-NK30	14.6	<0.1	<0.05	2.4	4.7	27.9	<0.02
JS-NK36	17	0.1	<0.05	5.9	4.51	22.5	<0.02
JS-NK37	36.8	0.1	<0.05	6.3	5.24	40.2	0.02
JS-NK38	103.7	0.3	<0.05	12.8	13.58	82.1	<0.02
JS-NK39	78.5	0.6	<0.05	17.7	17.18	160.2	<0.02
JS-NK41	27.4	<0.1	<0.05	7.8	7.94	47.6	<0.02
JS-NK42	146	0.5	<0.05	10.2	12.03	76.7	<0.02
JS-NK49	94.8	0.8	<0.05	8.6	18.08	73.8	0.03
JS-NK55	11.3	0.2	<0.05	2.5	4.73	15.4	<0.02
JS-NK56	13.3	0.2	<0.05	3.4	7.6	31	<0.02
JS-NK57	23	0.3	<0.05	3.2	6.67	24.9	<0.02
JS-NK61	3.3	<0.1	<0.05	4.1	2.76	16.3	<0.02
JS-NK62	4.4	0.1	<0.05	5	3.75	19.2	<0.02
JS-NK64	3	<0.1	<0.05	3	1.67	10.6	<0.02
JS-NK65	10.3	0.1	<0.05	3.3	2.82	11.6	<0.02
JS-NK67	10.1	<0.1	<0.05	1.9	6.62	33.1	<0.02
JS-NK68	22.3	<0.1	<0.05	2.8	8.83	47.7	<0.02
JS-NK69	105.5	0.6	<0.05	9.5	24.42	125	<0.02

	1T	1T	1T	1T	1T	1T	1T
	Re	Be	Li	Pr	Nd	Sm	Eu
	PPB	PPM	PPM	PPM	PPM	PPM	PPM
	1	0.1	0.1	0.02	0.02	0.02	0.02
name							
JS-NK2	3	0.1	1.8	0.89	3.98	0.82	0.17
JS-NK3	<1	0.2	2.4	2.55	10.6	2.13	0.49
JS-NK7	<1	<0.1	1.3	1.96	7.5	1.45	0.17
JS-NK12	<1	0.2	4.1	1.01	4.03	0.77	0.12
JS-NK17	<1	0.2	7	22.3	80.35	12.95	2.44
JS-NK20	<1	0.3	28	15.87	61.73	11.62	2.02
JS-NK22	<1	0.4	27.8	18.34	69.16	11.82	2.41
JS-NK23	<1	0.3	26.7	12.24	43.82	7.19	1.43
JS-NK26	<1	0.1	6.8	1.05	3.57	0.58	0.1
JS-NK27	<1	0.3	19.8	10	34.36	6.28	1.13
JS-NK30	<1	<0.1	2.7	2.76	9.6	1.42	0.46
JS-NK36	<1	0.1	3.2	2.51	9.9	1.68	0.38
JS-NK37	<1	0.1	4.3	5.29	19.57	3.27	0.62
JS-NK38	<1	0.5	8.2	11.66	41.65	6.46	1.31
JS-NK39	<1	0.4	5.6	22.93	84.47	13.55	2.67
JS-NK41	<1	0.1	2.1	5.27	20.79	3.41	0.77
JS-NK42	<1	0.5	10.1	9.17	34.91	6.06	1.24
JS-NK49	<1	0.3	29.1	9.2	35.22	6.03	1.29
JS-NK55	2	0.1	0.2	1.81	6.81	1.2	0.25
JS-NK56	<1	0.3	1.5	3.55	13.34	2.49	0.38
JS-NK57	<1	0.2	2.9	3.28	12.75	1.97	0.37
JS-NK61	<1	<0.1	0.1	1.69	5.79	0.69	0.33
JS-NK62	<1	<0.1	0.4	2.26	8.32	1.05	0.28
JS-NK64	<1	<0.1	0.1	1.08	3.57	0.5	0.17
JS-NK65	<1	0.1	0.4	1.37	4.75	0.71	0.17
JS-NK67	<1	0.1	0.9	3.76	15.6	2.43	0.57
JS-NK68	<1	0.3	2.3	5.54	20.79	3.52	0.68
JS-NK69	<1	0.3	25.9	15.44	57.77	10.6	1.79

	1T	1T	1T	1T	1T	1T	1T
	Gd	Tb	Dy	Ho	Er	Tm	Yb
	PPM	PPM	PPM	PPM	PPM	PPM	PPM
	0.02	0.02	0.02	0.02	0.02	0.02	0.02
name							
JS-NK2	0.87	0.13	0.63	0.16	0.47	0.07	0.32
JS-NK3	2.42	0.3	1.61	0.31	0.92	0.1	0.66
JS-NK7	0.81	0.14	0.62	0.07	0.18	0.03	0.18
JS-NK12	0.83	0.07	0.45	0.13	0.34	0.03	0.18
JS-NK17	12.12	1.6	7.63	1.02	2.43	0.34	2.13
JS-NK20	10.32	1.16	6.45	0.91	2.38	0.2	1.35
JS-NK22	11.83	1.49	7.73	1.12	2.56	0.22	1.53
JS-NK23	6.43	0.86	4.41	0.8	2.19	0.23	1.2
JS-NK26	0.53	0.08	0.62	0.11	0.49	0.04	0.42
JS-NK27	5.14	0.74	4.12	0.71	1.88	0.25	1.65
JS-NK30	1.77	0.14	1.1	0.17	0.49	0.06	0.48
JS-NK36	1.39	0.16	1.1	0.17	0.56	0.08	0.57
JS-NK37	2.46	0.3	1.48	0.21	0.55	0.07	0.68
JS-NK38	6.7	0.78	3.38	0.6	1.7	0.18	1.35
JS-NK39	12.4	1.39	5.78	0.73	1.88	0.13	1.24
JS-NK41	3.45	0.36	1.71	0.24	0.88	0.13	0.89
JS-NK42	4.54	0.66	2.99	0.5	1.27	0.19	1.31
JS-NK49	6.41	0.74	4.06	0.71	2.1	0.33	2.57
JS-NK55	1.42	0.17	0.8	0.19	0.6	0.08	0.58
JS-NK56	1.98	0.27	1.55	0.32	0.81	0.14	0.91
JS-NK57	2.27	0.24	1.3	0.3	0.71	0.09	0.61
JS-NK61	1.05	0.08	0.52	0.11	0.29	0.05	0.33
JS-NK62	1.33	0.12	0.79	0.13	0.44	0.06	0.38
JS-NK64	0.53	0.05	0.45	0.07	0.23	0.05	0.15
JS-NK65	0.87	0.12	0.77	0.11	0.27	0.05	0.3
JS-NK67	2.22	0.26	1.38	0.26	0.76	0.13	0.72
JS-NK68	3.9	0.43	1.95	0.35	1.2	0.15	0.89
JS-NK69	11.73	1.37	6.65	1.01	3.07	0.29	1.74

	1T	1T	1T	1F15	1F15	1F15	1F15
	Lu	Pd	Pt	Mo	Cu	Pb	Zn
	PPM	PPB	PPB	PPM	PPM	PPM	PPM
	0.02	10	2	0.05	0.02	0.02	0.2
name							
JS-NK2	0.04	<10	<2	0.08	1.54	12.89	13.8
JS-NK3	0.08	<10	<2	0.24	0.94	10.57	11.7
JS-NK7	<0.02	<10	5	0.15	1.72	7.97	6.1
JS-NK12	0.02	23	<2	0.08	1.4	3.14	12.3
JS-NK17	0.25	<10	4	0.08	3.81	19.06	42.2
JS-NK20	0.21	<10	<2	0.48	7.93	28.82	87
JS-NK22	0.15	<10	<2	0.1	0.7	18.88	88.5
JS-NK23	0.15	<10	<2	0.13	6.53	19.2	88.1
JS-NK26	0.05	10	<2	0.14	5.67	12.44	29.9
JS-NK27	0.19	48	<2	0.42	20.31	19.76	78.2
JS-NK30	0.08	<10	2	0.54	1.63	7.16	12.7
JS-NK36	0.08	23	<2	0.1	1.34	18.36	15.4
JS-NK37	0.1	10	<2	0.07	5.16	13.56	21.7
JS-NK38	0.22	<10	<2	1.14	6	834.23	96.3
JS-NK39	0.2	<10	<2	0.09	3.08	16.71	40
JS-NK41	0.14	<10	<2	0.1	1.63	16.32	12.4
JS-NK42	0.14	10	<2	0.24	146.5	18.29	87.4
JS-NK49	0.38	13	<2	0.16	2.56	20.36	99.6
JS-NK55	0.08	<10	<2	<0.05	3.38	8.71	13.1
JS-NK56	0.09	<10	<2	0.13	7.14	13.98	24.1
JS-NK57	0.06	<10	<2	0.06	3.15	8.16	14.1
JS-NK61	0.04	14	<2	0.13	1.09	9.37	6
JS-NK62	0.03	15	3	0.14	2.28	8.21	11.9
JS-NK64	0.05	<10	<2	0.1	1.6	8.04	5.9
JS-NK65	0.03	<10	<2	0.11	1.03	6.58	16.1
JS-NK67	0.11	<10	<2	0.07	0.63	8.46	4.7
JS-NK68	0.09	15	<2	0.1	0.79	11.17	11.6
JS-NK69	0.22	60	<2	0.66	1.53	19.23	70.7

	1F15	1F15	1F15	1F15	1F15	1F15	1F15
	Ag	Ni	Co	Mn	Fe	As	U
	PPB	PPM	PPM	PPM	%	PPM	PPM
	20	0.1	0.2	2	0.02	0.2	0.1
name							
JS-NK2	49	7.5	5.7	142	1.09	<0.2	0.7
JS-NK3	30	5.1	2.7	92	1.02	<0.2	0.9
JS-NK7	<20	2.3	1	61	0.6	<0.2	0.7
JS-NK12	<20	9.2	7.4	260	2.33	<0.2	2.4
JS-NK17	27	11.9	10.2	613	2.87	1.5	1.8
JS-NK20	58	27.1	17.9	1040	4.42	0.5	3.1
JS-NK22	28	26.8	17.1	1198	4.94	0.7	3
JS-NK23	29	32.8	21.8	979	4.61	1.6	3.4
JS-NK26	36	7	6	505	1.82	<0.2	2.3
JS-NK27	46	30.3	19.5	1633	4.79	0.8	3.4
JS-NK30	40	3.4	2.4	147	0.87	0.4	0.6
JS-NK36	29	3.3	1.8	371	1.04	<0.2	0.9
JS-NK37	27	3	3.2	549	1.3	<0.2	0.9
JS-NK38	885	21.3	15	737	3.35	7	2.7
JS-NK39	56	8.7	7.1	404	3.35	<0.2	3.6
JS-NK41	48	3.7	2.1	862	1.06	<0.2	1
JS-NK42	274	33.1	22.4	834	4.57	9.6	2.7
JS-NK49	56	27.9	19.2	1306	4.77	0.6	1.9
JS-NK55	<20	6.2	3.7	191	1.1	<0.2	1.1
JS-NK56	25	11.7	6.7	435	2.61	<0.2	2.6
JS-NK57	28	8.9	4.6	298	1.66	<0.2	1.6
JS-NK61	26	2.3	0.9	378	0.54	<0.2	0.4
JS-NK62	27	4.4	2.4	221	1.31	<0.2	1
JS-NK64	<20	3.3	1.3	197	0.45	0.8	0.5
JS-NK65	<20	8.3	6.5	233	1.7	<0.2	1
JS-NK67	<20	1.9	1.2	210	0.59	<0.2	0.4
JS-NK68	<20	5.5	2.8	119	1.22	<0.2	1.3
JS-NK69	<20	28.7	19.7	986	4.2	0.8	2.9

	1F15	1F15	1F15	1F15	1F15	1F15	1F15
	Au	Th	Sr	Cd	Sb	Bi	V
	PPM	PPM	PPM	PPM	PPM	PPM	PPM
	0.1	0.1	1	0.02	0.02	0.04	1
name							
JS-NK2	<0.1	3.9	102	0.04	0.11	0.23	17
JS-NK3	<0.1	3.5	128	0.03	0.11	0.09	18
JS-NK7	<0.1	3	100	0.03	0.18	0.08	12
JS-NK12	<0.1	3.7	52	<0.02	0.13	0.1	27
JS-NK17	<0.1	11.2	292	0.12	0.15	0.16	49
JS-NK20	<0.1	14.1	380	0.13	0.06	0.17	95
JS-NK22	<0.1	14.1	274	0.12	0.07	0.15	109
JS-NK23	<0.1	14.9	257	0.13	0.08	0.2	113
JS-NK26	<0.1	7.1	187	0.13	0.08	0.16	29
JS-NK27	<0.1	14.1	266	0.14	0.08	0.18	115
JS-NK30	<0.1	2.8	94	<0.02	0.08	0.18	14
JS-NK36	<0.1	4	182	0.08	0.12	0.06	17
JS-NK37	<0.1	4.1	202	0.04	0.17	<0.04	19
JS-NK38	<0.1	8.8	169	0.21	0.77	0.65	57
JS-NK39	<0.1	15.5	158	0.11	0.17	0.06	67
JS-NK41	<0.1	4.8	246	0.03	0.08	0.08	17
JS-NK42	<0.1	8.1	168	0.1	0.16	<0.04	69
JS-NK49	<0.1	7.8	332	0.12	0.21	0.11	66
JS-NK55	<0.1	4.5	125	0.03	0.24	0.05	18
JS-NK56	<0.1	10.7	497	0.11	0.6	0.13	61
JS-NK57	<0.1	6.2	200	<0.02	0.48	0.05	36
JS-NK61	<0.1	1.8	167	0.03	0.2	<0.04	7
JS-NK62	<0.1	2.8	97	<0.02	0.43	<0.04	16
JS-NK64	<0.1	1.7	122	<0.02	0.21	<0.04	5
JS-NK65	<0.1	3.4	85	0.05	0.27	<0.04	26
JS-NK67	<0.1	2.2	90	<0.02	0.09	<0.04	11
JS-NK68	<0.1	3.4	115	0.05	0.08	<0.04	27
JS-NK69	<0.1	16.4	245	0.08	0.22	0.1	98

	1F15	1F15	1F15	1F15	1F15	1F15	1F15
	Ca	P	La	Cr	Mg	Ba	Ti
	%	%	PPM	PPM	%	PPM	%
	0.02	0.001	0.1	1	0.02	1	0.001
name							
JS-NK2	0.11	0.006	3	8	0.16	436	0.132
JS-NK3	0.17	0.051	8.5	9	0.1	1080	0.139
JS-NK7	0.05	0.01	8	8	0.05	1263	0.105
JS-NK12	0.07	0.009	3.2	14	0.41	440	0.171
JS-NK17	1.22	0.036	85.1	29	0.53	430	0.468
JS-NK20	1.43	0.07	60.5	49	1.02	769	0.653
JS-NK22	0.82	0.085	70.5	63	1.12	1109	0.787
JS-NK23	0.7	0.092	42.8	58	1.08	1229	0.727
JS-NK26	0.39	0.011	4.4	16	0.37	492	0.247
JS-NK27	0.86	0.056	31.6	64	1.14	1199	0.702
JS-NK30	0.31	0.015	17.4	7	0.15	451	0.102
JS-NK36	0.79	0.013	9	14	0.14	1827	0.166
JS-NK37	0.91	0.011	18.1	16	0.19	1470	0.192
JS-NK38	0.48	0.055	45.5	37	0.53	1587	0.437
JS-NK39	0.15	0.013	79.7	37	0.27	1542	0.818
JS-NK41	1.34	0.013	16.8	16	0.17	1057	0.211
JS-NK42	0.7	0.06	31.9	43	0.78	1196	0.476
JS-NK49	1.98	0.045	32	39	1.06	384	0.479
JS-NK55	0.5	0.013	14.4	12	0.21	729	0.119
JS-NK56	1.72	0.034	27.8	28	0.4	455	0.503
JS-NK57	0.68	0.018	23.6	20	0.23	628	0.253
JS-NK61	0.94	0.003	9.6	6	0.05	415	0.048
JS-NK62	0.35	0.004	14	18	0.09	423	0.215
JS-NK64	0.43	0.003	7.8	4	0.05	457	0.026
JS-NK65	0.16	0.003	8.9	13	0.26	969	0.204
JS-NK67	0.74	0.003	11	9	0.04	1162	0.086
JS-NK68	0.39	0.153	18.1	16	0.13	1799	0.128
JS-NK69	0.65	0.071	46.3	65	0.93	1313	0.834

	1F15	1F15	1F15	1F15	1F15	1F15	1F15
	Al	Na	K	W	Zr	Sn	Be
	%	%	%	PPM	PPM	PPM	PPM
	0.02	0.002	0.02	0.1	0.2	0.1	1
name							
JS-NK2	3.33	1.343	1.99	0.3	86.1	0.8	2
JS-NK3	4.21	1.857	3.59	0.4	39.3	0.7	1
JS-NK7	4.11	1.874	3.96	0.2	39.7	0.3	<1
JS-NK12	3.59	1.33	1.96	0.5	43.1	0.9	1
JS-NK17	5.15	2.449	1.61	0.4	103.9	1.2	2
JS-NK20	7.49	2.854	2.21	0.5	135.7	2.8	4
JS-NK22	8.1	1.857	3.44	1.7	169	3.3	3
JS-NK23	8.21	1.664	3.99	2	178.4	4.1	2
JS-NK26	4.41	1.836	1.51	0.5	71	1.2	2
JS-NK27	8.42	1.728	3.87	1.7	119.3	4	3
JS-NK30	2.79	1.025	0.96	0.2	41.5	0.5	1
JS-NK36	5.13	2.495	3.88	<0.1	55.1	0.6	1
JS-NK37	5.33	2.802	3.63	0.2	60.9	0.5	<1
JS-NK38	6.75	3.182	3.58	0.5	115.1	2.2	3
JS-NK39	5.01	1.626	4.52	0.7	224.2	2.6	2
JS-NK41	4.95	2.615	3.03	0.2	72.7	0.5	1
JS-NK42	6.94	2.689	3.43	0.6	106.6	2	4
JS-NK49	6.4	2.004	1.88	0.5	125.6	2.2	3
JS-NK55	3.95	1.382	2.42	0.2	34.8	0.7	1
JS-NK56	4.34	1.289	1.43	0.3	123.3	2	2
JS-NK57	4.45	1.768	2.24	0.6	60.7	1.2	1
JS-NK61	2.5	0.795	1.87	<0.1	24.9	0.3	<1
JS-NK62	2.31	0.612	1.74	0.2	41.5	0.5	<1
JS-NK64	2.3	0.691	1.83	<0.1	18.5	0.3	<1
JS-NK65	4.43	0.683	3.72	0.3	43.2	0.6	1
JS-NK67	3.87	0.811	3.83	0.1	29	0.5	2
JS-NK68	5.81	0.855	5.59	0.4	51.4	0.9	1
JS-NK69	7.76	1.823	4.56	1.7	210.5	3.9	3

	1F15	1F15	1F15	1F15	1F15	1F15	1F15
	Sc	S	Y	Ce	Pr	Nd	Sm
	PPM	%	PPM	PPM	PPM	PPM	PPM
	0.1	0.04	0.1	0.02	0.1	0.1	0.1
name							
JS-NK2	1.4	<0.04	5.4	21.64	1	3.6	0.7
JS-NK3	2	<0.04	7.5	26.43	2.4	8.6	1.7
JS-NK7	1.6	<0.04	3.3	18.03	2.2	7.2	1.7
JS-NK12	3.6	<0.04	3.8	5.99	1	4.1	0.7
JS-NK17	7.1	<0.04	25.2	128.1	19.8	69.8	10.8
JS-NK20	14.2	<0.04	41.3	130.05	15.7	56	10.8
JS-NK22	19.8	<0.04	44.7	89.45	16	71.5	13
JS-NK23	14.6	<0.04	38.5	61.06	10.8	39.7	7.1
JS-NK26	3.8	<0.04	6.4	10.26	1.1	4.6	0.6
JS-NK27	16.5	<0.04	28.8	60.98	9.1	32.6	6.7
JS-NK30	1.4	<0.04	6	39.43	4.2	12.9	2.1
JS-NK36	3.5	<0.04	5.7	19.92	2.4	8.2	1.6
JS-NK37	3.9	<0.04	6.6	33.37	4.5	16.2	2.8
JS-NK38	9.2	<0.04	19.6	72.14	10.9	38.8	7.1
JS-NK39	6.5	<0.04	22.1	132.78	17.6	66.3	10.6
JS-NK41	3.5	<0.04	9.5	38.82	4.6	18	3
JS-NK42	9.8	<0.04	18.9	70.35	8.7	31.1	6.2
JS-NK49	8.8	<0.04	22.4	64.89	8.4	31.1	7.2
JS-NK55	2.2	<0.04	11.2	30	3.7	13.6	2.5
JS-NK56	6.1	<0.04	28.5	57.8	7.6	27.8	5.8
JS-NK57	4	<0.04	17	42.98	5.7	20.6	4
JS-NK61	0.9	<0.04	3.8	17.03	1.8	6.4	1.2
JS-NK62	1.2	<0.04	6.3	24.65	3	11.4	1.7
JS-NK64	0.6	<0.04	2.7	13.81	1.5	4.5	0.8
JS-NK65	3.1	<0.04	5.8	19.52	2.1	7.8	1.5
JS-NK67	1.7	<0.04	6.2	26.55	2.9	11.5	2.2
JS-NK68	2.4	<0.04	9.4	42.66	5.2	18.1	3.4
JS-NK69	13.9	<0.04	28.7	99.17	12.2	45	9.1

	1F15	1F15	1F15	1F15	1F15	1F15	1F15
	Eu	Gd	Tb	Dy	Ho	Er	Tm
	PPM	PPM	PPM	PPM	PPM	PPM	PPM
	0.1	0.1	0.1	0.1	0.1	0.1	0.1
name							
JS-NK2	0.1	0.8	0.2	1.2	0.2	0.6	0.1
JS-NK3	0.3	1.4	0.2	1.6	0.3	0.7	0.2
JS-NK7	0.2	1.3	0.2	0.8	0.1	0.4	<0.1
JS-NK12	<0.1	0.6	0.1	0.7	0.2	0.4	<0.1
JS-NK17	2.2	8.7	1.1	6	1	2.4	0.4
JS-NK20	1.9	8.7	1.4	7.4	1.5	5.2	0.7
JS-NK22	2.1	10.8	1.5	10.4	1.8	5.3	0.8
JS-NK23	1.3	6.4	0.9	6.3	1.5	4.8	1
JS-NK26	<0.1	0.5	<0.1	0.7	0.2	0.9	0.2
JS-NK27	1.1	4.1	0.8	4.7	1.3	4.4	0.9
JS-NK30	0.5	1.4	0.2	1.1	0.2	0.5	0.1
JS-NK36	0.3	1.4	0.2	1	0.3	0.7	0.1
JS-NK37	0.5	1.6	0.3	1.5	0.2	0.7	0.1
JS-NK38	1.3	5.1	0.8	4.2	0.8	2.2	0.3
JS-NK39	2.3	8	1.1	5.6	1	2	0.4
JS-NK41	0.5	2.1	0.3	1.7	0.4	1.1	0.2
JS-NK42	1.3	4	0.8	3.9	0.7	2	0.3
JS-NK49	1.3	4.6	0.7	4.2	0.8	2.6	0.5
JS-NK55	0.6	2.3	0.4	2.3	0.4	1.2	0.2
JS-NK56	1.2	5.3	0.9	5	1	3	0.5
JS-NK57	0.7	3.6	0.5	3.1	0.7	1.9	0.3
JS-NK61	0.3	0.8	0.1	0.6	0.2	0.4	<0.1
JS-NK62	0.5	1.3	0.1	1.3	0.2	0.6	0.1
JS-NK64	0.3	0.5	<0.1	0.6	0.1	0.2	<0.1
JS-NK65	0.3	0.9	0.2	0.9	0.2	0.5	<0.1
JS-NK67	0.3	1.3	0.2	1	0.2	0.7	0.1
JS-NK68	0.4	2.1	0.3	1.5	0.3	0.9	0.1
JS-NK69	1.7	7.7	1.2	5.7	1.2	2.9	0.4

	1F15	1F15	1F15	1F15	1F15	1F15	1F15
	Yb	Lu	Hf	Li	Rb	Ta	Nb
	PPM	PPM	PPM	PPM	PPM	PPM	PPM
	0.1	0.1	0.02	0.1	0.1	0.1	0.04
name							
JS-NK2	0.7	0.1	2.41	4.4	70.9	0.3	4.16
JS-NK3	0.8	0.1	1.19	3.3	93.5	0.3	4.43
JS-NK7	0.4	<0.1	1.2	2.3	101.8	0.3	3.33
JS-NK12	0.4	<0.1	1.27	5.4	78.3	0.3	5.46
JS-NK17	2.4	0.4	3.24	8.2	65.4	0.8	12.6
JS-NK20	4.7	0.7	3.97	31.2	103.3	1.1	17.5
JS-NK22	6.3	0.8	4.87	32.3	145.7	1.3	19.57
JS-NK23	5.7	0.8	4.79	35.3	143.7	1.2	20.61
JS-NK26	1.3	0.2	2.19	10.2	53.5	0.4	7.21
JS-NK27	5.2	0.8	3.48	23.8	126.7	1.2	17.36
JS-NK30	0.6	0.1	1.18	4.8	32.7	0.2	3.08
JS-NK36	0.8	0.1	1.72	3.9	92.5	0.3	5.11
JS-NK37	0.7	0.1	1.74	5.1	96.6	0.4	5.68
JS-NK38	2.1	0.4	3.3	12.7	160.3	0.7	11.58
JS-NK39	2	0.4	6.28	8.4	147.5	1.3	21.88
JS-NK41	1.2	0.2	2.24	3.4	76.1	0.4	6.31
JS-NK42	2	0.3	2.79	14.3	181.4	0.7	13.16
JS-NK49	3.1	0.5	3.45	35.9	108.7	0.8	14.27
JS-NK55	1.1	0.2	1.07	1.2	62.9	0.3	4.09
JS-NK56	3	0.4	3.42	2.9	56.3	0.9	12.67
JS-NK57	1.8	0.3	1.72	7.4	69.1	0.5	7.96
JS-NK61	0.4	<0.1	0.71	0.8	40.3	0.1	1.59
JS-NK62	0.7	<0.1	1.19	1.8	47.5	0.2	4.38
JS-NK64	0.4	<0.1	0.49	0.8	43.7	<0.1	1.16
JS-NK65	0.6	0.1	1.28	3.2	109.9	0.3	5.22
JS-NK67	0.7	0.1	0.87	2.9	95.6	0.2	3.45
JS-NK68	1.1	0.2	1.37	8	152.4	0.3	5.11
JS-NK69	2.8	0.4	5.69	42.1	157.9	1.4	22.25

	1F15	1F15	1F15	1F15	1F15	1F15	1F15
	Cs	Ga	In	Re	Se	Te	Tl
	PPM	PPM	PPM	PPM	PPM	PPM	PPM
	0.1	0.02	0.01	0.002	0.3	0.05	0.05
name							
JS-NK2	1.8	6.74	0.03	0.003	<0.3	0.08	0.64
JS-NK3	1.1	9.48	<0.01	<0.002	<0.3	0.06	0.71
JS-NK7	0.7	7.87	<0.01	<0.002	<0.3	<0.05	0.64
JS-NK12	1.5	9.79	0.02	0.004	<0.3	0.08	0.58
JS-NK17	2	11.2	0.04	<0.002	<0.3	<0.05	0.49
JS-NK20	4.5	22.75	0.07	0.002	<0.3	0.2	0.76
JS-NK22	5.1	27.36	0.13	<0.002	1	<0.05	0.75
JS-NK23	4.3	26.43	0.05	<0.002	<0.3	0.22	0.86
JS-NK26	1.6	10.07	0.02	<0.002	0.4	<0.05	0.35
JS-NK27	3.8	25.48	0.14	0.004	<0.3	<0.05	0.79
JS-NK30	0.7	5.43	0.02	<0.002	<0.3	0.09	0.24
JS-NK36	0.8	8.83	0.02	<0.002	<0.3	0.06	0.7
JS-NK37	0.9	9.89	0.03	0.002	<0.3	0.09	0.68
JS-NK38	3.1	16.7	0.06	0.004	<0.3	0.09	1.1
JS-NK39	2.3	15.62	0.06	0.002	<0.3	<0.05	0.96
JS-NK41	0.8	8.24	0.01	0.004	<0.3	<0.05	0.47
JS-NK42	4	18.22	0.06	0.002	<0.3	<0.05	1.1
JS-NK49	5.7	16.37	0.05	0.002	<0.3	<0.05	0.72
JS-NK55	0.8	8.44	0.02	0.004	0.3	0.05	0.33
JS-NK56	1.2	10.52	0.04	<0.002	<0.3	0.34	0.32
JS-NK57	1.6	9.29	0.03	0.004	<0.3	0.11	0.37
JS-NK61	0.4	4.06	<0.01	0.003	<0.3	0.13	0.26
JS-NK62	0.5	4.67	<0.01	0.005	<0.3	0.12	0.31
JS-NK64	0.4	4.01	0.01	<0.002	<0.3	0.11	0.27
JS-NK65	1.8	9.19	<0.01	<0.002	<0.3	<0.05	0.63
JS-NK67	0.5	6.47	<0.01	0.003	<0.3	<0.05	0.56
JS-NK68	1.1	15.63	0.04	<0.002	<0.3	0.07	0.89
JS-NK69	4.4	21.72	0.09	0.005	<0.3	<0.05	0.79



Norges geologiske undersøkelse
Postboks 6315, Sluppen
7491 Trondheim, Norge

Besøksadresse
Leiv Eirikssons vei 39, 7040 Trondheim

Telefon 73 90 40 00
Telefax 73 92 16 20
E-post ngu@ngu.no
Nettside www.ngu.no

*Geological Survey of Norway
PO Box 6315, Sluppen
7491 Trondheim, Norway*

*Visitor address
Leiv Eirikssons vei 39, 7040 Trondheim*

*Tel (+ 47) 73 90 40 00
Fax (+ 47) 73 92 16 20
E-mail ngu@ngu.no
Web www.ngu.no/en-gb/*